UNIVERSITAT DE BARCELONA

Desarrollo de sistemas nanoestructurados conteniendo Lactoferrina para el tratamiento de patologías oculares

Ana Laura López Machado

UNIVERSITAT DE BARCELONA

Facultad de Farmacia y Ciencias de la Alimentación

Desarrollo de sistemas nanoestructurados conteniendo Lactoferrina para el tratamiento de patologías oculares

Ana Laura López Machado

2022

UNIVERSITAT DE BARCELONA

PROGRAMA DE DOCTORADO

Investigación, Desarrollo y Control de Medicamentos

Desarrollo de sistemas nanoestructurados conteniendo Lactoferrina para el tratamiento de patologías oculares

Memoria presentada por **Ana Laura López Machado** para optar al título de doctora por la Universidad de Barcelona

Directoras

Dra. María Luisa García López

Dra. Elena Sánchez López

Doctoranda

Ana Laura López Machado

Tutora

Dra. María Luisa García López

A mi familia,

por su apoyo, confianza y amor incondicional.

"Defiende tu derecho a pensar, porque incluso pensar de forma errónea es mejor que no pensar"

Hipatia de Alejandría

AGRADECIMIENTOS

AGRADECIMIENTOS

Llegó el momento de dar fin a una etapa e inicio a otra y es importante mirar atrás y agradecer a todos los que han formado parte de mi vida, acompañándome en este camino. Quienes han estado presente en lo profesional guiándome en la investigación, y en lo personal, haciéndome este trayecto un poquito más fácil.

En primer lugar, agradezco a mi madre, por ser madre y estudiante universitaria a la vez, y llevarme a la piscina, toda mi niñez, con una bolsa llena de apuntes. Fue mi primer gran ejemplo a seguir. Gracias por creer en mí y demostrarme tu amor incondicional y por estar siempre.

Me siento muy afortunada por haber tenido la oportunidad de estar, estos últimos años, rodeada de grandes mujeres científicas, a las que admiro, y de quienes he podido absorber muchísimos conocimientos y experiencias, tanto profesionales como humanas.

Gracias a mis directoras de tesis, la Dra. Marisa García y Dra. Elena Sánchez, sin su guía y enseñanza, esta tesis no hubiese sido posible, les agradezco por todo el apoyo emocional y profesional que me han ofrecido a lo largo de estos años. A la Dra. Marta Espina, por su humanidad, apoyo, confianza, gran disposición y consejos, me llevo una amiga.

A la Dra. Josefa Badía y la Dra. Laura Baldomà por permitirme trabajar en el Departamento de Bioquímica y Fisiología de la Facultad de Farmacia y Ciencias de la Alimentación y a la Dra. Natalia Díaz quien no dudó en ayudarme y explicarme, siempre con la mejor disposición, el maravilloso mundo de los cultivos celulares.

AGRADECIMIENTOS

Agradezco la presencia de todos con quienes he compartido y trabajado a lo largo de este camino, porque todos me han enseñado algo. A todos los compañeros que han pasado por el laboratorio, gracias, ha sido un placer poder ayudar y sentirme ayudada siempre que lo he necesitado. Con el paso de los años el *lab 2* se había convertido en mi segunda casa (aunque probablemente por las horas pasadas en él, debería considerarlo la primera). A Amandita, gracias por convertirlo todo en risas que sanan, me has salvado muchas veces. Por tener esa alma tan bonita y ese cerebro tan brillante. A Cami, derrochas bondad y vitalidad, y eres una luchadora, gracias por tu aura. Gracias a Pauli, no sé qué hubiera sido de mi sin tus abrazos de madre en mis primeros años perdida en el *lab*, nuestros ataques de risa y tu ayuda con el Word. Gerard y Lorena, los jovencitos que vienen pisando fuerte, gracias por todos los favores de última hora, de agobios de etapa final de tesis. Gracias por ser un gran equipo.

Una mención especial a la Dra. Carmen Arévalo, quien ha sido mi inspiración desde segundo de carrera y probablemente la responsable de que me enamorara de la ciencia, el trabajo en el laboratorio y la docencia.

A mi familia, Mamá, Papá, Jose, Abuelo y Padrino, no tengo palabras para agradecer todo lo que han hecho por mí y el apoyo que me han brindado en todo momento, muchas gracias por estar siempre, en los buenos momentos, pero sobre todo en los malos, no fallan. Sin su apoyo no estaría donde estoy.

A mi familia del alma, Ana, Belén, Katia, María y Miguel, en Canarias tengo un tesoro, gracias por ser la familia que uno elige, por estar siempre desde la distancia, regalándome su tiempo, amor, consejos,

haciéndome la vida más vida, y más amena en los momentos difíciles, iluminan mi vida, gracias.

A Katya, Diana, Tania y Adri, cuatro mujeres increíbles que la vida me ha ido regalando en diferentes momentos, cuando más las necesitaba, gracias por hacer que mi vida en Barcelona fuera más divertida y fácil, he aprendido muchísimo de ustedes y me han hecho sentir como en casa.

Gracias al universo por poner en mi camino siempre a grandes profesionales que me han enseñado a ser mejor científica y, lo más importante, mejor persona. Gracias a todos ellos y a la vida que me ha permitido poco a poco ir alcanzando cada una de mis metas.

Gracias, gracias, gracias infinitas.

ÍNDICE

ÍNDICE

ABREVIATURAS

ABREVIATURAS

AA	Ácido araquidónico
AFM	Microscopía de fuerzas atómicas
BHA	Barrera Hematoacuosa
BHR	Barrera Hematorretiniana
COX	Ciclooxigenasa
CYP450	Citocromo P450
DAMP	Patrones moleculares asociados al daño
DLS	Dispersión dinámica de la luz
DoE	Diseño de experimentos
DSC	Calorimetría diferencial de barrido
EE	Eficiencia de encapsulación
EET	Ácido epoxieicosatetraenoico
EPR	Epitelio pigmentario de la retina
FLA_2	Fosfolipasa A_2
FTIR	Espectroscopia de infrarrojo con transformada de Fourier
HCE-2	Línea celular corneal humana
IFN-γ	Interferón-gamma
LF	Lactoferrina
bLF	Lactoferrina bovina
bLF-LIP	Liposomas cargados con Lactoferrina
bLF-NPs	Nanopartículas poliméricas cargadas con Lactoferrina
LOX	Lipoxigenasa
LPS	Lipopolisacárido
LT	Leucotrieno
MRP	Proteína asociada a la resistencia de múltiples fármacos

NF-κB	Factor de transcripción nuclear-κB
NK	Células Natural Killer
NPs	Nanopartículas
PEG	Polietilenglicol
PG	Prostaglandina
PLGA	Poli (ácido láctico-co-glicólico)
Rho	Rodamina
ROS	Especies reactivas de oxígeno
SOS	Síndrome del ojo seco
TEM	Microscopia electrónica de trasmisión
TLRs	Receptores tipo toll
TNF	Factor de Necrosis Tumoral
TX	Tromboxano
Zav	Tamaño promedio de partícula
ZP	Potencial zeta

RESUMEN - ABSTRACT

RESUMEN

La inflamación ocular es uno de los trastornos oftalmológicos más comunes y está asociada a un amplio abanico de patologías que afectan tanto al segmento anterior como posterior del ojo. El síndrome del ojo seco (SOS) o *queratoconjuntivitis sicca* es una patología de la superficie ocular, crónica y multifactorial, caracterizada por la pérdida de la homeostasis de la película lagrimal. Es la primera causa de consulta oftalmológica y está asociada a diferentes síntomas oculares como inestabilidad e hiperosmolaridad de la película lagrimal, inflamación en la superficie ocular, daño y anomalías neurosensoriales.

Existe una amplia variedad de alternativas terapéuticas para el tratamiento del SOS y las enfermedades inflamatorias oculares. Las lágrimas artificiales administradas por vía tópica, se utilizan para lubricar la superficie ocular, con el fin de mantener la humedad y evitar la desecación, produciendo un alivio instantáneo de los síntomas. Sin embargo, al no tener propiedades antinflamatorias, no actúan sobre la patogenia fundamental de la enfermedad, la inflamación. Por otro lado, los tratamientos habituales para combatir la inflamación ocular incluyen corticosteroides y antiinflamatorios no esteroideos (AINEs), desaconsejados para su uso prolongado debido al amplio número de efectos adversos que conlleva.

La Lactoferrina (LF) es una glicoproteína con numerosas propiedades terapéuticas, entre las que se incluye la capacidad antinflamatoria, antioxidante e inmunomoduladora. Está presente en las lágrimas basales y reflejas constituyendo un 20-30 % del proteoma, en pacientes sanos, disminuyendo significativamente en pacientes con la

enfermedad de ojo seco. Sin embargo, uno de los retos más importantes en el tratamiento ocular por vía tópica es la rápida eliminación vía conjuntiva y conducto nasolacrimal del activo administrado, dando como resultado una vida media precorneal limitada. Considerando lo anterior, el objetivo principal de esta investigación es el desarrollo y caracterización de dos sistemas nanoestructurados conteniendo LF, un vehículo polimérico basado en NPs de PLGA (bLF-NPs) y uno lipídico, basado en liposomas (bLF-LIP). Ambas formulaciones presentaron características fisicoquímicas adecuadas para la administración por vía ocular, así como un perfil biofarmacéutico de liberación prolongada de la LF. Los dos sistemas desarrollados mostraron una óptima tolerancia ocular, respaldada por los resultados in vitro (MTT y HET-CAM) e in vivo (test de Draize). Los ensayos de eficacia terapéutica in vitro e in vivo (en modelos de inflamación y sequedad ocular), demostraron su elevada eficacia tanto en la prevención y el tratamiento de la inflamación ocular del segmento anterior del ojo como en el tratamiento del síndrome de ojo seco. En conclusión y considerando los resultados obtenidos, ambos sistemas nanoestructurados de LF constituirían una alternativa prometedora, eficaz y segura para el tratamiento por vía tópica de patologías inflamatorias oculares.

ABSTRACT

Ocular inflammation is one of the most common ophthalmological disorders and is associated with a wide range of pathologies affecting both the anterior and posterior segments of the eye. Dry eye syndrome (DES) or *keratoconjunctivitis sicca* is a chronic, multifactorial ocular surface pathology characterised by loss of tear film homeostasis. It is the leading cause of ophthalmological consultation and is associated with different ocular symptoms such as tear film instability and hyperosmolarity, ocular surface inflammation, damage, and neurosensory abnormalities.

A wide variety of therapeutic alternatives exist for the treatment of DES and inflammatory ocular diseases. Topically administered artificial tears are used to lubricate the ocular surface to maintain moisture and prevent drying, producing instant relief of symptoms. However, it does not present anti-inflammatory properties, so it does not act on the fundamental pathogen of the disease, inflammation. On the other hand, the usual treatments to combat ocular inflammation include corticosteroids and non-steroidal anti-inflammatory drugs (NSAIDs), which are not recommended for prolonged use due to the large number of side effects associated with them.

Lactoferrin (LF) is a glycoprotein with numerous therapeutic properties, including anti-inflammatory, antioxidant and immunomodulatory capacity. It is present in basal and reflex tears and constitutes 20-30% of the proteome in healthy patients, decreasing significantly in patients with dry eye disease. However, one of the most important challenges in topical ocular treatment is the rapid elimination of the administered active via conjunctiva and nasolacrimal duct, resulting in a limited precorneal half-life. Considering

the above, the main objective of this research is the development and characterisation of two nanostructured systems containing LF, a polymeric vehicle based on PLGA NPs (bLF-NPs) and a lipidic one, based on liposomes (bLF-LIP). Both formulations presented physicochemical characteristics suitable for ocular administration, as well as a biopharmaceutical profile based on prolonged release of LF. Both systems developed showed optimal ocular tolerability, supported by *in vitro* (MTT and HET-CAM) and *in vivo* (Draize test) results. *In vitro* and *in vivo* therapeutic efficacy tests (in models of ocular inflammation and dry eye), demonstrated their high efficacy both in the prevention and treatment of ocular inflammation of the anterior segment of the eye and in the treatment of dry eye syndrome. In conclusion, and considering the results obtained, both nanostructured LF systems would constitute a promising, effective, and safe alternative for the topical treatment of ocular inflammatory pathologies.

1.

INTRODUCCIÓN

1.1 Características anatómicas y fisiológicas de la vía ocular

El ojo es uno de los órganos más pequeños y complejos del cuerpo humano. Su función es proporcionar la información visual del entorno, mediante la conversión de la luz en señales eléctricas y su transmisión, a través del nervio óptico, hacia la corteza visual del cerebro, donde son procesadas las imágenes (Willoughby et al., 2010). El globo ocular posee una forma esférica de aproximadamente 2,5 cm de diámetro anteroposterior y 7,5 cm de circunferencia, y dado que comparte numerosas propiedades anatómicas y fisiológicas con el cerebro, se considera una extensión del sistema nervioso central (Galloway et al., 2016; Groef and Cordeiro, 2018; Kels et al., 2015).

Su estructura se puede subdividir ampliamente en **dos segmentos**: anterior y posterior (Figura 1). El **segmento anterior** ocupa aproximadamente un tercio del globo, mientras que la porción restante pertenece al segmento posterior. Tejidos como la córnea, la conjuntiva, el humor acuoso, el iris, el cuerpo ciliar y el cristalino conforman el segmento anterior. El **segmento posterior** del ojo incluye la esclera, la coroides, la retina, el nervio óptico y el humor vítreo (Patel et al., 2013)

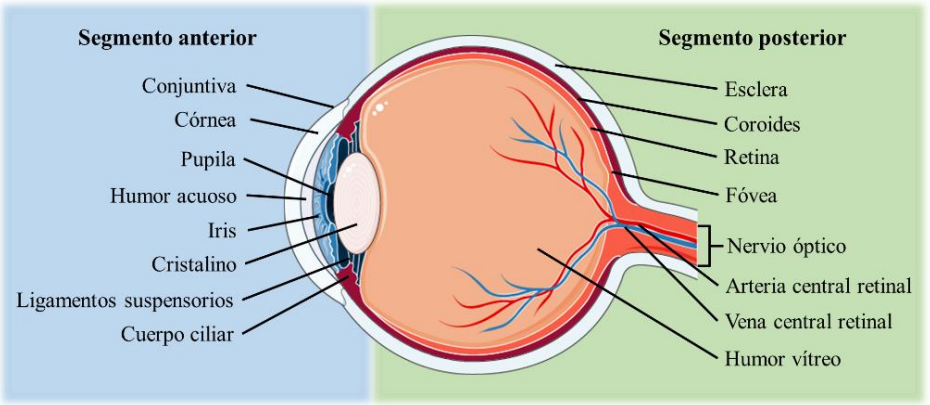

Figura 1. Segmentos y partes del globo ocular (adaptación de (Forrester et al., 2016).

El globo ocular está constituido por **tres capas** concéntricas principales. La variación anatómica y fisiológica de cada capa presenta una barrera significativa que dificulta el alcance de un fármaco a su diana tras su administración tópica (Gaudana et al., 2010).

La capa más externa es la **córneo-escleral**, la cual constituye la primera barrera del ojo y es una estructura fibrosa y protectora, constituida por la córnea y la esclera (Figura 2).

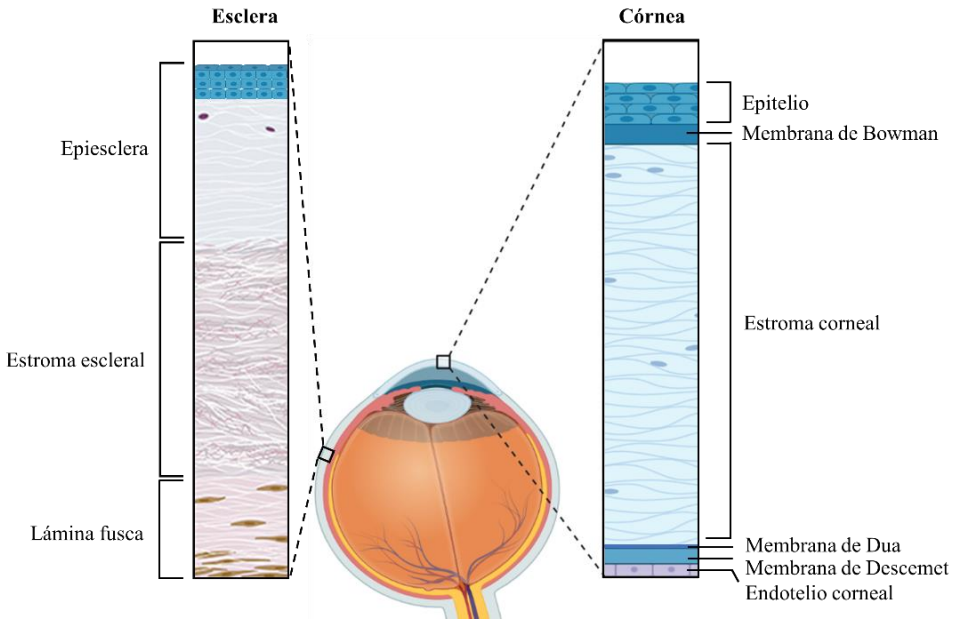

Figura 2. Estructura de la capa córneo-escleral (adaptación de (Galloway et al., 2016)).

La córnea se caracteriza por ser transparente, regular y avascular, lo cual es indispensable para la visión, y a su vez, está constituida por 6 capas de diferente naturaleza (de anterior a posterior: epitelio, membrana de Bowman, estroma, capa de Dua, membrana de Descemet y endotelio).

El epitelio corneal es un epitelio estratificado y está constituido por unas 4-6 capas de células no queratinizadas. Limita con la membrana de Bowman por una membrana basal firmemente adherida a través de fibras de colágeno. Sufre una renovación celular constaste mediante mitosis, gracias al flujo de células madre procedentes del limbo, dando lugar a una renovación celular completa, aproximadamente, cada 10 días (Galloway et al., 2016).

Sus funciones principales comprenden:

(1) diferentes mecanismos de protección ocular, tales como, la protección física de las capas más profundas debido a su superficie elástica y renovable; la estabilización ante un posible desgarro por la presencia de microvellosidades y pliegues; la función de barrera, favorecida por la presencia de uniones en hendidura o gap y uniones estrechas intercelulares frente al paso de líquidos y microorganismos; y la protección frente a radiaciones ultravioleta de longitud de onda corta;

(2) la producción de glucocálix y

(3) por último, su estructura uniforme le confiere la transparencia y capacidad refractiva fundamentales para la función visual (Downie et al., 2021).

Además de células epiteliales, en el epitelio corneal también pueden encontrarse células dendríticas presentadoras de antígenos y nervios sensoriales.

La lámina anterior limitante o membrana de Bowman es una red densa de fibras de colágeno orientadas al azar y es acelular, excepto en las zonas donde las fibras nerviosas del estroma penetran en el epitelio.

El estroma corneal, también llamado *sustancia propria*, confiere rigidez y espesor a la córnea. Está compuesto por fibras de colágeno y células de tejido conectivo, queratocitos, todo ello embebido una matriz extracelular. Además, presenta la inclusión de fibras nerviosas sensoriales.

Respecto a la membrana de Dua, delimita el estroma y la membrana de Descemet. Se presenta como una membrana acelular, delgada, resistente e impermeable al aire, constituida por fibras de colágeno altamente comprimidas. Fue descrita por primera vez en 2013 y existe cierta controversia en torno a su existencia (Dua et al., 2013).

La lámina posterior limitante o Membrana de Descemet es la membrana basal del endotelio corneal. El grosor y elasticidad de su estructura de colágeno, dispuesto de forma muy regular, le confieren gran resistencia frente a traumatismos o patologías.

Por último, el endotelio corneal, consiste en una monocapa de células escamosas que recubre la superficie interna de la membrana de Descemet y posteriormente se enfrenta a la cámara anterior. Está compuesta por nutrientes procedentes del humor acuoso y mantiene la hidratación del estroma a través de la bomba Na^+/K^+-ATPasa, lo que contribuye a la transparencia de la córnea (Downie et al., 2021).

Por su parte, la esclera, es un tejido opaco y blanquecino, no vascularizado y de naturaleza viscoelástica, formado por fibroblastos y una matriz de colágeno con haces dispuestos al azar. Posee tres capas principales: la epiesclera, formada por fibroblastos, proteoglicanos, melanocitos y glicoproteínas, entrelazados en una matriz de colágeno; el estroma escleral, constituido por fibras de colágeno más gruesas y ciertos melanocitos, que le confieren un color más oscuro; y la lámina fusca, formada por haces de colágeno más cortos y gran cantidad de melanocitos, situada adyacente a la úvea. Además, posee un surco que permite el paso de vasos ciliares y nervios. En la esclera se acoplan los músculos oculares, y

presenta funciones de protección y mantenimiento de la forma del globo ocular (Lawrenson, 2018).

La zona en la cual el epitelio de la superficie externa de la córnea continúa con la conjuntiva bulbar, una membrana mucosa delgada, suelta y transparente que recubre la parte anterior de la esclera, es decir, la unión entre ambas estructuras, se denomina limbo, y está constituido por un anillo de células madre altamente vascularizado, responsable de la regeneración del epitelio corneal (Galloway et al., 2016).

La **úvea**, la capa intermedia, se encuentra altamente vascularizada y pigmentada debido a la gran cantidad de melanocitos presentes (Forrester et al., 2016; Groef and Cordeiro, 2018).

La parte anterior de la úvea constituye el iris, que posee una apertura denominada pupila, cuya función consiste en regular la cantidad de luz que penetra en el globo ocular. El iris presenta unos capilares poco permeables a moléculas, debido a la presencia de la barrera hematoacuosa (BHA). Esta barrera consta de dos capas de células ubicadas en el epitelio del cuerpo ciliar del iris y en el endotelio de sus vasos sanguíneos. Ambas capas celulares expresan complejos de uniones estrechas, impidiendo así la entrada de solutos al humor acuoso (Gaudana et al., 2010).

La parte posterior de la úvea se denomina coroides y está compuesta por tejido conectivo vascular. Es la encargada de nutrir las diferentes capas de la retina.

La fracción que une el iris con la coroides es el cuerpo ciliar y sus tres funciones principales incluyen la secreción de humor acuoso, el ajuste del enfoque del cristalino y el drenaje del humor acuoso (Cholkar et al., 2012; Forrester et al., 2016).

La tercera capa es la **retina,** es la capa nerviosa del ojo y recubre el interior de la coroides. Está constituida por la retina neural, a su vez formada por grupos de neuronas y células interconectadas entre las que se encuentran las fotorreceptoras (conos y bastones); y el epitelio pigmentario de la retina (EPR), formado por una capa de células situadas entre la coroides y las células fotorreceptoras (Groef and Cordeiro, 2018).

Las uniones estrechas existentes entre el EPR y las células endoteliales vasculares conforman la barrera hematorretiniana (BHR) cuya función es restringir el transporte no especifico de moléculas entre la sangre circulante y la retina neural (Zuhaila García-Rubio and Lima-Gómez, 2014).

La retina se encuentra muy vascularizada y presenta gran sensibilidad a la luz, que produce la excitación de las células fotorreceptoras, desencadenando una cascada de reacciones bioquímicas capaces de generar señales eléctricas, que son enviadas mediante el nervio óptico al cerebro, originando el fenómeno de la visión (Dua et al., 2013; Galloway et al., 2016).

A su vez, el interior ocular se divide en tres compartimentos: la **cámara anterior**, situada entre la córnea y el iris, que contiene el humor acuoso; la **cámara posterior**, constituye el espacio entre la superficie posterior del iris y el cristalino; y la **cámara vítrea** que se sitúa entre la cara posterior del cristalino y la retina (Figura 3).

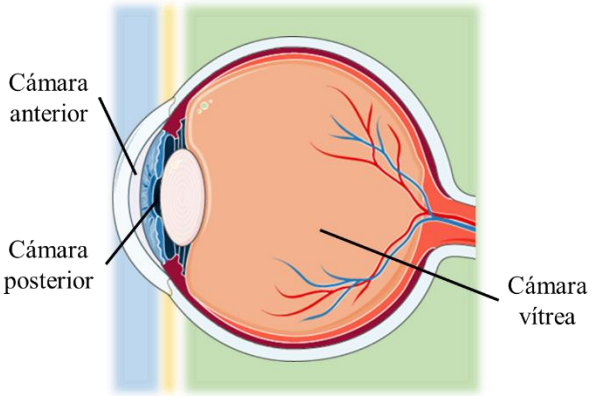

Figura 3. Compartimentos del globo ocular (adaptación de (Galloway et al., 2016)).

El volumen normal de **humor acuoso** es de 0,3 mL y sus funciones principales son nutrir al cristalino y a la córnea, y mantener la presión intraocular.

El **humor vítreo** consiste en una red tridimensional de fibras de colágeno y moléculas de ácido hialurónico polimerizado, capaces de contener grandes cantidades de agua. Posee un papel fundamental en el mantenimiento de la estructura ocular y de soporte de la retina (Galloway et al., 2016; Kels et al., 2015).

La **administración de moléculas con actividad farmacológica** a nivel ocular, por vía tópica, presenta numerosas ventajas. Al ser una técnica no invasiva, relativamente rápida, segura y fácil de usar, posee gran aceptación por el paciente. Sin embargo, la mala absorción y la biodisponibilidad deficiente del activo, por causa de las diferentes barreras anatómicas y fisiológicas, limitan su efectividad (Bachu et al., 2018; Patel et al., 2013).

En el momento en el que el colirio es administrado en la superficie ocular, un volumen de aproximadamente 40 μL entra en contacto con la película lagrimal y se enfrenta a la acción mecánica del parpadeo reflejo y al drenaje nasolacrimal. Esto produce un aumento en el volumen del fondo de saco conjuntival que favorece el aumento de la secreción de lágrimas y su drenaje, con la finalidad de restaurar su volumen promedio de 10 μL. Se produce la pérdida en un 95 % del activo disponible para ejercer la acción terapéutica en el área precorneal (Bachu et al., 2018). Por lo tanto, el tiempo de contacto del fármaco con los tejidos oculares será de 1-2 minutos. El conducto nasolacrimal, cuyas paredes están vascularizadas, traslada el fluido lagrimal desde el ojo hasta la cavidad nasal, lo que puede producir la absorción sistémica del activo, pudiendo potenciar sus efectos adversos a nivel extraocular.

La **película lagrimal** es una capa liquida protectora que recubre la superficie ocular y contiene lípidos, proteínas y electrolitos. Posee un espesor de aproximadamente 3-4 μm y se renueva a una velocidad de alrededor del 16 % por minuto mediante el parpadeo.

El concepto tradicional de un modelo de película lagrimal de tres capas ha sido reemplazado por un modelo que contempla una estructura más ordenada y compleja (Figura 4). Comprende una capa superficial lipídica, que recubre a una fase acuosa más amplia, compuesta por mucinas en suspensión y esta, a su vez, se superpone al glucocálix, también constituido por mucinas transmembrana, con largas estructuras filamentosas, unidas estrechamente a las microvellosidades de los epitelios corneal y conjuntival.

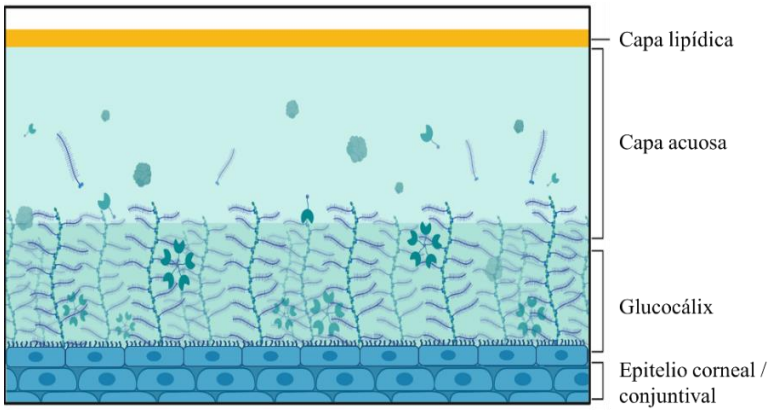

Figura 4. Estructura de la película lagrimal (adaptación de (Downie et al., 2021)).

La función principal de los lípidos es impedir la evaporación de la sección acuosa y reducir la tensión superficial de la lágrima, para favorecer su retención y su extensión por la superficie ocular (Downie et al., 2021).

Las mucinas ayudan a lubricar la superficie reduciendo la fricción durante el parpadeo.

El proteoma lagrimal describe una gran cantidad de proteínas y péptidos presentes. Entre otros, se encuentran la lizosima, lactoferrina, lipocalina-1, albumina e inmunoglobulinas, así como una amplia variedad de mediadores inflamatorios (Craig et al., 2017).

Los electrolitos presentes en la lagrima contribuyen a la homeostasis de la superficie ocular y son los principales responsables de la osmolaridad. Principalmente se encuentra sodio, potasio, cloro y bicarbonato (Downie et al., 2021).

Además, la lágrima contiene moléculas antioxidantes que ayudan a proteger la superficie ocular del estrés oxidativo, tales como el glutatión, el

ácido ascórbico, la cisteína, la tirosina o la lactoferrina (Downie et al., 2021; Georgiev et al., 2017).

Las moléculas que son capaces de atravesar la película lagrimal se enfrentan a **dos rutas de absorción**: la corneal y la no-corneal (conjuntiva-esclera) (Figura 5).

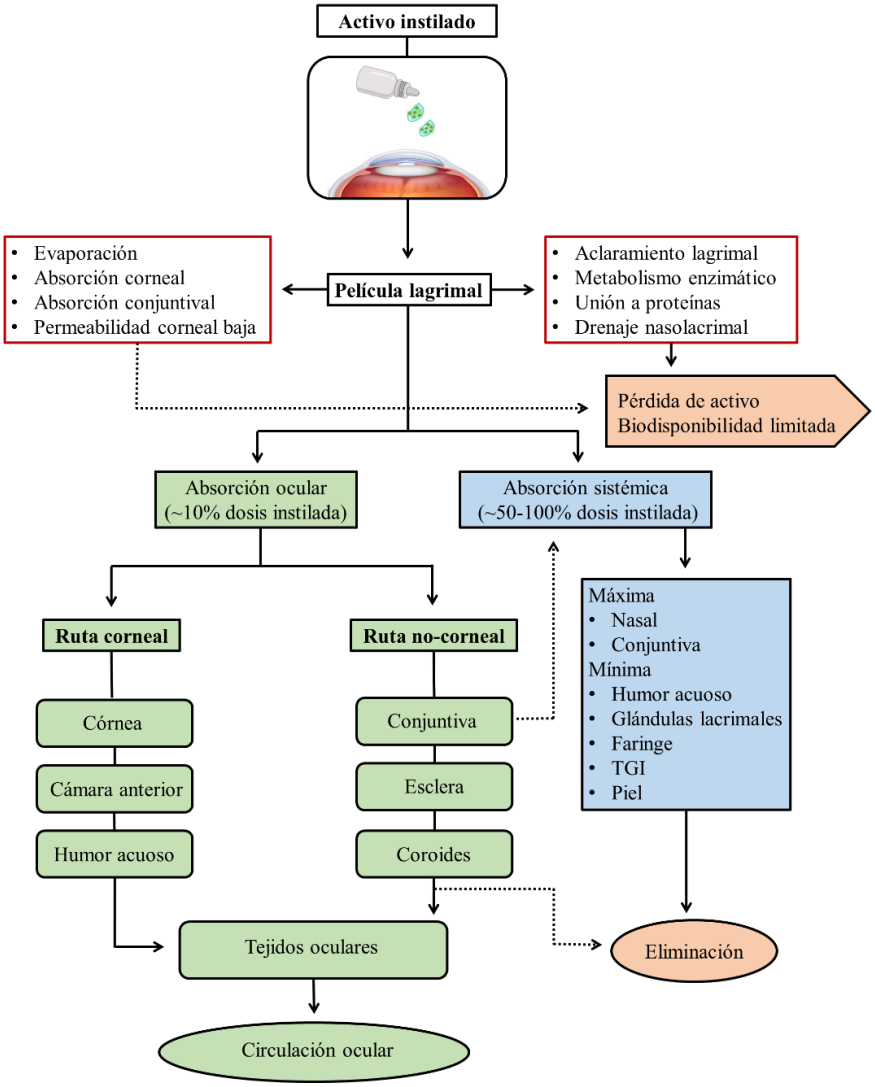

Figura 5. Rutas de absorción y eliminación de sustancias activas a nivel ocular (adaptación de (Swetledge et al., 2021)).

INTRODUCCIÓN

La **ruta corneal** implica el paso del activo a través de las 6 capas de la córnea. En primer lugar, por el epitelio corneal, cuyas células se encuentran de forma ordenada y compacta a través de uniones estrechas. Esto le confiere alta lipofilicidad, favoreciendo el paso de moléculas hidrofóbicas por permeación transcelular. Ciertas moléculas hidrofílicas que poseen un tamaño inferior a 350 KDa, podrían atravesar, también, el epitelio utilizando la ruta paracelular. Las células del epitelio corneal poseen carga neta negativa a pH fisiológico, por lo que se ve favorecida la permeación de moléculas cargadas positivamente (Bachu et al., 2018). El estroma, sin embargo, es una capa hidrofílica y gelificada que presenta el 90% del grosor de la córnea. Posteriormente, se encuentra el endotelio cuyas uniones intercelulares son amplias y permiten la entrada de compuestos hidrófilos (Mazet et al., 2020).

Una vez atravesada la córnea, la molécula alcanza la cámara anterior y es distribuida en el humor acuoso. El cual tiene una tasa de renovación de 2-3 μL por minuto. Desde ahí, la molécula es capaz de alcanzar diferentes tejidos del segmento anterior como el iris, el cristalino o el cuerpo ciliar por permeación a través de los tejidos o mediante la BHA (Hazare et al., 2016).

En el caso de la **ruta no-corneal**, la molécula entra en contacto con la conjuntiva bulbar, la membrana celular mucosa que recubre la esclera, cuyos espacios intercelulares son menos estrechos que en el epitelio corneal. Por esta capa, así como por la esclera, principalmente permearían las moléculas hidrofílicas y de alto peso molecular. Una vez atravesada la esclera, desde la coroides, altamente vascularizada, la molécula activa

lograría alcanzar los tejidos adyacentes donde ejercer su acción farmacológica (Lakhani et al., 2018).

Por otra parte, la absorción del activo se ve dificultada por la presencia de bombas de eflujo o proteínas de membrana, cuya función es la expulsión de sustancias desde el citoplasma celular al liquido extracelular. Entre ellas se encuentra la glicoproteína P (gp-P) presente en células de diferentes tejidos oculares, que restringe la entrada a moléculas anfipáticas y la proteína asociada a la resistencia de múltiples fármacos (MRP), transportador responsable de la expulsión de diferentes aniones orgánicos y compuestos conjugados del interior celular (Bachu et al., 2018).

La presencia de estas barreras oculares estáticas (diferentes capas de la córnea, esclera, retina y barreras hematoacuosa y hematorretiniana) y dinámicas (flujo sanguíneo coroideo y conjuntival, aclaramiento linfático, y dilución lacrimal) hace que la administración de fármacos por vía tópica presente un gran desafío, dando lugar al desarrollo de nuevas formas farmacéuticas nanotecnológicas que facilitan su administración y absorción hacia el tejido diana.

1.2 Enfermedades frecuentes del segmento anterior ocular

1.2.1 Síndrome del ojo seco

El síndrome del ojo seco (SOS) o *queratoconjuntivitis sicca* es una patología de la superficie ocular, crónica y multifactorial, caracterizada por la pérdida de la homeostasis de la película lagrimal. Es la primera causa de consulta oftalmológica y está asociada a diferentes síntomas oculares como inestabilidad e hiperosmolaridad de la película lagrimal, inflamación en la superficie ocular, daño y anomalías neurosensoriales. Se asocia con dolor y limitaciones en la realización de actividades cotidianas (Tsubota et al., 2020). Se denomina superficie ocular a la película lagrimal, las glándulas lagrimales y de Meibomio, la córnea, la conjuntiva y los párpados. La homeostasis consiste en el estado de equilibrio dinámico con respecto a las funciones y a la composición química de los tejidos y fluidos oculares (Craig et al., 2017).

El SOS es una de las afecciones oculares más frecuentes, que afecta a millones de personas en todo el mundo, con una prevalencia que oscila entre el 5 y el 50 % dependiendo de la zona (Agarwal et al., 2021; Roda et al., 2020). Se incluyen numerosos factores de riesgo, tales como edad avanzada, sexo femenino, síndrome de Sjögren, deficiencia de andrógenos, uso de algunos medicamentos como antihistamínicos, antidepresivos, ansiolíticos o anticonceptivos orales, enfermedad tiroidea, menopausia y tabaquismo, entre otros. Además, el uso continuo de lentes de contacto, ciertas condiciones ambientales como la contaminación elevada o la humedad baja y el uso excesivo de pantallas ha llevado a un aumento en la

incidencia del SOS, especialmente entre la población más joven (Joossen et al., 2020).

La función principal de la película lagrimal es el mantenimiento de la integridad de los tejidos de la superficie ocular subyacente, por lo que tiene gran influencia en la calidad de la visión. La película lagrimal normal tiene un índice de refracción de 1,337 y un pH de entre 6,8 y 8,2. Su viscosidad normal es mayor a 0,0082 Pa·s, viéndose reducida significativamente en el SOS. Los valores normales de osmolaridad, o concentración de partículas osmóticamente activas en la lagrima, varían de 270 a 315 mOsm/L y constituyen un indicador general del equilibrio entre la producción de lágrimas, la evaporación, el drenaje y la absorción. La inestabilidad de la lágrima da lugar a una evaporación excesiva del componente lagrimal acuoso, lo que genera la hiperosmolaridad lagrimal (Downie et al., 2021).

Esta hiperosmolaridad, junto al estrés oxidativo y mecánico celular producido en la superficie córneo-escleral conducen a irritación, inflamación de la superficie ocular, dolor, visión borrosa y alteraciones visuales, resultando en una disminución considerable de la calidad de vida del paciente (Agarwal et al., 2021).

Además, se genera un entorno proinflamatorio caracterizado por una gran liberación de citocinas, quimiocinas y células inmunitarias, que conduce a la degradación de la matriz extracelular y la ruptura de las uniones estrechas presentes entre las células epiteliales de la córnea. Estas condiciones dañan la superficie ocular y favorecen el reclutamiento de más células inflamatorias, generando un círculo vicioso inflamatorio que afecta

a la función e integridad ocular (Figura 6) (Anfuso et al., 2017; Joossen et al., 2020; Mazet et al., 2020; Seen and Tong, 2018).

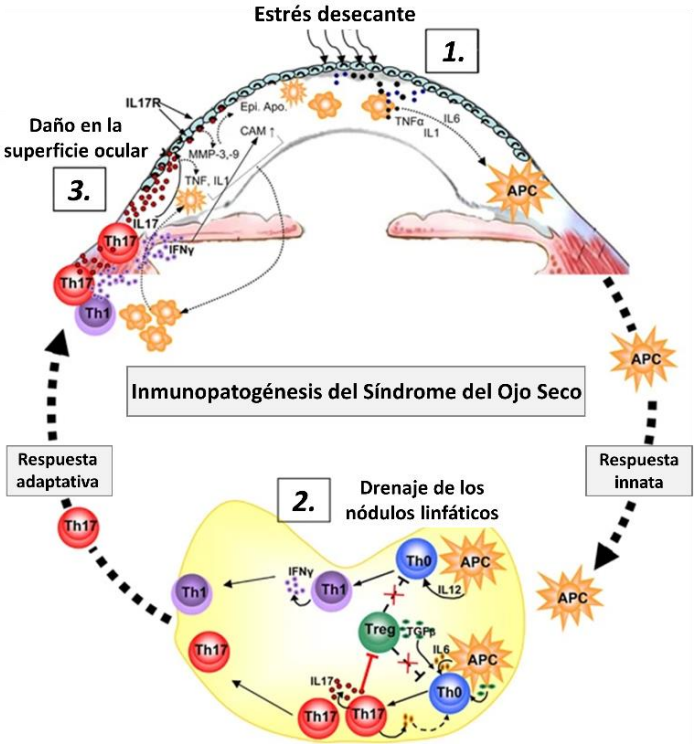

Figura 6. Inmunopatogénesis de la enfermedad del ojo seco, mecanismo inflamatorio asociado (adaptación de (Tsubota et al., 2020)).

1.2.2 Inflamación ocular

El fenómeno inflamatorio es una respuesta inmunológica, general e inespecífica del organismo, que se inicia como resultado de un trauma, lesión externa, enfermedad sistémica inflamatoria autoinmune o bien, frente a la presencia de agentes patógenos, sustancias xenobióticas, tóxicas o irritantes. Esta reacción puede variar en intensidad y duración y se presenta normalmente acompañada de enrojecimiento, calor, dolor, picor o pérdida de la función local. La inflamación es un proceso bioquímico complejo que

se caracteriza por el reclutamiento de células inmunitarias, producción de factores de crecimiento y citocinas proinflamatorias, cuyo objetivo es eliminar o aislar al agente etiológico que causa la alteración y reparar el daño a nivel local (Dennis and Norries, 2015; Gallo et al., 2017).

Ciertos estímulos causados por agentes infecciosos, radicales libres o lesiones en los tejidos generan una respuesta inmunitaria inducida por la liberación de proteínas y compuestos bioactivos procedentes de células muertas, lesionadas o infectadas. Estos factores endógenos se conocen como patrones moleculares asociados al daño (DAMP). Estos tienen afinidad por diversos receptores de membrana, en concreto, pueden interaccionar con los receptores tipo toll (TLRs), lo que desencadenaría la vía de inflamación mediada por el factor de transcripción nuclear-κB (NF- κB), el cual, en condiciones normales, se encuentra en el citosol asociado a una familia de proteínas quinasas denominada IκB (Rhen and Cidlowski, 2005). La fosforilación de IκB conduce a su ubiquitinación y degradación por el proteasoma, permitiendo la internalización nuclear de NF-κB, donde se une a ciertas secuencias de ADN, denominadas elementos NF-κB y estimula la transcripción de genes para citocinas, quimiocinas, moléculas de adhesión celular, ciclooxigenasas y óxido nítrico inducible. Estos mediadores son los responsable de la cascada inflamatoria con respuestas especificas e inespecíficas, y estimulan la producción de precursores de monocitos y neutrófilos en la medula ósea (Kruzel et al., 2017).

A su vez, tras el daño celular, por efecto de la enzima Fosfolipasa A_2 (FLA_2), se libera ácido araquidónico (AA) a partir de los lípidos de membrana, un mediador celular de la respuesta inflamatoria, que estimula

la producción de citoquinas proinflamatorias y el proceso de apoptosis. El AA, además, es precursor de los eicosanoides, los cuales poseen importantes funciones homeostáticas en los procesos inmunológicos e inflamatorios, incluyendo desde la modulación de la fuga vascular hasta la regulación de la agregación plaquetaria. El AA puede metabolizarse mediante dos vías: la vía de la *ciclooxigenasa* (COX) y la vía de la *lipooxigenasa* (LOX). La COX cataliza el metabolismo del AA dando lugar a prostaglandinas (PGs) y tromboxanos (TXs); y mediante el metabolismo por la LOX se generan leucotrienos (LTs) y otros metabolitos intermediarios. Finalmente, por la vía del citrocromo P450 (CYP450) se produce el ácido epoxieicosatetraenoico (EETs) (Dennis and Norries, 2015; White, 1999).

Paralelamente, el sistema del complemento, un conjunto de proteínas y péptidos enzimáticos presentes en la sangre y los fluidos corporales y el reclutamiento de células inmunitarias innatas, como los neutrófilos, macrófagos y células dendríticas, mediante quimiotaxis, conlleva a la producción de más mediadores inflamatorios como pueden ser la histamina, la serotonina, el factor activador de plaquetas, ciertas ROS, óxido nítrico, citoquinas y quimiocinas. Estos mediadores producen principalmente vasodilatación, aumento de la permeabilidad vascular, activación endotelial, dolor, fiebre y quimiotaxis, dando lugar a una retroalimentación positiva del proceso inflamatorio (Kruzel et al., 2017).

Las múltiples interconexiones entre las células inmunitarias, las citoquinas y las proteínas del complemento protegen contra el desarrollo de infecciones sistémicas y promueven la reparación de los tejidos dañados.

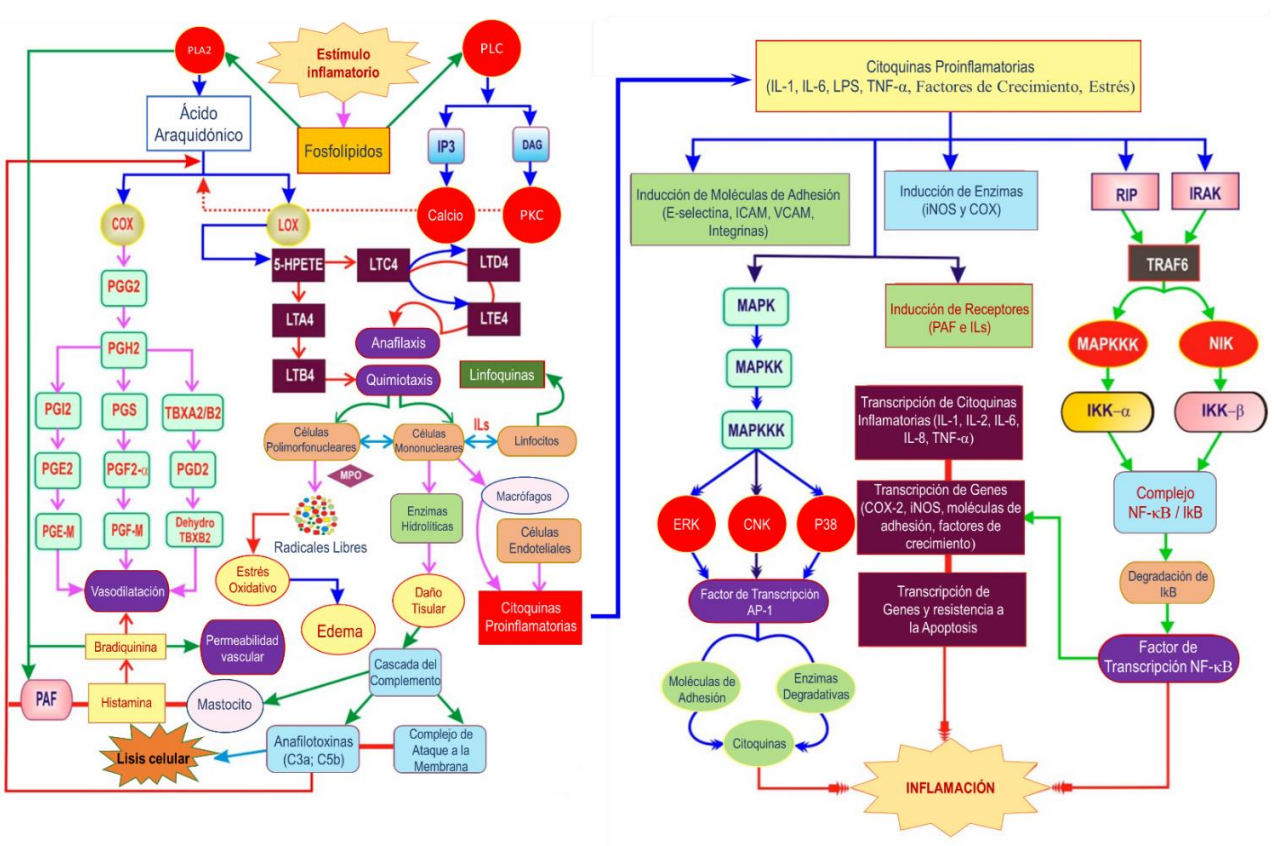

Figura 7. La cascada inflamatoria (adaptación de (Patil et al., 2019)).

INTRODUCCIÓN

La **inflamación ocular** es uno de los trastornos oftalmológicos más comunes y está asociada a un amplio abanico de patologías. Es una respuesta inespecífica a una agresión ocular, de origen externo o interno, que incluye diferentes mediadores proinflamatorios. Estos originan el reclutamiento y la activación de células inflamatorias y la liberación de diferentes mediadores inflamatorios. La inflamación puede tener diversas etiologías, incluyendo infecciones, traumatismos, efectos adversos a fármacos, respuestas autoinmunes, el SOS, o enfermedades inflamatorias sistémicas, como pueden ser la artritis reumatoide, la enfermedad de Crohn o el Lupus, entre otras (Schultz, 2018).

Clínicamente, la uveítis incluye la inflamación de las diferentes estructuras intraoculares de ambos segmentos, anterior y posterior, y los diferentes desórdenes se clasifican de acuerdo con su ubicación anatómica (Tabla 1).

Tabla 1. Tipos de uveítis según su clasificación anatómica (Foster et al., 2016).

Tipo	Zona afectada	Desórdenes asociados
Anterior	Cámara anterior	Iritis, iridociclitis, ciclitis anterior.
Intermedia	Vítreo	Pars planitis, ciclitis posterior, vitritis.
Posterior	Retina o coroides	Focal, multifocal, coroiditis difusa, coriorretinitis, retinitis, neurorretinitis.
Panuveítis	Todos los segmentos oculares implicados.	

Por otro lado, los fenómenos inflamatorios que afectan a las diferentes capas de la esclera se denominan escleritis o epiescleritis, caracterizándose este primero por ser muy doloroso y con mayor repercusión, pudiendo causar perdida visual o ceguera por complicaciones

graves como la necrosis escleral (Vergouwen et al., 2020). La episcleritis consiste en la inflamación de la capa delgada de tejido conectivo situada entre la esclera y la conjuntiva. Presenta un carácter agudo y suele ser idiopática. Las manifestaciones típicas incluyen eritema, malestar ocular leve y agudeza visual normal (Salama et al., 2018).

La inflamación de la conjuntiva (conjuntivitis) puede ser debida a un proceso infeccioso o no infeccioso. La conjuntiva es la membrana mucosa lubricante transparente que recubre la superficie del globo ocular (bulbar) y la superficie interior del párpado (palpebral). La conjuntivitis infecciosa puede tener diversas causas: bacterianas, virales, por clamidia, micóticas y parasitarias. Las causas de la conjuntivitis no infecciosa incluyen alérgenos, agentes tóxicos e irritantes (Alfonso et al., 2015).

1.2.3 Hemorragia subconjuntival

La hemorragia conjuntival o *hiposfagma*, consiste en una colección de sangre en el segmento anterior del ojo, específicamente en la *substancia propria*, situada entre la conjuntiva bulbar y la epiesclera, sin traspasar el limbo corneal. Generalmente se localiza en las áreas inferior y temporal de la conjuntiva. Se produce por la rotura de pequeños vasos sanguíneos o capilares que provocan esta acumulación de sangre. Su incidencia aumenta con la edad, particularmente a partir de los 50 años (Lim et al., 2015).

Normalmente se presenta indolora, no produce secreciones y no altera la agudeza visual. La hemorragia puede ocupar un espacio parcial o total en la esclera. Esta patología desaparece por reabsorción progresiva, sin producir consecuencias oculares, en un periodo de tiempo variable que puede ir desde los 7 días, hasta el mes. Sin embargo, si la hemorragia es de

gran tamaño y el área afectada se eleva debido a una alta cantidad de sangre presente, puede producir una alteración en la regularidad de la superficie ocular, causando sequedad ocular y molestias durante el parpadeo.

La hemorragia subconjuntival suele suceder de manera ocasional y sus causas son de naturaleza diversa, aunque en muchos casos es idiopática. Ocurre, principalmente, secundaria a hipertensiones venosas bruscas, tos, vómitos, traumas oculares, debilidad vascular, el uso de fármacos anticoagulantes y/o antiagregantes plaquetarios, enfermedades vasculares sistémicas, o en ciertas conjuntivitis. El uso de lentes de contacto puede inducir también la hemorragia, principalmente en pacientes con desordenes hematológicos, así como tras una cirugía ocular (Lim et al., 2015; Pitts et al., 1992; Sahinoglu-Keskek et al., 2013; Tarlan and Kiratli, 2013).

1.3 Lactoferrina: proteína multifuncional

La lactoferrina (LF) es una glicoproteína globular, de 80 KDa, que modula diferentes reacciones innatas y adaptativas del sistema inmunitario. Pertenece a la familia de las transferrinas y se considera una proteína multifuncional ya que presenta actividad antiinflamatoria, propiedades antioxidantes, antibacterianas, antifúngicas, antivirales, antiparasitarias e inmunomoduladoras, además posee actividad anticancerígena, juega un papel potencial en la preservación de la salud ósea, la regulación de la microbiota intestinal y mejora la función cognitiva en pacientes con enfermedades neurodegenerativas. (Connell et al., 2021; González-Chávez et al., 2009; Kanyshkova et al., 2001; Lee et al., 2020; Wang et al., 2017).

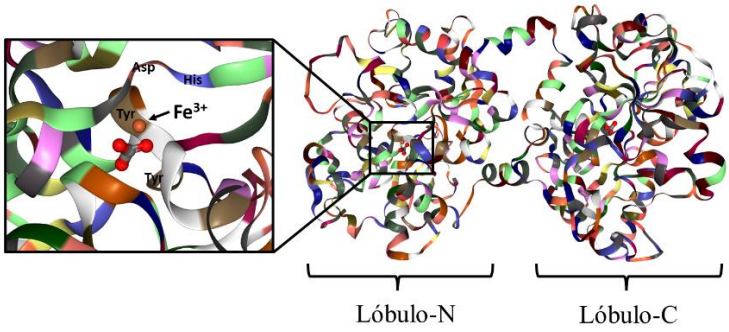

Figura 8. Estructura terciaria de la lactoferrina. Lóbulos diferenciados y posición especifica de los iones de hierro.

La estructura tridimensional de la LF revela una conformación plegada en dos lóbulos homólogos (N y C) conectados por una región bisagra o alfa-hélice flexible, con gran capacidad de unión a iones de hierro. Cada uno de los lóbulos puede unirse a iones Fe^{+2} o Fe^{+3} de forma estable y reversible, y simultáneamente, a un anión bicarbonato. En cuanto a su composición de aminoácidos, la cisteína proporciona grupos tiol para los

enlaces disulfuro intramoleculares 16 y 17 que estabilizan los lóbulos en LF humana y bovina, respectivamente. La asparagina proporciona sitios potenciales de glicosilación en ambos lóbulos. Una histidina, dos moléculas de tirosina y el ácido aspártico son esenciales para la unión del hierro y la arginina es fundamental para la unión del carbonato (Elzoghby et al., 2020).

La LF se une al hierro de manera reversible dando como resultado diferentes conformaciones 3D: apo-LF (sin hierro), LF monoférrico y holo-LF que está saturado con dos iones férricos. La Apo-LF tiene una conformación abierta y es más susceptible a la proteólisis, mientras que la holo-LF tiene una conformación cerrada por lo que presenta más resistencia. La LF humana está unida a glucanos poli-N-acetil-lactosamínicos en cada lóbulo, mientras que la LF bovina contiene restos de galactosa-α-1,3-galactosa (alfa-gal) en la ubicación terminal no reductora. Estos glucanos aumentan la estabilidad de la LF frente a las proteasas y el pH ácido (Elzoghby et al., 2020; Rascón-Cruz et al., 2021).

Presenta una carga neta positiva y punto isoeléctrico de entre 8,0 y 8,5. Es la única transferrina con capacidad de retener el hierro en un amplio rango de pH, incluyendo medios extremadamente ácidos. La proteína sufre la desnaturalización a dos temperaturas diferentes para los dos lóbulos; ~60 °C y ~90 °C (González-Chávez et al., 2009).

La LF es secretada por neutrófilos y glándulas exocrinas. Durante los procesos de inflamación o infección se ha observado que la concentración de LF aumenta considerablemente debido al reclutamiento de neutrófilos, donde se encuentra en cantidades considerables en sus gránulos (Zhang et al., 2021). El calostro y la leche presentan los niveles más altos

de esta glicoproteína, siendo la segunda proteína más abundante en la leche tras la caseína, pero también se encuentra en fluidos corporales como lágrimas, saliva o secreciones gastrointestinales (Tamhane et al., 2019) (Tabla 2).

Tabla 2. Principales fuentes y concentración de lactoferrina (Wang et al., 2019)

Fluidos biológicos	Concentración (mg/ml)
Calostro humano	5,80 ± 4,30
Calostro bovino	0,82 ± 0,54
Leche materna	2,00 - 3,30
Leche bovina	0,03 - 0,49
Lágrimas humanas	1,13 ± 0,29

A nivel citológico, la LF interacciona con los proteoglicanos de la superficie celular y se une específicamente a los receptores de membrana para estimular las vías ERK1/2 y PI3K/Akt (*extracellular signal-regulated protein kinase* y *phosphatidylinositol-3-kinase*), vías de señalización intracelular encargadas de controlar la multiplicación celular, diferenciación y apoptosis. Los receptores de membrana para la internalización de LF están constituidos por lipoproteínas de baja densidad (LRP1 y LRP2), receptores de membrana implicados en la endocitosis y receptores de unión a transferrina (TFR1, TFR2), así como ferritina y ferroportina necesarias para la transferencia de hierro. La expresión de estos receptores suele ser mayor en la superficie de las células cancerosas debido a su alta tasa metabólica. Además, la LF puede ingresar en las células mediante una interacción electrostática, entre su carga positiva y la carga negativa de los proteoglucanos de la superficie celular. También interactúa con la omentina-1, que es un receptor tipo lectina expresado en el epitelio intestinal y

responsable de la captación de LF. Además, puede unirse a receptores tipo Toll 4 (TLR4) jugando un papel inmunomodulador (Elizabeth Childs et al., 2020; Elzoghby et al., 2020).

La LF bovina (bLF) y la humana son dos proteínas que presentan alta homología en su secuencia de aminoácidos, lo que les confiere una gran similitud también en sus funciones principales en el organismo (Rosa et al., 2017). Por lo tanto, la mayor parte de los estudios *in vitro* e *in vivo* se han llevado a cabo empleando bLF, que es una sustancia reconocida como segura (GRAS) por la Administración de Alimentos y Medicamentos (FDA) y la Autoridad Europea de Seguridad Alimentaria (AESA) (European Food Safety Authority, 2012; Rosa et al., 2017).

A nivel ocular, la LF es una de las proteínas más abundantes de la lagrima, comprendiendo alrededor del 20-30 % en las lágrimas basales y reflejas (Hanstock et al., 2019). Además, está presente en el humor vítreo y en diferentes tejidos oculares, como la córnea, el iris y el epitelio pigmentario de la retina (Rageh et al., 2017).

La bLF es una sustancia inmunomoduladora natural que posee una fuerte **actividad antiinflamatoria** (Conneely and Conneely, 2013; Håversen et al., 2002; Rosa et al., 2017). Parte de esta actividad puede atribuirse a su capacidad para interactuar con receptores específicos de la superficie celular en células epiteliales y células del sistema inmunitario, mediada por la fracción de glucanos de la molécula, así como con su capacidad para unirse a patrones moleculares asociados a patógenos (PAMP), reconocidos principalmente por los receptores tipo Toll (TLR) (Legrand, 2016). La LF también juega un papel en la diferenciación,

maduración, activación, migración, proliferación y función de las células presentadoras de antígenos, como son las células B, neutrófilos, monocitos/macrófagos y células dendríticas, además de reducir el perfil inflamatorio, mediante la modulación de la respuesta inmune al regular a la baja las citoquinas proinflamatorias. Así mismo, promueve el aumento del número de células natural killers (NK), estimula el reclutamiento en la sangre de células polimorfonucleares e induce la fagocitosis (Drago-Serrano et al., 2017; Rascón-Cruz et al., 2021).

Además, tanto la LF humana como la bovina pueden ser internalizadas en las células epiteliales y penetrar en el núcleo, donde se encuentra el ADN, siendo el lóbulo N el responsable de su internalización, orientación y unión (Superti, 2020; Suzuki et al., 2009). Así, tienen la capacidad de modular la respuesta inflamatoria en las células del epitelio corneal atenuando la transcripción de genes inducida por NF-κB para diversos mediadores inflamatorios e inhiben citocinas proinflamatorias como el interferón-gamma (IFN-γ), el factor de necrosis tumoral-alfa (TNF-α) y diferentes interleucinas (ILs) (González-Chávez et al., 2009; Gu and Wu, 2016; Rascón-Cruz et al., 2021; Rosa et al., 2017)

La LF ejerce su **acción antimicrobiana** frente a una amplia gama de microbios como bacterias, hongos, virus y parásitos por dos mecanismos diferentes. (i) Actividad indirecta o microbiostática mediada por el secuestro de hierro libre esencial para el crecimiento y proliferación microbiana; (ii) función microbicida, actuando directamente, sobre las membranas. Específicamente, su actividad bactericida se lleva a cabo a través de la interacción del extremo N altamente catiónico, con el LPS cargado

negativamente de las bacterias gram-negativas, provocando daños en la membrana. Además, evita así la interacción de la proteína de unión de LPS (LPB) con la endotoxina para bloquear la unión de LPS a la proteína de membrana CD14, que daría lugar a la activación de monocitos y macrófagos (Elzoghby et al., 2020; Superti, 2020).

Al mismo tiempo, en el proceso inflamatorio también está involucrada la generación de especies reactivas de oxígeno (ROS) que influyen en la gravedad de la inflamación ocular y el daño en los tejidos. Las ROS provocan peroxidación de lípidos de la membrana celular, daño oxidativo en proteínas y la formación de nuevos radicales libres. Se ha descrito que los iones de hierro libres potencian las reacciones redox, aceptando o donando fácilmente electrones que contribuyen a la formación de estas ROS (Kanwar et al., 2015).

Niveles normales de LF en la película lagrimal pueden contribuir a la reducción de la concentración de hierro libre presente, mediante su secuestro o actividad quelante, e inhibir los efectos proinflamatorios de los radicales libres; además de ejercer actividad protectora frente a la radiación solar UV en el epitelio corneal (Chen et al., 2017; Flanagan and Willcox, 2009).

Actualmente, la LF puede encontrarse en diferentes productos comercializados en diversas formas farmacéuticas. La tabla 3 muestra algunos de ellos (Elzoghby et al., 2020).

Tabla 3. Productos farmacéuticos comercializados con lactoferrina (Elzoghby et al., 2020).

Nombre comercial	Forma de dosificación	Composición	Indicación clínica
Pravotin®	Granulado para suspensión	100 mg LF	Embarazo, enfermedades cardiovasculares, pacientes en hemodiálisis, deportistas y pediatría
Yili LF ShuHua Milk®	Leche suplementada con LF	(LF 5 mg/100 ml) (LF 10 mg/100 ml)	Inmunoestimulante, influenza humana, resfriado común
Biotene Oral Balance®	Gel	Lactoperoxidasa, Lisozima y LF	Boca seca, higiene bucal
Symbiotics Super Immune Colostrum Plus LF®	Comprimidos	931 mg Calostro bovino y fosfolípidos y 29 mg LF	Inmunoestimulante
Lattoglobina®	Cápsulas	LF liofilizada 9.75 g	Embarazo, anemia ferropénica
Reimmugen®	Cápsulas	Calostro bovino, LF 1.5%	Patologías cardiovasculares
Symbiotics LF®	Cápsulas	500 mg bLF	Inmunoestimulante
Life extension LF Caps®	Cápsulas	285 mg Apo-LF	Inmunoestimulante
Immune Care®	Cápsulas	250 mg Apo-LF	Inmunoestimulante y antioxidante
IronSorb® + LF	Cápsulas	18 mg hierro elemental + 200 mg LF	Anemia ferropénica, suplementación
Acacia®	Cápsulas	250 mg LF	Alivio de la diverticulitis y anemia
Elleffe 100®	Crema	4% LF	Adyuvante en afecciones cutáneas contra virus, hongos y bacterias
Kelapher®	Crema	LF Liposomal	Discromía hemosiderínica; equimosis postoperatoria; insuficiencia venosa, úlceras flebostáticas; tratamientos post-láser no ablativos

1.4 Sistemas nanoestructurados de liberación controlada de fármacos a nivel ocular

En las últimas décadas, las nuevas técnicas de administración de fármacos a nivel ocular han evolucionado considerablemente. Los objetivos principales de cualquier sistema ocular de administración de fármacos incluyen mantener las concentraciones terapéuticas del fármaco en su diana molecular, reducir la frecuencia de administración, con especial importancia en los tratamientos crónicos, y superar las barreras oculares estáticas y dinámicas. A la hora de formular un nanosistema se tiene en especial consideración que este produzca una disminución de los posibles efectos adversos provocados por el fármaco libre y un aumento de su biodisponibilidad (Tabla 4) (Tsai et al., 2018).

El segmento anterior del ojo suele ser tratado mediante el uso tópico de gotas oftálmicas, cuya principal desventaja es la baja biodisponibilidad debido a la renovación continua del fluido lagrimal y al elevado drenaje nasolagrimal. Los nanosistemas utilizados para la administración de fármacos oculares, que incluyen nanopartículas poliméricas y lipídicas, liposomas, nanomicellas, emulsiones, lentes de contacto con liberación sostenida de fármacos, implantes oculares y ungüentos, posibilitan un mayor tiempo de residencia en el área precorneal (Yang et al., 2022). Esto es debido a las interacciones que se producen entre los nanosistemas y las glicoproteínas presentes en la córnea y la conjuntiva, consiguiendo formar un depósito temporal, con la resultante liberación prolongada del principio activo.

Tabla 4. Tipos de nanopartículas coloidales biodegradables para el tratamiento de patologías oculares (Tsai et al., 2018).

Vehículo	Administración	Aplicaciones	Ventajas
Liposomas	▪ Administración tópica ▪ Inyección subconjuntival ▪ Inyección intravítrea	▪ SOS ▪ Queratitis fúngica ▪ Degeneración macular ▪ Glaucoma ▪ Uveoretinitis autoinmune	Estructura de bicapa de fosfolípidos biocompatible, transporta fármacos hidrofílicos y lipofílicos, alta eficiencia de encapsulación.
NPs PLGA	▪ Administración tópica ▪ Inyección intravítrea	▪ Trastornos inflamatorios de la córnea ▪ Uveítis ▪ Retinitis	Polímero bien investigado, hidrofilicidad, biodegradable y biocompatible, protege al fármaco de la degradación e induce su liberación controlada.
NPs lipídicas	▪ Administración tópica ▪ Inyección intravítrea ▪ Administración periocular	▪ SOS ▪ Degeneración macular ▪ Glaucoma ▪ Retinopatía diabética ▪ Uveítis	Bajos costos de producción, facilidad para penetrar en los tejidos oculares internos, biodegradable y biocompatible, protege al fármaco de la degradación e induce su liberación controlada.
NPs de quitosano	▪ Administración tópica ▪ Inyección en estroma corneal ▪ Inyección subretiniana	▪ Endoftalmitis bacteriana ▪ Enfermedades hereditarias de la córnea ▪ Enfermedades genéticas asociadas al EPR	Bajos costos de producción, la mucoadhesividad prolonga el tiempo de retención del fármaco en la superficie ocular, atraviesa los espacios de las uniones estrechas para superar las barreras oculares.
NPs de gelatina	▪ Administración tópica ▪ Inyección intravítrea	▪ Enfermedad bacteriana del segmento anterior ocular ▪ SOS ▪ Neovascularización corneal	Bajos costos de producción, componente del estroma corneal, polianfolito, biocompatible y biodegradable, fácil modificación superficial, fácil y eficiente encapsulación de activos.

Además, el uso de nanotransportadores resulta muy eficiente a la hora de atravesar barreras tisulares y membranas, por lo tanto, también resulta útil la administración de fármacos encapsulados en estos nanosistemas, por vía tópica, para el tratamiento de patologías oculares presentes en el segmento posterior del ojo (Gote et al., 2019; Nagarwal et al., 2009; Souto et al., 2019). En la Tabla 5 se muestran algunos ejemplos de nanoformulaciones indicadas para terapias oculares comercializadas y en fase de ensayos clínicos (Khiev et al., 2021).

La gran eficacia de los tratamientos farmacológicos a nivel ocular, no invasivos, mediante el uso de sistemas nanoestructurados, se debe a los siguientes factores (Lalu et al., 2017):

- Aumento del tiempo de residencia precorneal.
- Mejora de los problemas de solubilidad y biodisponibilidad.
- Direccionamiento al tejido diana y aumento de la penetración.
- Liberación sostenida y farmacocinética controlada.
- Protección del activo y aumento de su estabilidad fisicoquímica.

Tabla 5. Tratamientos oculares basados en nanosistemas llevados a ensayos clínicos y aprobados por la FDA (Khiev et al., 2021).

Producto	Nanoformulación	Indicación	Estado
Restasis®	Nanoemulsión	Ojo seco	Aprobado
Durezol®	Nanoemulsión	Inflamación ocular	Aprobado
Trivaris®	Suspensión de acetónido de triamcinolona	Uveítis	Aprobado
Retiro®	Implante no biodegradable de acetónido de fluocinolona	Uveítis no infecciosa	Aprobado
Kenalog®	Suspensión de acetónido de triamcinolona	Edema macular	Aprobado
Ozurdex®	Implante biodegradable de dexametasona	Edema macular, uveítis no infecciosa	Aprobado
Ilúvien®	Implante no biodegradable de acetónido de fluocinolona	Edema macular diabético	Aprobado
Triesencia®	Suspensión de acetónido de triamcinolona	Edema macular	Aprobado
Visudyne®	Liposomas	AMD	Aprobado
Macugen®	Nanopartículas poliméricas de aptámero	DMAE húmeda	Aprobado
SYSTANE®	Nanoemulsión a base de propilenglicol	Ojo seco	Aprobado
TLC399 (ProDex)	Nanopartículas lipídicas	Edema macular	Fase II
POLAT-001	Liposomas	Glaucoma	Fase II

1.4.1 Nanopartículas poliméricas

Las nanopartículas (NPs) poliméricas biodegradables constituyen uno de los sistemas coloidales más estudiados. La definición clásica de nanopartícula, formulada en la Enciclopedia de Nanociencia y

Nanotecnología, considera estos sistemas como partículas coloidales de tamaño comprendido en el rango de 1-1000 nm (1μm) formuladas con materiales macromoleculares en los que el principio activo está disuelto, encapsulado o atrapado en el interior y/o superficie de la matriz polimérica, funcionando como una unidad completa en términos de transporte y propiedades (Kreuter, 2004).

Estos sistemas poseen la habilidad de atravesar barreras fisiológicas y ser internalizados a nivel celular con mayor facilidad que fármacos o moléculas de elevado peso molecular o propiedades fisicoquímicas complejas, además de una gran capacidad de carga de activos. Debido a su elevada relación superficie-volumen, la unión de diferentes ligandos a su superficie favorece su penetración y direccionamiento a la diana terapéutica.

Las cadenas de polímero pueden ser de procedencia natural o sintética. Los polímeros naturales más utilizados incluyen quitosano, ácido hialurónico, alginato de sodio y carboximetilcelulosa de sodio. Entre los polímeros sintéticos, los más utilizados son los poliésteres como poli(ácido láctico-co-glicólico) o poli(ε-caprolactona) y poli(etilenglicol). Las NPs pueden clasificarse en 2 grupos según la disposición del polímero: nanocápsulas y nanoesferas (Figura 8). Las nanocápsulas son sistemas vesiculares compuestos por una membrana polimérica externa y un interior líquido. En cambio, las nanoesferas consisten en una matriz polimérica en la cual el fármaco se encuentra entrelazado.

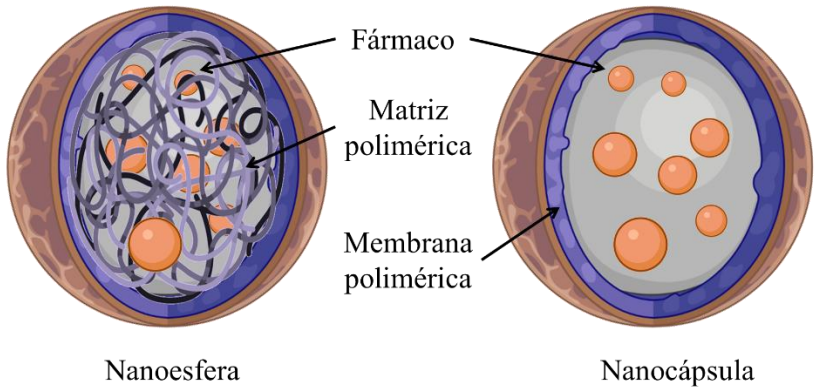

Figura 8. Nanopartículas poliméricas biodegradables (adaptación de (Suffredini et al., 2014).

Uno de los polímeros más utilizados actualmente para la fabricación de estos sistemas de administración de fármacos es el PLGA, es un co-polímero formado por monómeros consecutivos de ácido poliláctico (PLA) y poliglicólico (PGA). Este compuesto fue aceptado por la FDA en 1960, y actualmente está aprobado por la EMA para uso parenteral y tópico. Es considerado una sustancia segura (GRAS) para su utilización en humanos, por ser un material biocompatible, biodegradable y no tóxico (Sharma et al., 2016). El PLGA puede procesarse en casi cualquier forma y dimensión y encapsula moléculas de naturaleza y tamaños muy diversos. Constituye un tipo de NP ideal para el transporte, direccionamiento y liberación sostenida de fármacos o sustancias bioactivas, así como para la administración de tratamientos crónicos, por su capacidad para disminuir los efectos secundarios y el número de dosis necesarias para conseguir el efecto terapéutico. Una de las características de interés del PLGA es la predicción de su cinética de degradación, la cual depende de la proporción de láctico/glicólico del polímero. A medida que aumenta la proporción de láctico, la tasa de degradación disminuye. Además, este polímero se

considera no tóxico, debido a que sufre hidrólisis no enzimática, en el organismo, generando como productos el ácido glicólico y el ácido láctico, los cuales son metabolizados por el ciclo de Krebs (Jain, 2000; Makadia and Siegel, 2011).

La administración de NPs de PLGA por vía ocular resulta útil dada la protección que ejercen sobre el principio activo frente a su posible inactivación enzimática en la película lagrimal o el epitelio corneal. Su uso favorece, además, el tiempo de residencia precorneal y su penetración tisular y a través de la membrana de la córnea y evita los efectos adversos causados por sobredosificación. Esta situación se ve favorecida con el recubrimiento polimérico, con polietilenglicol (PEG) u otras moléculas que, adheridas a la superficie, confieran carga positiva a las partículas, aumentando el tiempo de permanencia en la superficie ocular. Esto es debido a su retención en la red de mucinas y lisozimas, mediante interacción electrostática y enlaces de hidrógeno. Por lo tanto, la encapsulación en NPs mejora la biodisponibilidad a nivel ocular del principio activo (Lynch et al., 2019).

Las vías de transporte por las que las NPs penetran en los tejidos de la superficie ocular son de gran interés. Diferentes autores han estudiado este tema y han observado diferencias en la profundidad de penetración en el tejido conjuntival y la córnea, dependiendo de la naturaleza, el activo encapsulado y las propiedades fisicoquímicas de la formulación. Se han propuesto diferentes vías para explicar la penetración, incluida la endocitosis y la ruta transcelular. La endocitosis mediada por clatrina se observa para vesículas de un tamaño de alrededor de 120 nm y mediada por caveolina en el caso de NPs de unos 60 nm, aproximadamente. Se ha

observado que NPs de tamaños intermedios, sobre los 90 nm, son internalizadas mediante endocitosis independiente de estas proteínas. Las NPs internalizadas por endocitosis mediada por clatrina se dirigen a la degradación lisosomal. Las internalizadas por endocitosis mediada por caveolina se acumulan en los endosomas (caveosomas) y se envían a otros compartimentos subcelulares distintos de los lisosomas.

El metabolismo intracelular de los activos administrados difiere según la vía de internalización. Esto implica su separación física del transportador y sus características fisicoquímicas determinarán la tasa de degradación, lo cual es clave para la actividad farmacológica de la molécula transportada. Se describen diferentes procesos cinéticos para controlar los perfiles de liberación de fármacos de las NP, incluidos la desorción del fármaco adsorbido o unido a la superficie, la difusión a través de la matriz de la NP o la pared del polímero, la erosión de la pared de la NP y una combinación de procesos de erosión y difusión. Para activos que se distribuyen uniformemente en la matriz polimérica, la difusión y la biodegradación rigen el proceso de liberación. Si la difusión del activo es más rápida que la degradación polimérica, la liberación del fármaco se produce principalmente por difusión; por el contrario, su liberación se producirá mediante la degradación del polímero (Diebold and Calonge, 2010).

Existen diferentes métodos de preparación de NPs poliméricas, la elección del más conveniente depende de las características fisicoquímicas del activo a encapsular con una eficiencia de encapsulación adecuada y de los requerimientos de su aplicación. Ampliamente, los métodos pueden ser

clasificados en dos grupos, de acuerdo con los que utilizan polímeros ya preformados o aquellos que polimerizan los monómeros durante el proceso de síntesis.

A continuación, se explican brevemente los métodos de preparación de NPs con polímeros preformados (Begines et al., 2020; Crucho and Barros, 2017).

- Emulsificación / Evaporación del disolvente

Fue la primera técnica de síntesis de NPs desarrollada y en la actualidad es una de las más utilizadas (Vanderhoff and El Aasser, 1979). Existen dos métodos generales dependiendo de la solubilidad del fármaco. En primer lugar, la emulsión simple (W/O) adecuada en el caso de los activos liposolubles. Tanto el polímero como el fármaco se disuelven en disolventes orgánicos volátiles, y se forma una emulsión con una fase acuosa que contiene los tensioactivos, para posteriormente eliminar el solvente orgánico mediante su evaporación. En el caso de fármacos hidrosolubles, el método de la doble emulsión ($W_1/O/W_2$) posee una modificación con respecto al método simple, requiriendo un aporte extra de energía para la formación del sistema. En este caso, el fármaco se disuelve en la fase acuosa interna (W_1) y se emulsiona en primer lugar con la fase oleosa que contiene el polímero disuelto. Esta primera emulsión se emulsiona nuevamente con una segunda fase acuosa (W_2) que contiene el tensioactivo, para finalmente evaporar el disolvente orgánico mediante agitación, obteniendo así una suspensión de NPs.

- Emulsificación / Difusión del disolvente

Este método consiste, en primer lugar, en la formación de una emulsión O/W entre un disolvente parcialmente miscible en agua que contiene el polímero y el fármaco y una solución acuosa que contiene el tensioactivo (Leroux et al., 1995). El solvente orgánico y el agua se encuentran saturados y equilibrio termodinámico. Posteriormente se diluye con una gran cantidad de agua la emulsión previamente formada, lo que induce la difusión del disolvente desde las gotas dispersas hacia la fase externa, dando como resultado la formación de las partículas coloidales.

- Emulsificación / Salting-out

Esta técnica consiste en la separación de un disolvente miscible en agua de una solución acuosa a través del efecto de *salting-out*. Tanto el fármaco como el polímero se disuelven en un disolvente miscible en agua, como podría ser acetona. La fase acuosa contiene el agente de salificación y el surfactante, el agente de salificación puede ser electrolitos como $MgCl_2$, $CaCl_2$ y $Mg(CH_3COO)_2$, o no electrolitos como la sacarosa. La emulsificación se logra de manera espontánea debida al efecto Ouzo, sin emplear fuerzas de alto cizallamiento. La miscibilidad de la acetona y el agua se reduce al saturar la fase acuosa, lo que permite la formación de una emulsión O/W a partir de las fases miscibles. Se obtiene el efecto *salting-out* mediante adición de un exceso de agua a la emulsión formada previamente, para promover la difusión del solvente orgánico en la fase acuosa, lo que lleva a la precipitación del polímero disuelto en las nanogotas de la emulsión y, por consiguiente, a la formación de las NPs (Pinto Reis et al., 2006).

- Nanoprecipitación

Denominada también técnica de “desplazamiento del solvente” (Fessi et al., 1989). En esta técnica el polímero se disuelve en un solvente orgánico semipolar y esta disolución se añade a una solución acuosa, en agitación constante, gota a gota o mediante una tasa de adición controlada. Debido a la rápida difusión espontánea de la solución de polímero en la fase acuosa, las NPs se forman instantáneamente en un intento de evitar el contacto con las moléculas de agua. Durante este proceso se produce una disminución de la tensión interfacial que aumenta el área superficial debido a la rápida difusión y conduce a la formación de pequeñas gotas de solvente orgánico. A medida que el solvente difunde desde las nanogotas, el polímero precipita y da lugar a la formación de las NPs.

- Diálisis

En esta técnica el polímero se encuentra disuelto en la fase orgánica y dentro de un tubo de diálisis, o membrana semipermeable, que presenta un tamaño de poro conforme al peso molecular del polímero. El disolvente orgánico es semipolar y el desplazamiento del agua a través de la membrana conlleva la agregación progresiva del polímero debido a su insolubilidad, dando lugar a la formación de suspensiones homogéneas de NPs (Jeon et al., 2000).

- Fluidos supercríticos

Es el método más novedoso y utiliza fluidos supercríticos y/o gases de alta densidad (Ej. CO_2) en lugar de disolventes orgánicos con el objetivo de disminuir el impacto medioambiental (Sanli et al., 2012).

En la Tabla 6 se presentan algunas formulaciones basadas en NPs de PLGA conteniendo diferentes fármacos, actualmente comercializadas.

Tabla 6. Tratamientos oculares basados en NPs de PLGA comercializados y su año de aprobación por la FDA de los últimos 20 años (Ghitman et al., 2020).

Producto	Nanoformulación	Indicación	Estado
Arestin®	Microesfera PLGA de clorhidrato de minociclina	Coadyuvante en la periodontitis del adulto	Aprobado 2001
Eligard®	PLGA - *N* -metil-2-pirolidona de acetato de leuprolida	Cáncer de próstata	Aprobado 2002
Risperdal Consta®	Microesfera PLGA de risperidona	Esquizofrenia y trastorno bipolar I	Aprobado 2003
Vivitrol®	Microesfera PLGA de naltrexona	Antagonista de opioides	Aprobado 2006
Ozurdex®	Microesfera PLGA de dexametasona	Corticosteroide	Aprobado 2009
Bydureon®	Microesfera PLGA de exenatida sintética	Diabetes tipo II	Aprobado 2012
Signifor Lar®	Microesfera PLGA de pamoato de pasireotida	Acromegalia	Aprobado 2014
Zilretta®	Microesfera PLGA de triamcinolona	Osteoartritis y terapia con corticosteroides	Aprobado 2017
Bydureon Bcise®	Microesfera PLGA de exenatida	Diabetes tipo II	Aprobado 2017
Kit Triptodur®	Microesfera PLGA de pamoato de triptorelina	Pubertad precoz	Aprobado 2017

1.4.2 Liposomas

Los liposomas fueron descubiertos por primera vez en la década de 1960 por el hematólogo británico Dr. Alec D. Bangham y colaboradores en el Instituto Babraham de la Universidad de Cambridge, y en 1964 se publicó el primer informe (Bangham and Horne, 1964). Estos sistemas se definen como una estructura esférica coloidal formada por el autoensamblaje de moléculas lipídicas anfifílicas en solución (Guimarães et al., 2021). Por lo tanto, se trata de vesículas de naturaleza lipídica conformadas por una o varias bicapas de fosfolípidos y un núcleo hidrofílico. Debido a su tamaño, su carácter anfipático y su biocompatibilidad, los liposomas han sido usados durante años como transportadores para la liberación de biomoléculas y como modelos biológicos para el estudio de biomembranas. Esta estructura organizada ofrece a los liposomas la capacidad de encapsular tanto sustancias hidrófilas, en su interior acuoso, como lipófilas, incluidas en la/s membrana/s lipídicas (Javier López-Cano et al., 2021).

Los liposomas se han usado durante décadas para encapsular un amplio número de agentes bioactivos, entre los cuales se incluyen fármacos anticancerígenos, antibióticos, material genético, proteínas, DNA, péptidos, vacunas o enzimas, entre otros. El activo cargado en el liposoma se encuentra protegido frente a los diversos eventos fisiológicos, como la degradación enzimática, la inactivación química e inmunológica o el rápido aclaramiento plasmático o el drenaje nasolacrimal, lo que contribuye a optimizar y prolongar su acción farmacológica. Además, la encapsulación minimizaría los efectos adversos de ciertos fármacos, tanto por la reducción

de su exposición a tejido sano, como por su direccionamiento al tejido diana (Antimisiaris et al., 2021; Guimarães et al., 2021; Souto et al., 2019) .

Los compuestos principales de los liposomas son los fosfolípidos y el colesterol, lo cuales también son los componentes básicos de las membranas biológicas. Los fosfolípidos son lípidos anfifílicos compuestos por una molécula de glicerol unida a un grupo fosfato y a dos cadenas de ácidos grasos que pueden ser saturadas o insaturadas. Este grupo fosfato, a su vez, también puede estar unido a otra molécula orgánica. Según este grupo orgánico, los fosfolípidos de procedencia natural se clasifican en ácido fosfatídico (PA), fosfatidilcolina (PC), fosfatidiletanolamina (PE), fosfatidilinositol (PI), fosfatidilglicerol (PG) y fosfatidilserina (PD). Los fosfolípidos pueden ser naturales o sintéticos dependiendo de su obtención. Los naturales utilizados con más frecuencia son PC y PE. Las fuentes de extracción de fosfolípidos naturales principales son la yema de huevo y la soja. Otro tipo de fosfolípidos se puede producir, de manera sintética, a partir de lípidos naturales por modificación de grupos funcionales, cadenas alifáticas o alcoholes dando lugar a una gran variedad de fosfolípidos sintéticos que presentan alta estabilidad (Guimarães et al., 2021).

En cuanto a la administración ocular por vía tópica, uno de los fosfolípidos más empleados hasta el momento ha sido la PC procedente de la soja, debido a su baja inmunorreactividad y sus beneficios en la regeneración corneal. Además de ser el fosfolípido presente en las membranas celulares más común, posee un perfil rico y extenso de ácidos grasos, como el palmítico (C16: 0), esteárico (C18:0), oleico (C18:1), linoleico (C18:2) y linolénico (C18:3). Algunos de ellos son insaturados,

por lo que podrían proporcionar un efecto antioxidante en la superficie ocular (Thomas et al., 2016).

El colesterol es otro componente esencial en la formulación de los liposomas. Se ha descrito como un estabilizador de las fuerzas intermoleculares entre los fosfolípidos de la bicapa mejorando la estabilidad y evitando su dispersión, además modula la fluidez de la membrana y favorece la retención de activos encapsulados disminuyendo su permeación (Javier López-Cano et al., 2021).

Estos sistemas clasifican según su tamaño y número de bicapas lipídicas o lamelaridad. De este modo, se pueden categorizar como vesículas pequeñas unilamelares (SUV, por sus siglas en inglés) (10 nm -100 nm), grandes unilamelares (LUV) (>100 nm), gigantes unilamelares (GUV) (>1μm), vesículas multilamelares (MLV) si poseen más de una bicapa concéntrica y un diámetro promedio de partícula superior a 300 nm y sistemas multivesiculares (MVV), que poseen una estructura multicompartimental donde una bicapa de mayor tamaño engloba diversas vesículas independientes en su interior (Souto et al., 2019) (Figura 9). Los sistemas unilamelares pequeños y grandes suelen ser utilizados para la incorporación de moléculas hidrófilas en su interior acuoso, mientras que los sistemas multivesiculares se presentan como una buena opción para incorporar moléculas hidrófobas debido a su mayor región lipídica presente en las numerosas bicapas. Las vesículas gigantes unilamelares, han sido ampliamente utilizadas como modelos de membranas biológicas debido a su mayor tamaño, que permite su visualización mediante microscopia óptica y la macromanipulación de vesículas individuales (Has and Sunthar, 2020).

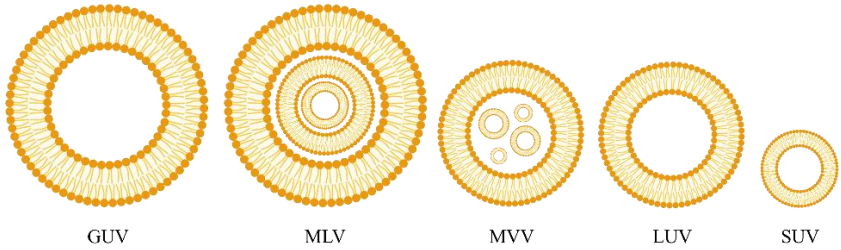

Figura 9. Clasificación de los liposomas en función de su tamaño y lamelaridad (adaptación de (Souto et al., 2019)).

Existe una gran variedad de técnicas para la fabricación de liposomas, incluyendo los propios métodos de formulación liposomal y los métodos de reducción de tamaño. Los diferentes procedimientos influyen en las propiedades finales de la formulación, a nivel fisicoquímico, tamaño y lamelaridad de los liposomas, así como en la eficiencia de encapsulación de activos. Por lo general, todos los métodos de preparación incluyen 4 pasos básicos comunes. Estos incluyen lípidos disueltos en solventes orgánicos, la eliminación del solvente orgánico, la purificación y aislamiento de los liposomas resultantes y el análisis fisicoquímico del producto final. A continuación, se explican brevemente los principales mecanismos de producción de liposomas (Guimarães et al., 2021; Has and Sunthar, 2020; Javier López-Cano et al., 2021).

- Rehidratación de la película lipídica

Es uno de los métodos más utilizados, y el primer método descrito por Bangham et al, donde se disuelve una mezcla de lípidos en un solvente orgánico para posteriormente evaporarse al vacío y dar lugar a la película lipídica seca, la cual se rehidrata en una solución tampón formando estas estructuras multicapa denominadas liposomas (Bangham et al., 1967).

Normalmente estos tipos de métodos tienen a producir MLV, por lo que se requiere de un método posterior complementario como la extrusión, ciclos de congelación-descongelación o sonicación para homogeneizar los tamaños y estabilizar la dispersión (Javier López-Cano et al., 2021).

- Evaporación de fase inversa

La técnica de evaporación de fase inversa consiste en la formación de un sistema de dos fases compuesto por micelas invertidas en una fase acuosa o una emulsión de agua en aceite (W/O), y una fase orgánica como cloroformo, etanol, metanol o una combinación de ellos. Inicialmente se forma la película lipídica en el evaporador rotatorio, se agrega un solvente orgánico y un tampón. Luego, el disolvente orgánico se elimina de nuevo mediante el rotavapor. Finalmente, la muestra liposomal puede someterse a otros procesos como sonicación, extrusión o congelación-descongelación para obtener la dispersión liposomal deseada. Actualmente, la tecnología de fluidos supercríticos ha optimizado el procedimiento de esta técnica. En este caso, el fluido supercrítico disuelve la película lipídica y mientras se agrega el tampón acuoso, el solvente se elimina por completo. Debido a que es un solvente económico e inocuo para el medio ambiente, el CO_2 supercrítico es el fluido de elección para llevar a cabo esta técnica (Pattni et al., 2015).

- Inyección de éter y etanol

La inyección de éter se utiliza para conseguir suspensiones de SUV únicas y homogéneas con un tamaño promedio de partícula de 100 a 300 nm. Este método consiste en preparar una solución lipídica en éter, éter dietílico o etanol y posteriormente añadirla lentamente a una solución acuosa o tampón donde se formará la dispersión liposomal (Guimarães et al., 2021).

- Eliminación de detergente

En este método, los fosfolípidos se solubilizan con detergentes en concentraciones críticas micelares. Tras la eliminación del detergente, mediante cromatografía en columna o diálisis, y la adición de un medio acuoso adecuado, las moléculas de fosfolípidos se autoensamblan para dar lugar a los liposomas (Pattni et al., 2015).

- Método de deshidratación- rehidratación

Este método tiene como objetivo desarrollar nuevos liposomas mediante la fusión de liposomas ya fabricados. Utiliza deshidratación y rehidratación controlada para obtener MLV y SUV, mediante centrifugación, liofilización y rehidratación lenta y controlada. Con esta técnica se podrían atrapar moléculas grandes como el ADN logrando altos índices de carga (Kirby and Gregoriadis, 1984).

- Método de congelación-descongelación

La congelación-descongelación es una técnica ampliamente utilizada para aumentar la eficiencia de encapsulación de activo en MLV. Este proceso ocurre porque en cada paso de congelación y descongelación, los MLV se destruyen y se vuelven a ensamblar, reduciendo el número de bicapas en cada ciclo (Li and Deng, 2004).

- Sonicación

Los ultrasonidos también se utilizan para homogeneizar y reducir el tamaño de las MLV para formar SUV. Las altas presiones creadas por los ultrasonidos rompen bruscamente los liposomas que se vuelven a ensamblar

espontáneamente en otros de tamaño más reducido, formando las SUV (Szoka and Papahadjopoulos, 1980).

- Homogenización a alta presión

En las técnicas de homogeneización los liposomas son forzados a pasar a través de un orificio a alta presión para reducir su tamaño, dando como resultado un concepto de colisión por alta velocidad (Brandl et al., 1990).

- Microfluidos

La microfluídica es la tecnología que tiene como objeto manipular los fluidos, como mezclas de lípidos y soluciones acuosas, a escala micro o nano. Esta técnica permite monitorizar cada parámetro para ser capaz de controlar y ajustar el tamaño medio de partícula, índice de polidispersión o lamelaridad (Kuribayashi et al., 2006).

Además, el mecanismo mediante el cual el principio activo es encapsulado en los liposomas puede llevarse a cabo de manera pasiva o activa. El método de carga pasiva del activo consiste en la incorporación del agente durante el proceso de fabricación. Los fármacos hidrófilos se situarán dispersos en la fase acuosa (dentro y fuera de los liposomas), mientras que los fármacos hidrófobos se quedarán atrapados en la membrana. Por el contrario, los métodos basados en la carga activa, también denominada carga remota, consisten en la introducción del agente activo después de la formación completa de la vesícula. Implica la creación de un gradiente iónico o de pH transmembrana que impulsa de manera eficiente el activo, solubilizado en el medio acuosos externo, a través de la bicapa lipídica, hacia el interior del liposoma.

Los liposomas se consideran sistemas adecuados para la administración ocular de activos debido a su alta biocompatibilidad y baja toxicidad, dado que poseen estructura y composición similar a la membrana celular y a su adecuada eficiencia para encapsular fármacos hidrófilos o lipófilos y administrarlos eficazmente en ambos segmentos oculares.

En relación con el segmento anterior del ojo, una estrategia capaz de aumentar el tiempo de residencia en los tejidos precorneales consiste en la utilización de lípidos con carga positiva o el recubrimiento de estos con polímeros con propiedades mucoadhesivas. Estos liposomas de naturaleza catiónica exhiben mayor capacidad para administrar activos en los tejidos oculares con respecto a los liposomas con carga neutra o negativa, como consecuencia de su interacción electrostática con las cargas negativas de superficie de la córnea (Souto et al., 2019).

Además, los liposomas pueden penetrar a través de la superficie ocular por varios mecanismos biológicos como la fusión con las membranas celulares, la adsorción, la endocitosis y el intercambio de lípidos (Lalu et al., 2017; Sánchez-lópez et al., 2017). Por lo general provocan una cinética de orden cero del patrón de liberación del activo con una liberación inicial rápida característica acompañada de una liberación sostenida en el tiempo. Asimismo, la superficie de los liposomas se puede modificar o funcionalizar con la adición de diferentes estructuras moleculares o ligandos específicos que mejoran sus características como sistema de administración de fármacos, lo que da lugar a una nueva categoría de liposomas denominada liposomas dirigidos o funcionalizados. Existen diferentes estrategias como la incorporación de tensioactivos, el recubrimiento polimérico, por ejemplo,

de polietilenglicol (PEG), mediante el cual se consigue una mejora en la biodisponibilidad además de carga superficial positiva, y al mismo tiempo, en la superficie de la bicapa lipídica puede incorporarse un amplio número de moléculas como pueden ser carbohidratos, péptidos, proteínas, anticuerpos o sus fragmentos, o aptámeros, mediante los cuales se consigue el direccionamiento de los nanosistemas al lugar de acción (Riaz et al., 2018).

En la actualidad, se está estudiando una amplia gama de formulaciones farmacéuticas que utilizan liposomas, sin embargo, solo un número restringido se envía a ensayos clínicos y preclínicos y un número aún más escaso está disponible comercialmente (Tabla 7) (Souto et al., 2019).

Tabla 7. Productos comercializados que contienen liposomas (adaptación de (Antimisiaris et al., 2021)).

Producto	Adm. / Activo	Indicación	Compañía
Arikayce®	Inhalación (con nebulizador) / amikacina	Infección pulmonar por complejo *Mycobacterium avium* (MAC)	Insmed Netherlands BV (estado de medicamento huérfano)
Estrasorb®	Emulsión tópica / Estradiol hemihidrato USP	Sofocos menopáusicos;	Novavax
Exparel®	iv e infiltraciones locales / bupivacaína	Analgesia regional posquirúrgica	Pacira pharmaceuticals, Inc
Alveofacto®	Intratraqueal / Bovactant	Síndrome de dificultad respiratoria (SDR)	Boehringer Ingelheim GmbH
Lipotalon®	Intraarticular / Dexametasona 21-palmitato	Trastornos reumáticos	Merckle Recordati GmbH
Arikayce®	Inhalación (con nebulizador) / amikacina)	Infección pulmonar por complejo *Mycobacterium avium* (MAC)	Insmed Netherlands BV (estado de medicamento huérfano)

1.5 Liofilización de nanosistemas

La mayoría de las nanopartículas se fabrican en solución acuosa, lo que provoca tanto inestabilidad química como física. Según la naturaleza de la NP y su carga superficial, esta puede sufrir diferentes procesos químicos durante su almacenamiento en medio acuoso, entre los que se incluyen la oxidación, la hidrólisis, la desamidación, el pardeamiento y/o la formación/intercambio de enlaces disulfuro. Mientras que la inestabilidad física hace que las NPs se vean sometidas, frecuentemente, a fenómenos de agregación y fusión de partículas, especialmente cuando son almacenadas durante periodos de tiempo prolongados (Fonte et al., 2016). La estabilización electrostática, descrita en la teoría de Derjaguin-Landau-Verwey-Overbeek (DLVO), puede contrarrestar esta inestabilidad física, pero solo es aplicable en el caso de sistemas coloidales con carga superficial elevada (Trenkenschuh and Friess, 2021).

La acción del solvente acuoso sobre la matriz polimérica o lipídica puede dar lugar a su degradación, lo que provocaría la fuga del activo encapsulado, modificando su biodistribución *in vivo* y sus propiedades farmacocinéticas, así como su liberación sostenida. Además de la formación de productos de degradación no deseados que puedan llegar a ser tóxicos para el organismo (Fonte et al., 2016; Hussain et al., 2020). Al mismo tiempo, la presencia de agua promueve el desarrollo y crecimiento de microorganismos en este tipo de suspensiones coloidales, por lo que lo más conveniente es trabajar bajo condiciones de esterilidad. Además, la esterilidad es un requerimiento para la administración oftálmica (Kaur and Kanwar, 2002).

La transformación de estas suspensiones a estado sólido, mediante la eliminación del agua, se presenta como una alternativa para evitar estos inconvenientes. Existen diferentes métodos para llevar a cabo este proceso de secado, entre los cuales destacan la liofilización (*freeze-drying)*, el secado por aspersión (*spray-drying*) y el secado por aspersión a temperatura reducida (*spray-freeze-drying*). Sus principales características se recogen en la Tabla 8. (Degobert and Aydin, 2021; Kawasaki et al., 2019).

En este trabajo, dada sus numerosas ventajas y su aptitud para llevar a cabo el proceso de escalado a nivel industrial, la liofilización fue el método seleccionado para eliminar el componente acuoso de los nanosistemas (recogido en Anexo-Patente).

La liofilización es un proceso de deshidratación que se lleva a cabo con el objetivo de mejorar la estabilidad de la nanosuspensión, aumentando su vida útil y, a la vez, facilitando su manipulación y almacenamiento. Consiste, simplificadamente, en congelar la muestra y eliminar el disolvente mediante su sublimación al vacío.

Tabla 8. Ventajas y limitaciones de los diferentes procesos de secado (Degobert and Aydin, 2021).

Procedimiento de secado	Ventajas	Inconvenientes
Liofilización (*freeze drying*)	▪ Baja temperatura, apta para productos termolábiles ▪ Cierre de viales bajo gas inerte apto para productos sensibles al oxígeno ▪ Dosificación precisa ▪ Tiempo de reconstitución corto debido a la alta porosidad ▪ Contenido de humedad controlado ▪ Proceso estéril	▪ Largo tiempo de procesamiento ▪ Configuración costosa ▪ Proceso complejo ▪ Costo de mantenimiento ▪ Exposición a la interfaz hielo-agua
Spray drying	▪ Proceso de secado rápido ▪ Bajo costo ▪ Buena fluidez de los polvos obtenidos ▪ Polvo aerosolizable	▪ Rendimiento (50–70%) ▪ No apto para productos termolábiles ▪ No apto para productos sensibles al oxígeno
Spray freeze drying	▪ Congelación rápida ▪ Alto rendimiento ▪ Buena fluidez de los polvos obtenidos ▪ Polvo aerosolizable	▪ Largo tiempo de procesamiento ▪ Alto costo ▪ Partículas frágiles ▪ Proceso complejo ▪ Requiere nitrógeno líquido

El proceso de liofilización se puede dividir en tres etapas: congelación (solidificación), secado primario (sublimación del hielo) y secado secundario (desorción de agua no congelable) (Figura 10).

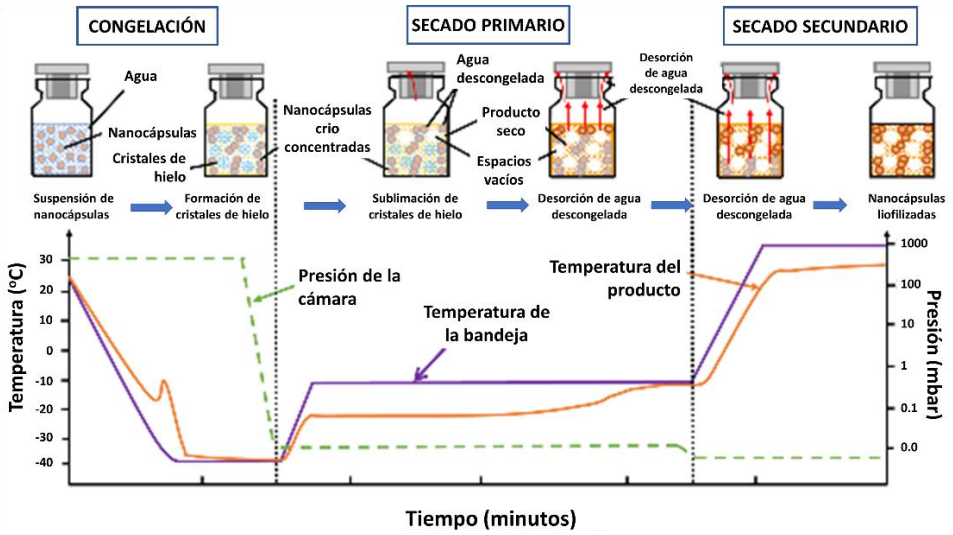

Figura 10. Etapas del proceso de liofilización, evolución de los parámetros del proceso y el estado correspondiente del producto a liofilizar (Degobert and Aydin, 2021).

La **primera etapa** del proceso es la **congelación** y ocurre a presión atmosférica. Durante esta etapa, la preparación se enfría y comienza la nucleación o formación de cristales. Durante el proceso de congelación, las moléculas de agua contenidas en la preparación cristalizan y empiezan a formar hielo. Esto conduce a un aumento de la concentración de solutos y, por consiguiente, a un aumento de la viscosidad, que alcanza valores de 10^{11} a 10^{12} Pa·s. Este líquido altamente concentrado y viscoso se solidifica e inhibe la posterior cristalización del hielo. La preparación, en este momento, se divide en una fase cristalina, constituida por el hielo y una fase amorfa que contiene los solutos. La temperatura a la ocurre este proceso se denomina temperatura de transición vítrea del soluto crioconcentrado (T_g'). La velocidad de enfriamiento y su duración influyen en el tamaño de partícula e índice de polidispersión tras su posterior reconstitución. Si la etapa de congelación se lleva a cabo a velocidad alta, se produciría la

formación de un gran número de cristales de hielo pequeño, lo que aumentaría la porosidad de la matriz y, por lo tanto, el tiempo de secado se vería reducido, sin embargo, también favorecería la agregación de las nanopartículas presentes, siendo este un paso crítico en el proceso (Degobert and Aydin, 2021).

La **segunda etapa** consiste en el **secado primario**. Esta etapa involucra la sublimación del hielo y ocurre a presión reducida. Durante este proceso, se transfiere calor desde la bandeja del liofilizador a la solución congelada. El hielo se sublima y el vapor de agua formado pasa a través de la porción seca del producto (el secado comienza desde la parte superior hasta el fondo del vial). Al final de la etapa de sublimación se forma un tapón poroso. Los poros corresponden a los espacios que fueron ocupados por cristales de hielo (Trenkenschuh and Friess, 2021).

Durante esta etapa, se debe controlar la temperatura del producto y mantenerlo en un margen seguro, de 2 a 5 °C por debajo de su temperatura de transición vítrea, especialmente en el caso de biomoléculas o fármacos inestables (Kawasaki et al., 2019). Esto es debido al paso de estado vítreo a estado líquido sobreenfriado, que ocurre cuando el producto se somete a temperaturas superiores a la T_g', da lugar a materiales con consistencia viscosa, debido a la flexibilidad parcial de sus moléculas, lo que le confiere una mayor susceptibilidad a cambios físicos y químicos.

La **tercera etapa** se denomina **secado secundario** e implica la eliminación, por evaporación, del agua adsorbida en el producto, también llamada humedad residual. Se trata de la porción de agua que no se congeló durante la primera etapa. Este proceso requiere más energía que el anterior,

por lo que implica trabajar a presión baja y temperatura más elevada. Para mantener el producto en su estado vítreo, en esta etapa, la temperatura tampoco debe sobrepasar su temperatura de transición vítrea del producto seco (T_g) (Kawasaki et al., 2019; Parra et al., 2015; Trenkenschuh and Friess, 2021).

Tras la liofilización, la formulación debe permanecer protegida del medio y, a nivel industrial, el vial se sella mediante un mecanismo de cierre hidráulico o de tornillo que posee el liofilizador, que presiona el tapón hacia el interior del recipiente. Tras el proceso de tapado de los envases, el producto puede retirarse con seguridad del liofilizador y el tapón puede reforzarse con una banda metálica para proporcionar un sellado permanente al producto (Przic et al., 2004).

2.

HIPÓTESIS - OBJETIVOS

La hipótesis de la presente tesis doctoral se basa en la propuesta de dos sistemas de liberación controlada de fármacos, conteniendo Lactoferrina, como alternativa para el tratamiento eficaz del síndrome del ojo seco y otras enfermedades inflamatorias oculares. La evidencia científica sugiere que la administración ocular de LF, encapsulada en nanosistemas de naturaleza polimérica o lipídica, biocompatibles, podría solventar los problemas de estabilidad y biodisponibilidad de la proteína, así como optimizar su eficacia en el tratamiento de dichas patologías.

El objetivo principal se centra en el desarrollo y caracterización de dos sistemas nanoestructurados, incluyendo un sistema de naturaleza polimérica (nanopartículas/nanoesferas) y uno de naturaleza lipídica (liposomas), ambos conteniendo LF, así como la evaluación del comportamiento biofarmacéutico, el perfil toxicológico y la eficacia terapéutica.

Objetivos Específicos

- Desarrollar y optimizar dos sistemas nanoestructurados conteniendo bLF: nanopartículas poliméricas (bLF-NPs) y liposomas con recubrimiento de ácido hialurónico (bLF-LIP).
- Determinar las características fisicoquímicas y la estabilidad de los sistemas optimizados a diferentes temperaturas de almacenamiento.
- Estudiar el comportamiento biofarmacéutico y demostrar que ambos sistemas presentan un perfil de liberación prolongado del activo.
- Estudiar los efectos de la esterilización mediante radiación ionizante en los sistemas.

HIPÓTESIS - OBJETIVOS

- Evaluar la internalización celular de los sistemas poliméricos mediante microscopía confocal.
- Evaluar el efecto citotóxico *in vitro* producido por los nanosistemas en células córneales (cultivo celular) y la tolerancia ocular mediante técnicas *in vitro* (HET-CAM) e *in vivo* (Test de Draize).
- Evaluar la eficacia anti-inflamatoria *in vitro* (determinación de citoquinas) e *in vivo* (estimulación con lipopolisacárido) de ambos sistemas.
- Estudiar la eficacia terapéutica *in vivo* en el ojo seco inducido en un modelo de conejo (Test de Schirmer).

3.

RESULTADOS

RESULTADOS

El desarrollo de la presente investigación dio lugar a dos publicaciones en forma de artículos científicos y una patente.

3.1. Development of topical eye-drops of lactoferrin-loaded biodegradable nanoparticles for the treatment of anterior segment inflammatory processes.

3.2. Development of Lactoferrin-Loaded Liposomes for the Management of Dry Eye Disease and Ocular Inflammation.

ANEXO. Liposomes for the treatment of ocular diseases.

3.1. Development of topical eye-drops of lactoferrin-loaded biodegradable nanoparticles for the treatment of anterior segment inflammatory processes.

Ana López-Machado, Natalia Díaz, Amanda Cano, Marta Espina, Josefa Badía, Laura Baldomà, Ana Cristina Calpena, Martina Biancardi, Eliana B. Souto, María Luisa García, Elena Sánchez-López.

International Journal of Pharmaceutics

Año: 2021

ISSN: 10.1016/j.ijpharm.2021.121188

Factor de impacto: 6,510

Resumen Gráfico

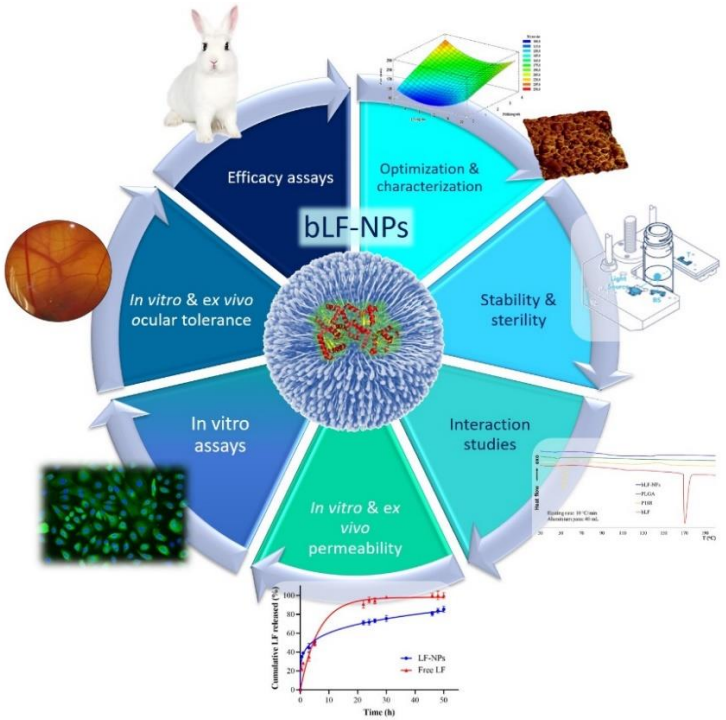

International Journal of Pharmaceutics 609 (2021) 121188

Contents lists available at ScienceDirect

International Journal of Pharmaceutics

journal homepage: www.elsevier.com/locate/ijpharm

Development of topical eye-drops of lactoferrin-loaded biodegradable nanoparticles for the treatment of anterior segment inflammatory processes

Ana López-Machado [a, b], Natalia Díaz [c, d, e], Amanda Cano [a, b, f], Marta Espina [a, b], Josefa Badía [c, d, e], Laura Baldomà [c, d, e], Ana Cristina Calpena [a, b], Martina Biancardi [g], Eliana B. Souto [h, i], María Luisa García [a, b, f, *, 1], Elena Sánchez-López [a, b, d, *, 1]

[a] Department of Pharmacy, Pharmaceutical Technology and Physical Chemistry, Faculty of Pharmacy and Food Sciences, University of Barcelona, Barcelona, Spain
[b] Institute of Nanoscience and Nanotechnology (IN2UB), University of Barcelona, Barcelona, Spain
[c] Department of Biochemistry & Physiology, Faculty of Pharmacy & Food Sciences, University of Barcelona, Barcelona, Spain
[d] Institute of Biomedicine, University of Barcelona (IBUB), Barcelona, Spain
[e] Institut de Recerca Sant Joan de Deu (IRSJD), Barcelona, Spain
[f] Biomedical Research Networking Centre in Neurodegenerative Diseases (CIBERNED), Madrid, Spain
[g] Technology Dedicated to Care, Barcelona, Spain
[h] Department of Pharmaceutical Technology, Faculty of Pharmacy, University of Coimbra, Portugal
[i] CEB—Centre of Biological Engineering, Campus de Gualtar, University of Minho, 4710-057 Braga, Portugal

ARTICLE INFO

Keywords:
Lactoferrin
Nanoparticles
PLGA
Ocular anti-inflammatory
Drug delivery
Cytotoxicity

ABSTRACT

Ocular inflammation is one of the most common comorbidities associated to ophthalmic surgeries and disorders. Since conventional topical ophthalmic treatments present disadvantages such as low bioavailability and relevant side effects, natural alternatives constitute an unmet medical need. In this sense, lactoferrin, a high molecular weight protein, is a promising alternative against inflammation. However, lactoferrin aqueous instability and high nasolacrimal duct drainage compromises its potential effectiveness. Moreover, nanotechnology has led to an improvement in the administration of active compounds with compromised biopharmaceutical profiles. Here, we incorporate lactoferrin into biodegradable polymeric nanoparticles and optimized the formulation using the design of experiments approach. A monodisperse nanoparticles population was obtained with an average size around 130 nm and positive surface charge. Pharmacokinetic and pharmacodynamic behaviour were improved by the nanoparticles showing a prolonged lactoferrin release profile. Lactoferrin nanoparticles were non-cytotoxic and non-irritant neither *in vitro* nor *in vivo*. Moreover, nanoparticles exhibited significantly increased anti-inflammatory efficacy in cell culture and preclinical assays. In conclusion, lactoferrin loaded nanoparticles constitute a safe and novel nanotechnological tool suitable for the treatment of ocular inflammation.

1. Introduction

Ocular inflammation constitutes one of the most common consequences associated to ophthalmic disorders and it is associated to a wide range of pathologies (Mazet et al., 2020). It is a non-specific response to an external insult that includes different molecular and functional mediators, involving recruitment and activation of inflammatory cells and release of inflammatory mediators, such as cytokines, interleukins, prostaglandins and enzymes (Anfuso et al., 2017).

Regarding the anterior segment of the eye, a wide range of ocular

Abbreviations: AFM, Atomic force microscopy; NSAIDs, Anti-inflammatory drugs; Z_{av}, Average particle size; bLF, Bovine LF; DSC, Differential scanning calorimetry; EE, Encapsulation efficiency; FTIR, Fourier transform infrared; GRAS, Generally recognized as safe substance; HCE-2, Human corneal epithelial cells; IL-8, Interleukin 8; P188, Kolliphor P188®; LF, Lactoferrin; LPS, Lipopolysaccharide; NPs, Nanoparticles; NF-κB, Nuclear transcription factor kappa B; PLGA, Poly (lactic-co-glycolic acid); PI, Polydispersity index; ROS, Reactive oxygen species; Rho, Rhodamine 110; SA, Sodium arachidonate; MTT, Tetrazolium bromide; TEM, Transmission electron microscopy; TFA, Trifluoroacetic acid; TNF-α, Tumour necrosis factor α; ZP, Zeta potential.

* Corresponding authors at: Department of Pharmacy, Pharmaceutical Technology and Physical Chemistry, Faculty of Pharmacy and Food Sciences, University of Barcelona, Barcelona, Spain.
E-mail addresses: marisagarcia@ub.edu (M.L. García), esanchezlopez@ub.edu (E. S´anchez-Lo´pez).
[1] Both have equally contributed.

https://doi.org/10.1016/j.ijpharm.2021.121188
Received 23 June 2021; Received in revised form 30 September 2021; Accepted 11 October 2021
Available online 14 October 2021

pathologies are tightly associated with ocular inflammation including dry eye disease or keratoconjunctivitis *sicca* (Chen et al., 2019), microbial or viral infection (Pearlman et al., 2013), post-operative inflammation, seasonal allergic conjunctivitis, blepharitis (Tamhane et al., 2019), or uveitis related to patients with psoriatic arthritis (Abbouda et al., 2017; Foster et al., 2016).

In this area, topical administration is the most suitable route for ocular treatments due to its ease of handling, non-invasiveness, and effectiveness avoiding systemic side effects associated with oral administration (Mazet et al., 2020).

Current treatment for ocular inflammation consists mainly on the administration of corticosteroids and non-steroidal anti-inflammatory drugs (NSAIDs), in monotherapy or in combination. Nonetheless, its prolonged use include severe adverse events (Caplan et al., 2017; Carnahan and Goldstein, 2000; Foster et al., 2016).

To address these issues, the research for alternatives in the treatment of ocular inflammation is crucial. Therefore, recently, lactoferrin (LF) is an iron-binding glycoprotein that modulates the innate and adaptive reactions of the immunological system. This protein is associated to anti-inflammatory effects as well as antibacterial, antifungal, antiviral, antiparasitic and immunomodulatory properties. Moreover, it has been investigated due to its multifunctional capacities to combat several ocular diseases (Gonz´alez-cha´vez et al., 2009; Kanyshkova et al., 2001; Lee et al., 2020; Wang et al., 2017).

LF three-dimensional structure reveals a protein folded into two highly homologous lobes with iron-binding capacity. Each of these lobes can bind a ferric ion stably and reversibly, with the simultaneous binding of a bicarbonate anion. LF is secreted by neutrophils and exocrine glands. Colostrum and milk present the highest levels of this glycoprotein, but it is also detected in fluids such as tears, saliva, or gastrointestinal secretions (Tamhane et al., 2019). During infection or inflammation processes it has been observed that LF concentration increases due to neutrophil recruitment (Ward et al., 2005). Specifically, at ocular level, LF is one of the most abundant proteins in the tear fluid, comprising around 20–30 % in basal and reflex tears (Hanstock et al., 2019). Moreover, LF is presented in vitreous humour and different ocular tissues, such as cornea, iris and retinal pigment epithelium (Rageh et al., 2016).

Human and bovine LF possess similar functions due to their high sequence homology (Rosa et al., 2017). Therefore, most of the *in vitro* and *in vivo* studies have been carried out employing bovine LF (bLF), generally recognized as safe substance (GRAS) by the Food and Drug Administration (FDA) and the European Food Safety Authority (EFSA) (European Food Safety Authority, 2012; Rosa et al., 2017). bLF has a powerful anti-inflammatory activity (Håversen et al., 2002). It is internalized from the apical side of the host cells and located in the nucleus, being N-lobe the responsible for the union, internalization and orientation (Suzuki et al., 2009). Thus, it has the capacity of modulating the inflammatory response in corneal epithelial cells attenuating the nuclear transcription factor kappa B (NF-κB)-induced transcription of genes for various inflammatory mediators (Gu and Wu, 2016; Rosa et al., 2017).

In addition, the generation of reactive oxygen species (ROS) is also involved in the inflammation process. It has been described that free iron is responsible for potentiating redox reactions, as it can easily accept or donate electrons that contribute to the formation of ROS (Kanwar et al., 2015). Therefore, eliminating free iron and inhibiting redox activities through chelation is a potentially useful therapeutic strategy to treat inflammatory ocular diseases (Chen et al., 2017).

Nonetheless, bLF presents some instability in aqueous solution (Wang et al., 2019). In addition, hydrophilic substances administered as eye drops are rapidly eliminated via conjunctiva and nasolacrimal duct. It results in a pre-corneal drug half-life of 1–3 min and it has been reported that, due to tear turnover, only 5 % of the dose penetrates the cornea and reaches intraocular tissues (Liu et al., 2015; Sa´nchez-Lo´pez et al., 2016).

During recent years, ocular active administration using controlled release systems has been emerging owing to improved permeability, bioavailability and stability, providing great advantages over conventional pharmaceutical dosage forms (Cano et al., 2017).

Therefore, to overcome these problems, drug encapsulation into biodegradable polymeric nanoparticles (NPs) has been carried out in order to increase its stability, therapeutic activity, and half-life in the ocular tissues allowing its release in a sustained way (Shi et al., 2010).

One of the most widely used polymers in these drug delivery systems is poly (lactic-co-glycolic acid) (PLGA), due to its biocompatibility and biodegradability. This compound is accepted by European Medicines Agency (EMA) and Food and Drug Administration (FDA) as Generally regarded as safe subtance (GRAS) that possess the ability of vectorization of the organism towards the therapeutic target (Sharma et al., 2016).

Hence, the aim of this study was the physicochemical development of polymeric bLF-NPs as topical ophthalmic drug delivery system for the treatment of ocular inflammation. This study highlights the incorporation of high molecular weight proteins like bLF within nanostructured systems. Moreover, the evaluation of their cytotoxicity and anti-inflammatory efficacy has been carried out by both *in vitro* and *in vivo* studies. Furthermore, corneal permeability and prolonged release of the active compound were decisive in the formulation assembly. Thus, the objective of improving the pharmacokinetic and pharmacodynamic drug profile was also pursued.

2. Experimental

2.1. Materials

bLF was purchased from Azienda Chimica e Farmaceutica (Italy); PLGA Resomer® 50:50 503H was acquired from Boehringer Ingelheim (Germany); ethyl acetate and Kolliphor®P188 (P188), ethyl-3-(3-dimethylaminopropyl) carbodiimide (EDC), N-hydroxysuccinimide (NHS), N-diisopropylethylamine (DIEA), rhodamine 110 (Rho) chloride, trypsin-EDTA (1X), insulin, hydrocortisone, lipopolysaccharide (LPS) and tetrazolium bromide (MTT) were purchased from Sigma Aldrich (MO, USA). Keratinocyte serum-free medium, human recombinant epidermal growth factor, bovine pituitary extract, penicillin, streptomycin, fetal bovine serum, IL-8 and TNF-α Human ELISA Kit were obtained from Thermo Fisher Scientific (Life Technologies, CA, USA). Human corneal epithelial cell line immortalized with adenovirus 12-SV40 hybrid virus (HCE-2, ATCC® CRL-11135) was purchased from LGC Standards (Barcelona, Spain). Water filtered through a Millipore® MilliQ system was used for all the experiments and all the other reagents used were of analytical grade.

2.2. Fabrication of nanoparticles

bLF loaded NPs were produced by a modified double emulsion method described elsewhere (Lamprecht et al., 2000; Tao Meng et al., 2003). Briefly, the organic phase (o) was formed dissolving a predetermined amount of PLGA in 2 mL of ethyl acetate. Aqueous phase (w_1) was obtained by dissolving bLF in 2.5 mL of deionized water. The primary emulsion (w_1/o) was formed by applying ultrasonic energy during 30 s. Secondary emulsion ($w_1/o/w_2$) was formed by mixing the w_1/o emulsion with 1.5 mL of deionized water containing P188 (1.8 $mg{\cdot}mL^{-1}$) following by the application of ultrasonic energy. Then, 1 mL of P188 (0.02 $mg{\cdot}mL^{-1}$) was added dropwise under magnetic stirring, and the organic solvent was evaporated overnight (Sa´nchez-Lo´pez et al., 2018).

The production of NPs fluorescently labelled with rhodamine 110 (Rho) followed the same approach above described, but adding 20 % of Rho-PLGA from the total amount of PLGA (Gonzalez-Pizarro et al., 2019a; Iqbal et al., 2015). Briefly, for the obtention of polymer Rho-PLGA, a quantity of PLGA 503H reacted with NHS and EDC dissolved in chloroform. Subsequently, the activated PLGA (NHS-PLGA) was

subjected to a procedure of washing/precipitation three times with cold diethyl ether. The resultant NHS-PLGA was dried and labelled with Rho by dissolving in chloroform with DIEA. The obtained polymer was submitted to three washing/precipitation cycles by adding an 80/20 mixture of diethyl ether and cold methanol. Finally, it was lyophilized and stored at − 20 °C (Gonzalez-Pizarro et al., 2019a).

2.3. Design of experiments

To obtain the optimal formulation, a design of experiments (DoE) was employed using a 2^3 central composite design matrix generated by StatGraphics Centurion XVI.I. This design was developed to analyse the effects of the independents variables (bLF, PLGA and P188 concentrations) on the dependent parameters (average particle size (Z_{av}), polydispersity index (PI), zeta potential (ZP) and encapsulation efficiency (EE)) (Nekkanti et al., 2015). Each factor was studied at five different levels (see Table 1) and the responses were modelled through the full second-order polynomial Eqn 1:

$$Y=\beta_0+\beta_1X_1+\beta_2X_2+\beta_3X_3+\beta_{11}X_1^2+\beta_{22}X_2^2+\beta_{33}X_3^2+\beta_{12}X_1X_2+\beta_{13}X_1X_3+\beta_{23}X_2X_3 \quad (1)$$

where Y is the measured response, β_0 to β_{23} are the regression coefficients and X_1X_2 and X_3 are the studied factors (Cano et al., 2018).

2.4. Physicochemical characterization

Different physicochemical parameters were determined to characterize the bLF-NPs using a ZetaSizer NanoZS (Malvern Instruments, Malvern, UK). Z_{av} and PI of NPs were determined by dynamic light scattering. ZP was determined measuring particle electrophoretic mobility using a combination of Laser doppler velocimetry and phase analysis light scattering (PALS). Samples were diluted (1:20) and measurements were carried out by triplicate in 10 mm diameter cells and disposable capillary cells DTS1070 (Malvern Instruments), respectively, at 25 °C (Anaraki et al., 2020).

2.5. Encapsulation efficiency

2.5.1. Indirect determination of encapsulation efficiency

With the objective of elucidating the percentage of bLF encapsulated in the NPs, the EE was determined indirectly by measuring the non-entrapped drug in the dispersion medium. The non-loaded drug was separated from NPs by ultracentrifugation at 4 °C and 45000 rpm for 60 min (Beckman Optima®, Ultracentrifuge, California, USA). Then, supernatant was used to evaluate the EE according to the following Eqn 2 (Gonzalez-Pizarro et al., 2018):

$$\text{EE (\%)} = \frac{\text{Total amount of bLF Free amount o fbLF}}{\text{Total amount of bLF}} \cdot 100 \quad (2)$$

The amount of the bLF in the aqueous phase was quantified by a reverse-phase high-performance liquid chromatography (RP-HPLC) method (Aguilar, 2004). The methodology used was validated in accordance with international guidelines (EMEA, 2011), including the evaluation of linearity, sensitivity, accuracy, and precision. Briefly, samples were quantified using HPLC Waters 2695 (Waters, Massachusetts, USA) separation module and a Europa® Protein 300 C_8 column (5 µm, 250 × 4.6 mm) with a mobile phase formed by a water phase of 0.1 % trifluoro acetic acid (TFA) and an organic phase of acetonitrile/water/TFA (95:5:0.1), in a gradient (from 95 % to 25 % of water phase in 4 min and back in next 4 min, maintaining this ratio until 25 min) at a flow rate of 0.75 mL·min^{-1}. A calibration curve with a bLF concentration ranges from 0.1 to 1 mg·mL^{-1} was prepared. A diode array detector Waters® 2996 at a wavelength of 219 nm was used to detect the bLF and data were processed using Empower 3® Software.

Table 1
Matrix of the factorial design including coded levels and their corresponding values in the experimental design.

	Levels				
Factor	− 1.68	− 1	0	+1	+1.68
cbLF (mg·mL^{-1})	1.60	5	10	15	18.40
cPLGA (mg·mL^{-1})	0.32	1	2	3	3.68
cP188 (mg·mL^{-1})	7.28	10	14	18	20.72

2.5.2. Direct determination of the encapsulation efficiency: Immunohistochemical method

Electrophoresis of bLF was carried out using the polyacrylamide gel in the presence of sodium dodecyl sulphate (SDS). This technique is used to separate and identify proteins based on their molecular weight. Proteins in the presence of SDS are denatured and negatively charged so they migrate to the anode in an electric field based on molecular weight. Gels with a polyacrylamide concentration of 10 % were used. The molecular weight marker used was the BENCHMARK® Prestained Protein Ladder (Invitrogen®). Subsequently, gel staining was performed with Coomassie bright blue, and protein analysis was carried out by Western Blot (Pillai-Kastoori et al., 2020). The protein present in the samples was detected using antibodies specific for bLF.

2.6. Morphological characterization

Morphology of the optimized formulation of bLF-NPs was determined by Transmission Electron Microscopy (TEM), performed on a JEM 1010 microscope (JEOL, Akishima, Japan). Copper grids were activated with UV light and diluted bLF-NPs (1:5) were placed on the grid surface, previously subjected to negative staining with uranyl acetate (2 %) (Cano et al., 2018).

Surface morphology and roughness were characterized by Atomic Force Microscopy (AFM) on a Dimension Icon microscope (Bruker, Massachusetts, USA). bLF-NPs were taped onto a glass slide and scanned in tapping mode (scan size of 2 µm, scan rate of 0.894 Hz, samples/line of 512) (You et al., 2020).

2.7. Interaction studies

bLF-NPs were ultracentrifuged (Beckman Optima® Ultracentrifuge, California, USA) at 45000 rpm and 4 °C, for 60 min, and the pellet was dried and pulverized to obtain the dry powder samples. Then, thermograms were obtained by Differential Scanning Calorimetry (DSC) on a Mettler T A 4000 system (Greifensee, Switzerland) equipped with a DSC-25 cell. Samples were weighed using a Mettler M3 Microbalance (Mettler Toledo, Ohio, USA), in perforated aluminium pans and heated under a flow nitrogen at a rate of 10 °C/min. Data were evaluated using 9.01 DB Metter STARe V software (Mettler Toledo, Ohio, USA) (Sa´nchez-Lo´pez et al., 2016).

Fourier Transform Infrared (FTIR) spectra of bLF-NPs and their components were carried out using a Thermo Scientific Nicolet iZ10 with an ATR diamond and DGTS detector. The scanning range was 525–4000 cm^{-1}, the spectral resolution was 4 cm^{-1} and 32 scans (Carvajal-Vidal et al., 2019).

2.8. γ-Irradiation sterilization

With the aim of eliminating any source of bacterial contamination, bLF-NPs were sterilized using a dose of 25 kGy of ^{60}Co as γ-irradiation source (Aragogamma, Barcelona, Spain). According to the European Pharmacopoeia, this dose represents the adequate absorbed dose for the purpose of sterilizing pharmaceutical products when bioburden is not known (Bozdag et al., 2005), maintaining a valid sterility assurance level (SAL) of 10^{-6} (Ramos Yacasi et al., 2016). The influence of γ-irradiation on the physicochemical properties of the NPs was evaluated.

2.9. Biopharmaceutical behaviour

2.9.1. In vitro drug release

In vitro release profile was evaluated using a direct dialysis bag technique due to the water solubility of bLF (Cano et al., 2018). The release medium was 0.1 M phosphate buffer saline solution (PBS) at pH 7.4, and bLF-NPs were place in 1 mL dialysis bags (Float-A-Lyzer® dialysis device, 1000 kDa) (Repligen®, Massachusetts, USA). Dialysis medium was PBS buffer, and it was maintained under magnetic stirring at 37 °C. At different time intervals, 1 mL of sample was taken from the release medium and replaced with fresh buffer solution. It was analysed by RP-HPLC method previously described and data were adjusted to the most common pharmacokinetic models (Cano et al., 2019).

2.9.2. Ex vivo corneal permeation study

The ex vivo bLF permeation study from bLF-NPs was carried out using isolated cornea from New Zealand rabbits (2.5–3.0 kg males), according to the Ethics Committee of Animals Experimentation from the University of Barcelona (CEEA-UB), and under veterinary supervision. Animals were anesthetized with intramuscular administration of ketamine HCl (35 $mg{\cdot}kg^{-1}$) and xylazine (5 $mg{\cdot}kg^{-1}$) and euthanized by an overdose of sodium pentobarbital (100 $mg{\cdot}kg^{-1}$) administered through marginal ear vein under deep anaesthesia (Sa´nchez-Lo´pez et al., 2016). Eyes were removed, immediately excised, and transported in artificial tear solution to the laboratory. Corneas were fixed in Franz cells between the donor and receptor compartment with a diffusion area of 0.64 cm^2. In all experiments, 1 mL of the test formulation (bLF-NPs or 9.32 $mg{\cdot}mL^{-1}$ of free bLF) was incubated in the donor compartment and immediately covered to avoid the sample evaporation. The receptor compartment was filled with PBS at 32 ± 0.5 °C and it was kept under magnetic stirring. 300 µL were withdrawn from the receptor compartment at pre-selected times during 6 h and replaced by an equivalent volume of fresh receptor medium at the same temperature. Sink conditions were maintained throughout the experiment.

The cumulative amount of bLF permeated was calculated, at each time point, from bLF amount in receptor medium and plotted as function time (Gonzalez-Pizarro et al., 2018). Samples were measured using the RP-HPLC method (Smith et al., 1985; Wang et al., 2017).

To quantify the sample inside the tissue, recovery of the corneal structure was analysed. The tissue was washed with distilled water, weighted, and sonicated in MQ® water for an hour, using an ultrasound bath.

Values were reported as the mean ± SD. Three replicates of each sample were carried out. Permeation parameters were obtained by plotting the cumulative bLF permeated versus time, calculating x-intercept by linear regression analysis. The permeability coefficient (K_p) ($cm{\cdot}h^{-1}$), steady-state flux (J) ($\mu g{\cdot}h^{-1}{\cdot}cm^{-2}$) and amount of permeated at 24 h (Q24) (µg) were calculated (Gómez-Segura et al., 2020).

2.10. NP short-term stability

The stability of bLF-NPs stored at different temperatures (4 and 25 °C) was studied by multiple light scattering using Turbiscan® Lab (Iesmat, Madrid, Spain). This technique identifies the different destabilization phenomena of the colloidal suspension such as creaming, sedimentation, flocculation, and coalescence. For this purpose, a glass measurement cell was filled with 20 mL of sample. The light source is a pulsed near infrared light source (λ = 880 nm) and it is received by backscattering detector at an angle of 45° from the incident beam due to the opacity of the NPs formulation. Backscattering data were acquired at 1, 15 and 30 days for 24 h at intervals of 1 h. Moreover, morphometric parameters (Z_{av}, PI and ZP) were also measured.

2.11. Cell culture assays

2.11.1. Cytotoxicity assays

Human corneal epithelial cells (HCE-2) were used to perform cytotoxicity assays. As these cells belong to corneal tissue, they present a greatly suitable line to carry out the *in vitro* studies of bLF-NPs for ocular administration. Keratinocyte serum-free medium was the culture medium for HCE-2 cells. It was supplemented with bovine pituitary extract 0.05 $mg{\cdot}mL^{-1}$ and epidermal growth factor 5 $ng{\cdot}mL^{-1}$ containing insulin 0.005 $mg{\cdot}mL^{-1}$, 10 % (v/v), fetal bovine serum, hydrocortisone 500 $ng{\cdot}mL^{-1}$ and penicillin 100 $U{\cdot}mL^{-1}$ plus streptomycin 100 $mg{\cdot}mL^{-1}$. Cells were grown on a culture flask to 80 % confluency in a humidified 10 % CO_2 atmosphere at 37 °C.

To highlight the possible cytotoxicity of the formulations, cell viability tests were performed on HCE-2 corneal cell line using MTT (Bromide of 3-(4,5-dimethyl-2-thiazoyl)-2,5-diphenyltetrazole as an indicator of viability. 0.1 mL of a cell density of 1×10^5 were seeded in 96-well plates and incubated at 37 °C for 24 h. Later, cells were exposed to bLF-NPs and free bLF at different drug concentrations (0.04–0.1 $mg{\cdot}mL^{-1}$). After 24 h of incubation, cells were washed with PBS and incubated with 0.25 % MTT in fresh medium for 2 h. Then, this medium was extracted, and DMSO was added for cell lysis. The absorbance was measured at λ = 560 nm by an automatic Modulus™ Microplate Photometer (Turner BioSystems, CA, USA). Data were analysed by calculating the percentage of MTT reduction and expressed as percentage of control (untreated cells).

2.11.2. Determination of proinflammatory cytokines

To evaluate the anti-inflammatory activity of the bLF-NPs and free bLF, HCE-2 cells were seeded (1×10^5 $cell{\cdot}mL^{-1}$) in 12-well plates and grown until 90 % confluency. Samples were added to the culture medium at 0.2 $mg{\cdot}mL^{-1}$ (drug concentration of loaded NPs) and inflammation was induced with lipopolysaccharide (LPS) (1 $\mu g{\cdot}mL^{-1}$). Cells stimulated only with LPS were used as a positive control and untreated cells as a negative control. After 24 h incubation, the supernatants were collected and centrifuged (16000 g for 10 min) at 4 °C and stored at −80 °C until use. Unknown levels of the pro-inflammatory cytokines, interleukin 8 (IL-8) and tumour necrosis factor α (TNF-α), were quantified using ELISA kits (BD Biosciences, CA, USA) according to manufacturer's instructions. Results were expressed as $pg{\cdot}mL^{-1}$.

2.11.3. Cellular uptake assay

To evaluate the internalization of NPs in HCE-2 cells, 1×10^5 $cell{\cdot}mL^{-1}$ HCE-2 were grown in eight-well chamber slider (ibidi®, Gra¨felfing, Germany) until 80 % confluence and posteriorly incubated with bLF-NPs at different dilutions ratios (1:10; 1:50 and 1:100) at 37 °C for 48 h. Non-internalized NPs were removed by washing three times with PBS and cells were fixed with 3 % paraformaldehyde for 30 min at 25 °C. Subsequently, cells were subjected to triple PBS washes and then, the nuclei were stained with 4´,6-diamidino-2-phenylindole (DAPI) for 15 min at 25 °C. Finally, mounting solution (PBS) was added for microscopic analysis. Images were acquired using a Leica TCS SP5 confocal laser scanning microscopy (Leica Microsystems, Wetzlar, Germany) with a 63x oil immersion objective lens (Gonzalez-Pizarro et al., 2019a).

2.12. Ocular tolerance

2.12.1. In vitro study: HET CAM test

In vitro ocular tolerance was assessed using the HET-CAM test to ensure that the formulation of bLF-NPs was non-irritating when administered as eye-drops. Irritation, coagulation, and haemorrhage phenomena were measured by applying 300 µL of the formulation

studied on chorioallantoic membrane of a fertilized chicken egg and monitoring it during the first 5 min after the application.

This assay was conducted according to the guidelines of ICCVAM (The Interagency Coordinating Committee on the Validation of Alternative Methods). The development of the test was carried out using 3 eggs for each group (free bLF, bLF-NPs, positive control (NaOH 0.1 M) and negative control (0.9 % NaCl)). The ocular irritation index (OII) was calculated by the sum of the scores of each injury according to the following expression (Eqn 3):

$$OII = \frac{(301 - H)\cdot 5}{300} + \frac{(301 - V)\cdot 7}{300} + \frac{(301 - C)\cdot 9}{300} \quad (3)$$

where H, V and C are times (s) until the start of haemorrhage (H), vasoconstriction (V) and coagulation (C), respectively. The formulations were classified according to the following: OII ≤ 0.9 non-irritating; 0.9 < OII ≤ 4.9 weakly irritating; 4.9 < OII ≤ 8.9 moderately irritating; 8.9 < OII ≤ 21 irritating (Derouiche and Abdennour, 2017; Shalom et al., 2017).

2.12.2. In vivo study: Draize test

The formulations were evaluated using primary eye irritation test of Draize to ensure the results obtained from the HEM-CAM test (Sánchez-López et al., 2016). For this experiment, New Zealand male albino rabbits (2.0–2.5 kg, St. Feliu de Codines, Barcelona, Spain) were used. 50 μL of each sample were instilled in the ocular conjunctival sac (n = 3/group) and a mild massage was applied to guarantee the passage of the sample through the eyeball. The possible appearance of irritation signs (corneal opacity and area of corneal involvement, conjunctival hyperemia, chemosis, ocular discharges, and iris abnormalities) was observed at the time of instillation and after 1 h from its application and if necessary, at predefined intervals: 24 h, 48 h, 72 h, 7 days, and 21 days after administration. The opposite untreated eye was used as a negative control. Draize test score was determined directly by observing the anterior segment of the eye and changes in the structures of the cornea (turbidity or opacity), iris and conjunctiva (congestion, chemosis, swelling and secretion).

2.13. In vivo efficacy studies

2.13.1. Prevention of inflammation

The evaluation of the prevention of inflammation ability of bLF-NPs in comparison with the free bLF and the control group (NaCl 0.9 %) was carried out. First, each sample was administered and subsequently, an inflammatory stimulus was applied in New Zealand male albino rabbits (n = 3/group). The study consisted of the application of 50 μL of each formulation. After 30 min of exposure, 50 μL of 0.5 % sodium arachidonate (SA) dissolved in PBS was instilled in the right eye and the left eye was used as a control. The evaluation of prevention of inflammation was carried out from the application of formulations up to 210 min, according to the Draize modified test scoring system (Sánchez-López et al., 2016).

2.13.2. Inflammation treatment

The induction of inflammation with the objective of evaluating the anti-inflammatory effect of bLF-NPs compared to the free protein and the control group (NaCl 0.9 %), was carried out using New Zealand male albino rabbits (n = 3/group). The study was conducted with the application of 50 μL of 0.5 % sodium arachidonate (SA) dissolved in PBS in the right eye, using the left eye as a control. After 30 min of exposure, 50 μL of each formulation was instilled. Evaluation of inflammation was performed from the application of formulations up to 180 min according to Draize modified scoring system (Sánchez-López et al., 2016).

2.14. Statistical analysis

Two-way ANOVA, followed by Tukey *post hoc* test, was performed for multi-group comparison. Student's *t* test was used for two-group comparisons. All the data are presented as the mean ± S.D. Statistical significance was set at $P < 0.05$ by using GraphPad Prism 8.4.3 and ImageJ was used to analyse images.

3. Results and discussion

3.1. Design of experiments

A composite central factorial design was carried out with the objective of optimizing the formulation, evaluating the effect of the concentrations of bLF, PLGA and P188 on the physicochemical properties of the developed NPs. The response parameters and their magnitudes for each of the 16 experiments are given in Table 2.

The response surface (Fig. 1a) and the Pareto diagram (Fig. 1b) showed that bLF concentration influences the EE, increasing the encapsulation of bLF at middle concentrations. At bLF concentrations between 8 and 11 $mg{\cdot}mL^{-1}$, an increase in EE was observed, reaching the 50–60 % encapsulation. Accordingly, the Pareto diagram (Fig. 1b) confirmed that only the bLF concentration exerted a significant influence on EE. With concentrations lower than 7 $mg{\cdot}mL^{-1}$, and higher than 12 $mg{\cdot}mL^{-1}$, EE markedly decreases. With regard to PLGA, although its influence is not statistically significant, from the surface responses plots, it can be observed that until reaching concentration values around 19 $mg{\cdot}mL^{-1}$, a directly proportional relationship between PLGA and EE is observed (at fixed P188 concentration of 1.8 $mg{\cdot}mL^{-1}$, and a bLF concentration around 9 $mg{\cdot}mL^{-1}$). However, after exceeding this concentration the EE begins to decrease. This trend may be explained by the limited polymer incorporation capacity and the bLF high molecular weight (87 kDa). Thus, meaning that at 19.01 $mg{\cdot}mL^{-1}$ the maximum loading capacity is reached.

Regarding the average size of the NPs, the response surface (Fig. 1c) reveals that at a constant concentration of PLGA (19.01 $mg{\cdot}mL^{-1}$), an intermediate concentration of bLF and low concentrations of surfactant favour lower particle sizes. In all cases, the NPs obtained have an average size bellow 250 nm, so they are all suitable for ocular administration (Wadhwa et al., 2009).

Likewise, the response surface (Fig. 1d) analysing the PI, shows that the surfactant concentration affects the values obtained significantly, observing that at higher concentrations of P188 and PLGA, the PI reaches values of 0.2 in the range of monomodal systems. Instead, at lower P188 concentrations optimal values of PI was obtained (<0.1), characteristic of a monodispersed system. This tendency can be explained by the phenomenon of absorption in the polymeric surface of the substances, given the positive charge that bLF-NPs possess. It is possible that bLF is being placed both inside the polymer matrix and on its surface. The surfactant is also placed on the NPs surface. Increasing the surfactant concentration, the surface of the NPs would be saturated, thus increasing the PI and their average size (Masoudipour et al., 2017). Yan et al. observed that the surface absorption of the surfactant can change the smooth polymeric NPs appearance into a slightly rough one (Yan et al., 2010).

The PLGA used possess a great negative ZP, due to the ionization on the surface of polymer of carboxylic end groups. However, it has been reported that the presence of surfactant P188 can lead to a reduction in their surface charge (Vega et al., 2012). The hydrophobic polyoxypropylene chains bind the surface of the NP, and the hydrophilic polyoxypropylene chains remain protruding in the medium around it, masking the negative surface charge present in the NPs. In this case, besides the surfactant, the active principle to be encapsulated, bLF, has a positive charge at medium pH, so it also covers the negative charge of the polymer, obtaining as a result a ZP of approximately + 30 mV. The positive charge prolongs the residence time on the epithelial layer of the cornea and thus facilitates drug penetration and achieves a sustained release (Andrés-Guerrero et al., 2017).

From the results obtained in the factorial design, an optimized

Table 2
Values of the 2^{3+} star central composite rotatable factorial design, parameters, and measured responses.

	cbLF		cP188		cPLGA		Z_{av}	PI	EE
	Coded level	(mg·mL^{-1})	Coded level	(mg·mL^{-1})	Coded level	(mg·mL^{-1})	(nm)		(%)
Factorial points									
1	− 1	5	− 1	1	− 1	10	135.1 ± 2.5	0.122 ± 0.044	43.96
2	1	15	− 1	1	− 1	10	130.6 ± 1.9	0.138 ± 0.034	32.39
3	− 1	5	1	3	− 1	10	112.0 ± 3.2	0.090 ± 0.021	34.67
4	1	15	1	3	− 1	10	110.2 ± 2.8	0.089 ± 0.031	23.26
5	− 1	5	− 1	1	1	18	133.1 ± 4.5	0.077 ± 0.002	44.83
6	1	15	− 1	1	1	18	116.7 ± 1.6	0.074 ± 0.022	30.23
7	− 1	5	1	3	1	18	187.0 ± 4.2	0.141 ± 0.010	49.36
8	1	15	1	3	1	18	146.5 ± 1.3	0.125 ± 0.021	44.83
Axial points									
9	1.68	1.6	0	2	0	14	134.7 ± 2.7	0.220 ± 0.024	35.18
10	− 1.68	18.4	0	2	0	14	243.1 ± 7.6	0.083 ± 0.009	45.56
11	0	10	1.68	3.68	0	14	148.6 ± 1.2	0.143 ± 0.046	50.75
12	0	10	− 1.68	0.32	0	14	157.4 ± 1.6	0.122 ± 0.028	47.87
13	0	10	0	2	1.68	20.72	148.2 ± 4.1	0.181 ± 0.012	37.94
14	0	10	0	2	− 1.68	7.28	125.1 ± 1.3	0.144 ± 0.005	49.03
Center points									
15	0	10	0	2	0	14	146.0 ± 5.1	0.100 ± 0.027	55.82
16	0	10	0	2	0	14	132.2 ± 3.7	0.158 ± 0.019	50.60

Results presented as mean ± standard deviation.

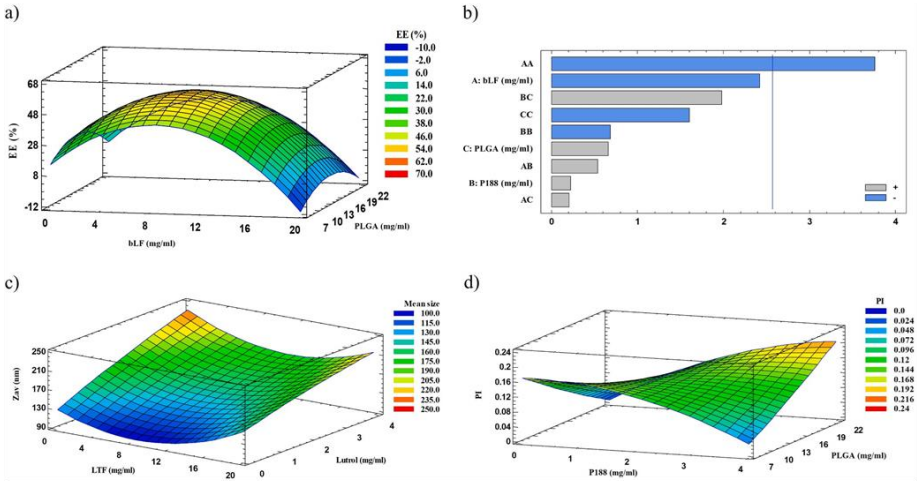

Fig. 1. (a) EE (%) surface response at a fixed P188 concentration (1.8 mg·mL^{-1}); (b) Pareto diagram for EE (%); (c) Z_{av} surface response at a fixed PLGA concentration (19.01 mg·mL^{-1}); (d) PI surface response at a fixed bLF concentration (9.32 mg·mL^{-1}).

Table 3
Physicochemical parameters of optimized bLF-NPs formulation.

cbLF (mg·mL^{-1})	cP188 (mg·mL^{-1})	cPLGA (mg·mL^{-1})	Z_{av} (nm)	PI	ZP (mV)	EE (%)
9.32	1.80	19.01	128.4 ± 5.0	0.058 ± 0.030	31.0 ± 0.8	56.00 ± 3.00

Data presented as mean ± standard deviation.

formulation was selected focusing mainly on the EE values (%) and on the adequate homogeneity of the sample (PI). It can be noted in Table 3, the optimized bLF concentration was 9.32 mg·mL^{-1}, 19.01 mg·mL^{-1} of polymer and 1.80 mg·mL^{-1} in the case of P188. The morphometry (Z_{av}, PI) and surface charge (ZP) of optimized formulation, determined by photon correlation spectroscopy and laser doppler velocimetry, respectively (Table 3) are suitable for ocular administration (Sa´nchez-Lo´pez et al., 2016). The EE of bLF in the nanoparticles was 56.00 ± 3.00 %.

The NPs were ultracentrifuged, and the pellet and supernatant were separated. A polyacrylamide gel electrophoresis was carried out in

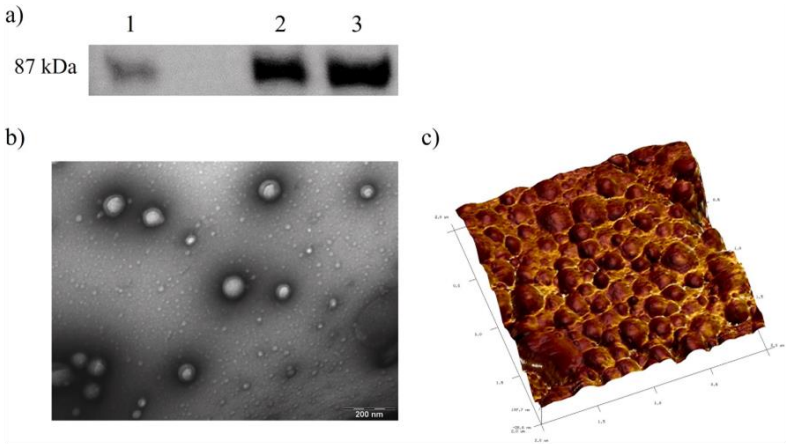

Fig 2. (a) bLF western blot analysis: 1. bLF control; 2. bLF in NPs; and 3. bLF in supernatant. (b) Microscopy studies of bLF-NPs by TEM; and (c) by AFM.

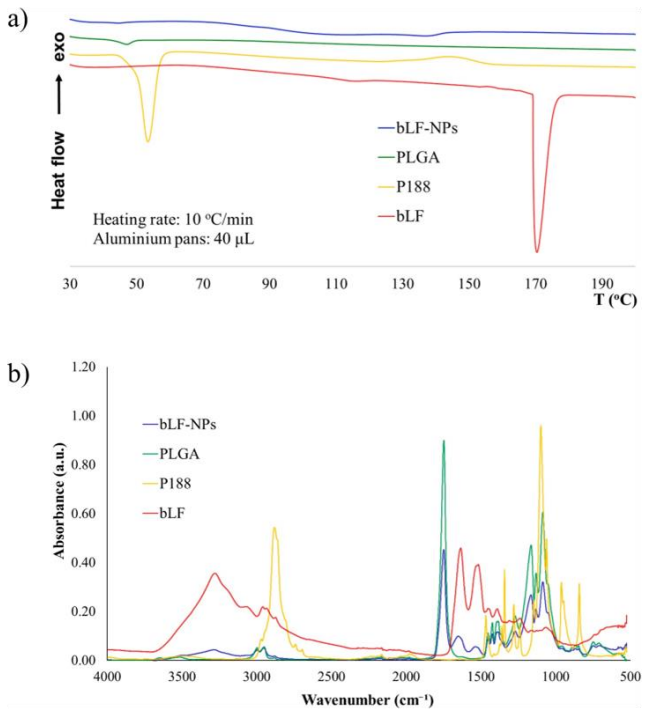

Fig. 3. Interaction studies of bLF-NPs. (a) DSC thermograms. (b) FTIR spectra.

denaturing conditions to separate the protein based on its molecular weight, then a western blot was carried out using anti-bLF antibodies. It was observed that 50 % of the initial bLF is within the systems thus confirming the results of EE (%) obtained by the HPLC method (Fig. 2a).

3.2. Morphological characterization

The morphological characterization of the optimized formulation of bLF-NPs was carried out by imaging using TEM and AFM (Fig. 2b and 2c). Images revealed a spherical shape of NPs, without any signs of aggregation phenomena and average particle diameters like those obtained in the morphometry tests performed by PCS.

3.3. Interaction studies

A factor that greatly affects the release of the active substance in *in vitro* and *in vivo* studies is the physical state of the drug inside the NPs. Therefore, a DSC study was carried out presenting the thermograms of bLF, P188, PLGA and bLF-NPs in the Fig. 3a. The bLF thermogram shows an acute endothermic accident that corresponds to its fusion, with a maximum temperature (T_{max}) of 170.41 °C which was not detected in bLF-NPs. This data suggest that bLF is encapsulated within the polymer matrix in an molecular dispersion or a solid solution state (Cano et al., 2019; Vega et al., 2012). P188 surfactant revealed a sharp melting endotherm characterized by a $\Delta H = 132.69\ J \cdot g^{-1}$ and a $T_{max} = 53.46$ °C (Gonzalez-Pizarro et al., 2018). It is noted a peak belonging PLGA that shows the onset of the glass transition (T_g) at 47.09 °C and in the bLF-NPs at 44.55 °C. This slight decrease of NPs T_g is attributed to the interaction between bLF and the polymer matrix (Sa´nchez-Lo´pez et al., 2017).

To evaluate the interaction between bLF and PLGA, the FTIR analysis was performed (Fig. 3b). There was no evidence of covalent bonds between the protein and PLGA. The IR spectrum of bLF showed protein characteristic peaks, amide I at 1638 cm^{-1} due to C = O and C–N stretching vibration and amide II at 1520 cm^{-1} corresponding to the N–H bending with contribution of C–N stretching vibration. At 3279 cm^{-1} the band is given by the signal of the stretching vibration of O–H in water molecules, indicating the presence of residual H_2O (Wang et al., 2017; Yao et al., 2014). In the PLGA analysis, a characteristic strong band appeared at 1750 cm^{-1} due to stretching vibration of the carbonyl group. The weak peaks at 3002 and 2956 cm^{-1} correspond to stretching vibration of the alkanes and it appeared the medium peaks at the band of 1159 and 1088 cm^{-1} corresponding to the stretching vibration C–O and C–O–O, respectively (Gonzalez-Pizarro et al., 2018). In the case of P188 two strong peaks are showed, at 2874 cm^{-1} corresponding to the stretching vibration of CH and at 1096 cm^{-1} signal given by the stretching vibration of C–O (Yan et al., 2010). bLF-NPs showed a similar profile to PLGA and P188 with further weak intensity peaks due to bLF (amide I, II and O–H).

3.4. Effects of γ-irradiation on bLF-NPs

Since bLF-NPs were going to be administered as eye-drops, the formulation should be sterilized. In this sense, bLF-NPs were γ-irradiated and morphometrically characterized to ensure that the irradiation process did not affect the chemical structure of the system. As seen in Table 4, the results obtained demonstrated that γ-irradiation had no effect on the physicochemical parameters of the optimized NPs. It has shown not significant differences between NPs before and after sterilization. In this area, some authors reported that higher doses of γ-irradiation might favour the tendency to decrease particle size and ZP and increase the PI value of polymeric NPs. The difference in the case of bLF-NPs could be due to the use of a different surfactant that does not present the "long chain extension" phenomenon that leads to the chain scission, such as polyvinyl alcohol molecule, and a consequent reduction in NP molecular weight. However, these physicochemical changes generate a barely perceptible effect on the PLGA NPs. therefore, these slight modifications do not affect the medical properties of bLF-NPs (Ramos Yacasi et al., 2016; Tapia-Guerrero et al., 2020).

Table 4
Physicochemical properties and EE of bLF-NPs before and after sterilitzation.

	Average size (nm)	PI	ZP (mV)	EE (%)
bLF-NPs	131.6 ± 0.8	0.061 ± 0.019	30.4 ± 0.2	60.00 ± 3.00
bLF-NPs 25 kGy	134.7 ± 0.8	0.084 ± 0.020	28.5 ± 0.2	57.00 ± 1.00

Data presented as mean ± standard deviation.

3.5. Biopharmaceutical behaviour

3.5.1. In vitro drug release

The *in vitro* release of bLF from bLF-NPs and free bLF was carried out using a direct dialysis bag technique. The cumulative drug release profile revealed a controlled and prolonged release of bLF from NPs. Fig. 4a shows a faster release of the bLF from the NP during the first 5 h than free bLF, due to the drug weakly bound on the surface of NPs (Carvajal-Vidal et al., 2019). After that, the release speed decreases significantly, performing a sustained release without reaching a plateau (83.6 % after 48 h). PLGA matrix of controlled release systems usually presents an initial burst with a zero-order release profile and a posterior slower release from the polymeric matrix by diverse routes as diffusion through the polymer, erosion of the PLGA matrix or a combination of both (Cano et al., 2018; Fu and Kao, 2010; Sa´nchez-Lo´pez et al., 2016). The Korsmeyer-Peppas model was the best one that adjusted the NPs formulation ($r^2 = 0.99$, AIC = 57.37). Free bLF showed a faster release, reaching 95 % after 22 h. The most appropriate release profile corresponds to a first-order equation ($r^2 = 0.97$, AIC = 80.76), characterized by a rapid release followed by a constant release (Fangueiro et al., 2016). To obtain the kinetic model that better fits for bLF release, data were adjusted to the most common kinetic models (Table 5).

3.5.2. Ex vivo corneal permeation

Ex vivo corneal permeation of bLF-NPs and free bLF were carried out to study its behaviour and compare different permeation parameters (Fig. 4b). According to Table 6, the bLF-NPs formulation presents statistically significant differences ($p < 0.05$) against free bLF in all examined permeation parameters, except for the case of bLF retained amount (QR). With respect to the steady-state flux (J) value is one third higher in the case of bLF-NPs, hence bLF from NPs permeated the cornea faster than free bLF. This fact is due to the greater lipophilicity of polymer than free protein, since the epithelium layer of the cornea is composed of lipid, and restricts the entry of hydrophilic substances, acting as a rate limiting factor for the eye level drug administration (Soni et al., 2019; Talluri et al., 2010). The different permeation parameters follow the same ratio, with the permeability coefficient (K_p) and the quantity permeated at 24 h (Q24) higher in the case of bLF-NPs than in the free bLF. It justifies the effect of bLF on the cornea and aqueous humor (Sa´nchez-Lo´pez et al., 2016). Otherwise, no significant differences in the bLF QR in both formulations can be observed. Regarding the NPs formulation, the retained quantity may be from the non-encapsulated percentage of bLF and the initial burst from the fraction of bLF weakly bound or adsorbed on the surface area of the NPs (Vega et al., 2012).

Therefore, this formulation may deliver the drug effectively to the specified area by releasing bLF slowly across the corneal tissue, which would be beneficial for the treatment of ocular inflammation such as that induced by allergens, traumatisms or microbial infection (Schultz, 2018).

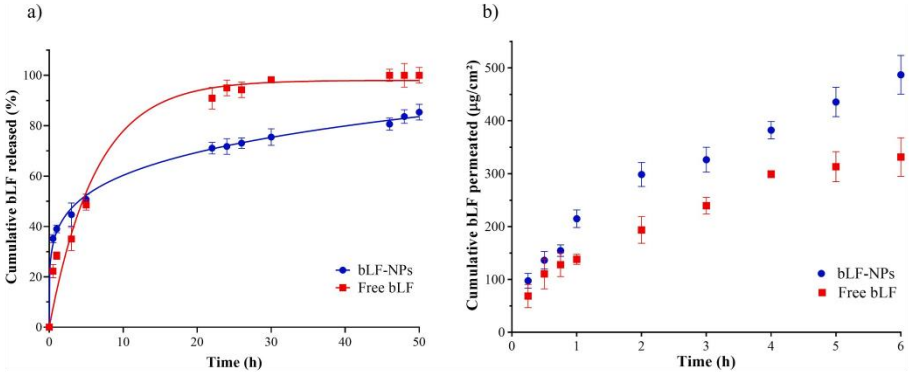

Fig. 4. (a) *In vitro* release profile of bLF-NPs (Korsmeyer-Peppas equation) against free bLF (first order equation). (b) *Ex vivo* corneal permeation profile of bLF-NPs compared with free bLF.

Table 5
Parameters for kinetic models of bLF-NPs and free drug solution.

Models	bLF-NPs		Free bLF	
	AIC	R^2	AIC	R^2
Zero Order	94.45	0.75	100.99	0.79
First Order	89.67	0.84	80.76	0.97
Higuchi	85.44	0.89	88.21	0.93
Hyperbola	82.79	0.91	77.88	0.97
Korsmeyer-Peppas	n = 0.007		n = 0.022	
	57.37	0.99	80.64	0.97

Table 6
Pharmacokinetic parameters adjusted to linear regression of the *ex vivo* corneal permeation of bLF-NPs against bLF.

Parameters	Free bLF	bLF-NPs
J ($\mu g \cdot h^{-1} \cdot cm^{-2}$)	70.55 ± 8.53	100.69 ± 16.75*
Kp · 10^3 ($cm \cdot h^{-1}$)	7.57 ± 0.91	10.80 ± 1.79*
Q24 (µg)	1081.63 ± 130.77	1544 ± 257.31*
QR ($\mu g \cdot g^{-1} \cdot cm^{-2}$)	1.07 ± 0.01	1.04 ± 0.01

Statistical significance: *p < 0.05. J, steady-state flux; Kp, permeability coefficient; Q24, permeated amount at 24 h; QR, retained amount.

3.6. Stability of nanoparticles

The prediction of the accelerated stability of the bLF-NPs was studied for 30 days. The optimized formulation was evaluated after 1, 15 and 30 days of storage at 4 and 25 °C. Turbiscan® Lab was used to determine destabilization processes such as the variation in the speed of migration of the particles (vertical sections of the graph) and the variation in size (horizontal section of the graph) (Fig. 5).

The migration of the particles to the upper part of the cell leads to a decrease in the concentration in the lower part. This is shown as a decrease in the backscatter signal (negative peak) and vice versa for the phenomena that occurs in the upper part of the vial. The backscatter profile with a deviation of ± 5 % is considered that it does not present significant variations in particle size. Variations of ± 10 % indicate that the formulation is unstable (Cano et al., 2017). This system allows predicting the instability processes of NPs before they can be detected by other techniques (Celia et al., 2009). It was observed that the back-scattered light profile did not show fluctuations greater than 5 %, which indicates that the sample remained stable stored at 4 °C. The stability is associated with the high ZP of the NPs, approximately + 30 mV, avoiding electrostatic interaction between particles and its flocculation and precipitation (Retamal Marín et al., 2017).

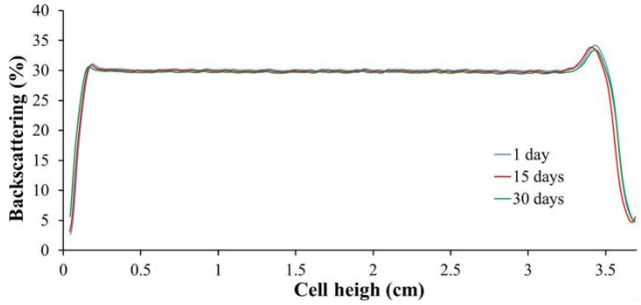

Fig. 5. Backscattering profile of bLF-NPs stored at 4 °C.

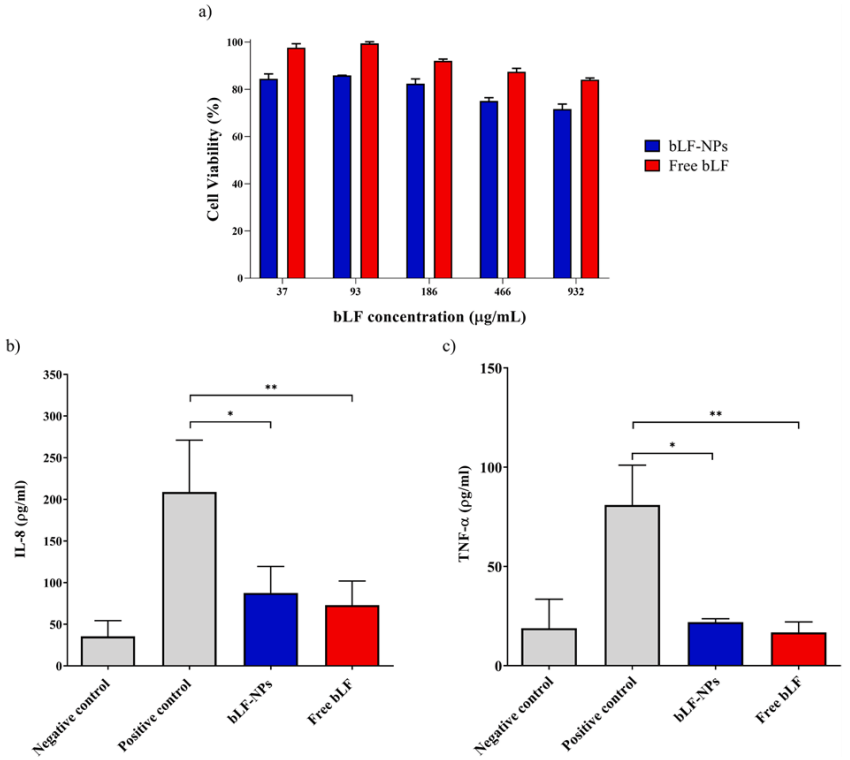

Fig. 6. (a) Effect of bLF-NPs on the viability of HCE-2 cells. The 100 % cell viability correspond with the average of MTT reduction values of untreated cells. (b) Quantification of secreted IL-8 proinflammatory cytokine in LPS-stimulated HCE-2 cells; (c) Quantification of secreted TNF-α. Negative control: no treatment; Positive control: LPS. Values are expressed as the mean ± SD; *p < 0.05; **p < 0.01 significantly lower than LPS-induced cytokine concentration.

3.7. Cytotoxicity of nanoparticles

Safety of bLF-NPs was assessed in HCE-2 cells. Results are shown in Fig. 6a. After 24 h of incubation, bLF-NPs did not show relevant cytotoxic effects. For concentrations up to 186 $\mu g \cdot mL^{-1}$, cell viability was higher than 80 %. At higher concentrations cell viability was close to 80 %. Free bLF showed no cytotoxic effects at all concentrations tested, since viability was kept close to 100 %.

LF is one of the most abundant components in the healthy tear fluid and contributes to iron retention mechanisms against pathogens and mitigates oxidative stress (Seen and Tong, 2018). Tear LF represents 20–30 % of the total proteins with concentrations ranging between 0.63 and 2.9 $mg \cdot mL^{-1}$, depending on sex and age, in healthy patients (Flanagan and Willcox, 2009; Lawrenson, 2018). Upon stimulation, such as oxidative stress or acute inflammation, the basal tear flow (1 $\mu L \cdot min^{-1}$) is significantly increased (Hanstock et al., 2019). bLF-NPs could provide a long-lasting protein concentration since the formulation is 3-fold more concentrated in lactoferrin than healthy tears. This fact improves its bioavailability, for cases in which the tears LF concentration is compromised (Ponzini et al., 2020).

Considering other formulation components, it has been reported that PLGA is a biocompatible, biodegradable, and safe polymer for the internalization and delivery of substances with pharmacological activities (Han et al., 2016).

Finally, the slight decrease in HCE cell viability, not observed for free bLF, may be due to the presence of the P188 surfactant. However, surfactants have been widely used as emulsifiers to prevent protein aggregation during manufacturing processes, shipping or storage (Wang et al., 2019; Yan et al., 2010). Although the most commonly used surfactants in biological products are polysorbates due to their widely known degradation, the evaluation of alternatives such as P188 has provided promising results. In fact, P188 is the surfactant that has been used in the production of commercialized biological drug products (Wang et al., 2019).

These results confirm the biocompatibility of the developed bLF-NPs with corneal cells, according to the generally recognized as safe (GRAS) designation of the formulation components (Han et al., 2016).

3.8. Anti-inflammatory activity of nanoparticles in HCE-2 cells

The ability of NPs to inhibit the inflammatory response produced by LPS was evaluated in HCE-2 cells through the analysis of IL-8 and TNF-α secreted cytokines (Fig. 6b and 6c). In the absence of NPs (positive control) LPS induced high secretion levels of both cytokines (Diaz-

Garrido et al., 2019). Treatment with bLF-NPs significantly decreased the expression of both cytokines to levels similar to that triggered by free bLF ($p < 0.05$).

There is evidence that in many ocular disorders involving chronic inflammation, tears present depleted levels of some proteins such as LF or lysozyme (Tamhane et al., 2019). In turn, these pathologies involve overexpression of different inflammatory mediators, specially IL-8 and TNF-α cytokines (Chen et al., 2019). It has been reported that elevated tear levels of IL-8 cause migration of neutrophils, basophils, and T lymphocytes causing exacerbation of the symptoms (Tamhane et al., 2019). Multiple studies have shown the presence of elevated levels of TNF-α, which is thought to represent a measure of the general inflammatory state of the ocular surface in patients with different ophthalmopathies (Aketa et al., 2017; Chen et al., 2019; Ghasemi, 2018).

LF has been reported to modulate the expression of several cytokines through different mechanisms (Lee et al., 2020). This protein is known to interact with cell surface receptors involved in the inflammatory response. For example, LF competes with bacterial LPS for binding to CD14 receptor, thus diminishing NF-κB-induced transcription of various genes for inflammatory mediators (Håversen et al., 2002; Kruzel et al., 2017). Meanwhile, in the context of iron sequestration, LF can control oxidative burst from neutrophils and macrophages that trigger the inflammatory response (Rosa et al., 2017). These results indicated that an anti-inflammatory effect was achieved with the bLF-NPs.

3.9. Cellular uptake of Rho-bLF-NPs

After 48 h incubation of HCE-2 cells with Rho-bLF-NPs at different concentrations (1:10; 1:50 and 1:100), the NP associated green fluorescence was visualized by confocal fluorescence microscopy. The nucleus was stained with DAPI. In the merged images, the Rho-NPs were found in the cytoplasm. As expected, untreated control cells did not show any green fluorescence signal from rhodamine, but nuclei were properly dyed with DAPI emitting blue florescent light (Fig. 7).

Different studies have proved the cellular internalization of PLGA NPs within corneal cells (Gonzalez-Pizarro et al., 2019a; Li et al., 2021; Sah et al., 2017; Sa´nchez-Lo´pez et al., 2016). The uptake is dependent on the NPs size, concentration, and incubation time. It is showed that 100 nm NPs are internalized mainly by receptor-mediated endocytosis in corneal cells, rather than larger NPs that present absorption on the cell surface (Qaddoumi et al., 2004). Furthermore, the low density lipoprotein receptor-related protein 1 (LRP1) has been identified by Higuchi et al. as the primary LF receptor in corneal epithelium (Higuchi et al., 2016). The LRP1 expression levels were 8.7-fold higher than intelectin-1, another LF corneal receptor (Higuchi et al., 2016). This fact suggested that the bLF-NPs uptake may also be carried out through LRP1 pathway.

3.10. Ocular tolerance results

3.10.1. In vitro ocular tolerance of NPs

To stablish ocular tolerance, HET-CAM *in vitro* test was applied. bLF-NPs and free bLF were tested in the CAM of 3 eggs for formulation, to determine the possible rapid irritation reaction. The addition of 1 M NaOH (positive control) produced an intense vasoconstriction and haemorrhage. In contrast, 0.9 % NaCl (negative control) produced no reaction over the time tested. Similarly, the application of free bLF solution or bLF-NPs into the CAM did not expose any sign of intolerance or vascular alteration. Considering Fig. 8, it is possible to confirm the suitability for ocular administration. As a result of the study, bLF-NPs are classified as a non-irritating substance at the ocular level (Table 7). These results are in agreement to those acquired by other authors with regard to polymeric NPs and bLF loaded for ocular administration (Abrego et al., 2015; S´anchez-Lo´pez et al., 2016; Varela-Ferna´ndez et al., 2021).

3.10.2. In vivo ocular tolerance of NPs

The optimized NPs formulation was evaluated using the primary irritation test or Draize test (Sa´nchez-Lo´pez et al., 2016). Due to the sensitive nature of the eye, possible irritating effects or ocular damage, the *in vivo* ocular irritation test was of great relevance. Rabbit model are preferred to carry out this assay since its eyes are wide and well-reported physiologically, in addition to its handling and availability. Despite this advantages, its eyes are normally more predisposed to irritation than the human eye (Yousry et al., 2017). The Draize test was carried out with the certainty that each of the instilled substances has already been tested by other authors individually (Gonzalez-pizarro et al., 2019b; Sa´nchez-

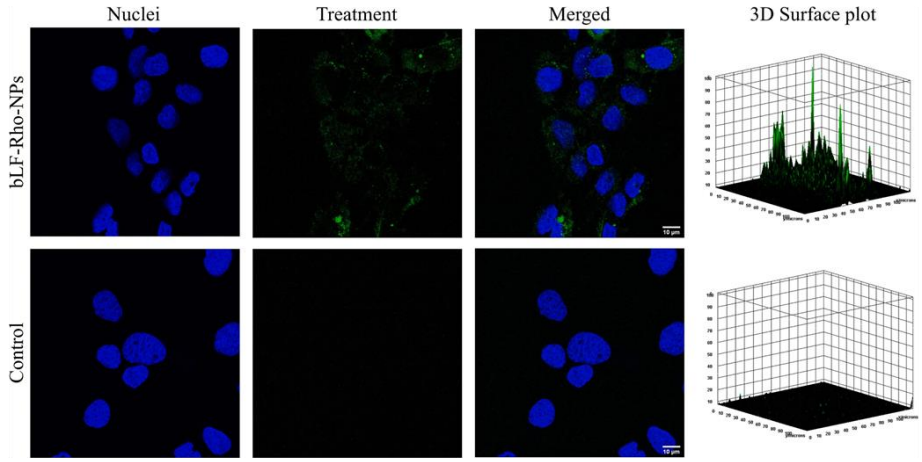

Fig 7. Cellular uptake of bLF-NPs (dilution 1:50). Images are representative of three independent biological experiments. 3D surface mapping analysis of internalized NPs (green signal).

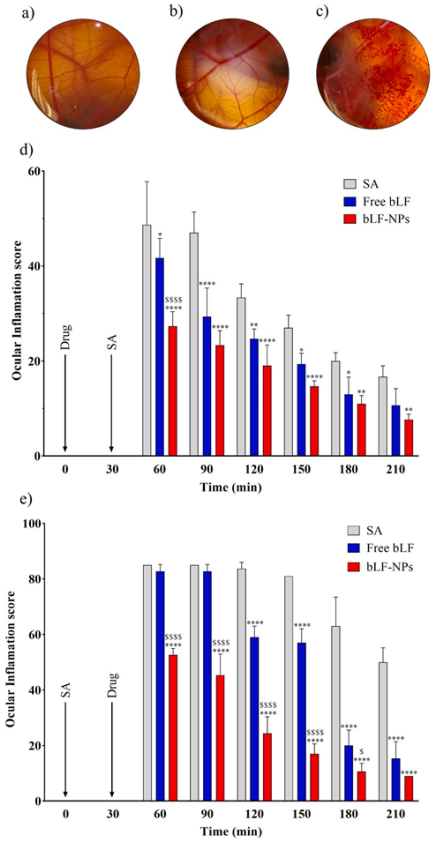

Fig. 8. HET-CAM test: (a) Free bLF; (b) bLF-NPs and (c) Positive control. (d) Ocular inflammation prevention. (e) Ocular inflammation treatment test. Values are expressed as mean ± SD; *p < 0.05, ** p < 0.01 and ***p < 0.001 and ****p < 0,0001 significantly lower than the inflammatory effect induced by SA; $p < 0.05, $$p < 0.01 and $$$p < 0.001 and $$$$p < 0,0001 significantly lower than the inflammatory effect induced by free bLF.

Table 7
In vitro ocular tolerance (HET-CAM).

Formulation	Medium score	Classification
bLF-NPs	0.07	Non-irritant
Free bLF (9.32 mg·mL^{-1})	0.07	Non-irritant

López et al., 2016). Draize test was accomplished considering the formulation safety, obtained in the previously performed *in vitro* irritation test. According to the obtained results, the total score for all rabbits was zero, without signs of ocular inflammation, redness, or increased tear production after instillation of bLF-NPs. Hence, the NPs could be classified as non-irritant substances.

3.11. *In vivo* anti-inflammatory efficacy

Two studies were carried out to determine the anti-inflammatory efficacy of the NPs, to confirm its capacity to prevent and treat ocular inflammation.

In vivo inflammatory prevention capacity of the formulations developed was evaluated. First, the formulations (bLF-NPs or free bLF) were applied, after 30 min, a drop of 0.5 % arachidonic acid (SA), the inflammation agent, was instilled. In the case of the positive control, physiological serum was administered instead of the bLF formulations. Notable differences were shown between the inflammation produced by SA and treated with bLF formulations or physiological serum. However, a slightly faster recovery and decrease in inflammation was observed in the case of those treated with bLF-NPs rather than free bLF over the time, probably due to tear clearance (Sánchez-López et al., 2016). bLF-NPs showed significant differences regarding positive control ($p < 0.0001$). Therefore, polymeric bLF-NPs exerted a preventive effect of inflammation due to the long-lasting release of bLF in the medium and its internalization on the corneal cells (Fig. 8d).

In vivo inflammatory treatment was also evaluated. Inflammation with significant hyperaemia was induced by SA after 30 min exposure (Fig. 8e). Then, bLF-NPs and free bLF were applied and the degree of inflammation was measured. It was observed that both formulations presented anti-inflammatory activity. However, the administration of bLF-NPs produced a statistically significant reduction of inflammation signs to a greater extent and faster than free bLF. This fact may be due to the improved ocular surface adherence of bLF-NPs, thus the residence time in the cornea might be longer (Sa´nchez-Lo´pez et al., 2016). In addition, bLF-NPs also promote bLF stability in aqueous solution (Wang et al., 2019; Wang et al., 2017). Therefore, bLF-NPs prolonged release and protection exerted by the polymeric matrix might increase corneal bLF concentration producing an anti-inflammatory action that lasted for a longer period. Polymeric nanostructured systems provide an enhanced bioavailability of bLF on the ocular surface, at the corneal level, and, as previously reported, possess the ability to reach deeper tissues such as vitreous humor or retina, being beneficial in the treatment of inflammation (Bisht et al., 2017; Gonzalez-Pizarro et al., 2018).

4. Conclusions

In summary, we have developed a novel nanotechnological tool in the treatment of ocular inflammation based on the incorporation of bLF, an anti-inflammatory and antioxidant high molecular weight protein, into polymeric NPs. This controlled release system has demonstrated to be stable without signs of flocculation or precipitation. Furthermore, corneal permeability and prolonged release of the active compound has been achieved improving the pharmacokinetic and pharmacodynamic drug profile. Both *in vitro* and *in vivo* studies confirm that these systems do not present any sign of cytotoxicity or ocular irritation. Moreover, the bLF-NPs present *in vivo* anti-inflammatory efficacy either in the prevention and in the treatment of symptoms. Therefore, bLF loaded PLGA NPs constitutes a suitable system to treat and prevent ocular inflammation.

CRediT authorship contribution statement

Ana López-Machado: Conceptualization, Methodology, Investigation, Writing – original draft, Visualization. **Natalia Díaz:** Methodology. **Amanda Cano:** Formal analysis, Writing – original draft, Visualization. **Marta Espina:** Formal analysis. **Josefa Badia:** Methodology, Resources, Writing – review & editing, Funding acquisition. **Laura Baldomà:** Methodology, Resources, Writing – review & editing, Funding acquisition. **Ana Cristina Calpena:** Methodology, Formal analysis. **Martina Biancardi:** Investigation. **Eliana B. Souto:** Writing – original draft. **María Luisa García:** Conceptualization, Resources, Writing – review & editing, Funding acquisition. **Elena Sánchez-López:** Conceptualization,

Investigation, Writing – review & editing.

Declaration of Competing Interest

The authors declare that they have no known competing financial interests or personal relationships that could have appeared to influence the work reported in this paper.

Acknowledgements

This work was supported by Portuguese Science and Technology Foundation (FCT/MCT) and from European Funds (PRODER/COMPETE) under the project reference UIDB/04469/2020 (strategic found), co-financed by FEDER, under the Partnership Agreement PT2020: UIDB/04469/2020.

References

Abbouda, A., Abicca, I., Fabiani, C., Scappatura, N., Pen˜a-García, P., Scrivo, R., Priori, R., Paroli, M.P., 2017. Psoriasis and Psoriatic Arthritis-Related Uveitis: Different Ophthalmological Manifestations and Ocular Inflammation Features. Semin. Ophthalmol. 32, 715–720. https://doi.org/10.3109/08820538.2016.1170161.

Abrego, G., Alvarado, H., Souto, E.B., Guevara, B., Halbaut, L., Parra, A., Calpena, A., Luisa, M., 2015. Biopharmaceutical profile of pranoprofen-loaded PLGA nanoparticles containing hydrogels for ocular administration. Eur. J. Pharm. Biopharm. 95, 261–270. https://doi.org/10.1016/j.ejpb.2015.01.026.

Aguilar, M., 2004. HPLC of Peptides and Proteins. Methods and Protocols, 1st ed. Methods in Molecular Biology. Humana Press, Totowa, NJ. Doi: 10.1385/1592597424.

Aketa, N., Yamaguchi, T., Asato, T., Yagi-Yaguchi, Y., Suzuki, T., Higa, K., Kurihara, T., Satake, Y., Tsubota, K., Shimazaki, J., 2017. Elevated Aqueous Cytokine Levels in Eyes With Ocular Surface Diseases. Am. J. Ophthalmol. 184, 42–51. https://doi.org/10.1016/j.ajo.2017.09.029.

Anaraki, N.I., Sadeghpour, A., Iranshahi, K., Toncelli, C., Cendrowska, U., Stellacci, F., Dommann, A., Wick, P., Neels, A., 2020. New approach for time-resolved and dynamic investigations on nanoparticles agglomeration. Nano Res. 13, 2847–2856. https://doi.org/10.1007/s12274-020-2940-4.

Andr´es-Guerrero, V., Bravo-Osuna, I., Pastoriza, P., Molina-Martinez, I.T., Herrero-Vanrell, R., 2017. Novel technologies for the delivery of ocular therapeutics in glaucoma. J. Drug Deliv. Sci. Technol. 42, 181–192. Doi: 20180227537138945O.

Anfuso, C.D., Olivieri, M., Fidilio, A., Lupo, G., Rusciano, D., Pezzino, S., Gagliano, C., Drago, F., Bucolo, C., 2017. Gabapentin attenuates ocular inflammation: In vitro and in vivo studies. Front. Pharmacol. 8, 1–10. https://doi.org/10.3389/fphar.2017.00173.

Bisht, R., Mandal, A., Jaiswal, J.K., Rupenthal, I.D., 2017. Nanocarrier mediated retinal drug delivery: overcoming ocular barriers to treat posterior eye diseases. Wiley Interdiscip. Rev. Nanomedicine. Nanobiotechnology e1473, 1–21. https://doi.org/10.1002/wnan.1473.

Bozdag, S., Dillen, K., Vandervoort, J., Ludwig, A., 2005. The effect of freeze-drying with different cryoprotectants and gamma-irradiation sterilization on the characteristics of ciprofloxacin HCl-loaded poly(D, L-lactide-glycolide) nanoparticles. J. Pharm. Pharmacol. 57, 699–707. https://doi.org/10.1211/0022357056143.

Cano, A., Ettcheto, M., Chang, J.H., Barroso, E., Espina, M., Kühne, B.A., Barenys, M., Auladell, C., Folch, J., Souto, E.B., Camins, A., Turowski, P., García, M.L., 2019. Dual-drug loaded nanoparticles of Epigallocatechin-3-gallate (EGCG)/Ascorbic acid enhance therapeutic efficacy of EGCG in a APPswe/PS1dE9 Alzheimer's disease mice model. J. Control. Release 301, 62–75. https://doi.org/10.1016/j.jconrel.2019.03.010.

Cano, A., Ettcheto, M., Espina, M., Auladell, C., Calpena, A.C., Folch, J., Barenys, M., S´anchez-Lo´pez, E., Camins, A., García, M.L., 2018. Epigallocatechin-3-gallate loaded PEGylated-PLGA nanoparticles: A new anti-seizure strategy for temporal lobe epilepsy. Nanomedicine Nanotechnology. Biol. Med. 14, 1073–1085. https://doi.org/10.1016/j.nano.2018.01.019.

Cano, A., S´anchez-Lo´pez, E., Espina, M., Egea, M.A., García, M.L., 2017. Polymeric nanoparticles of (-)-epigallocatechin gallate: A new formulation for the treatment of ocular diseases. J. Control. Release 259, e5–e195. https://doi.org/10.1016/j.jconrel.2017.03.046.

Caplan, A., Fett, N., Rosenbach, M., Werth, V.P., Micheletti, R.G., 2017. Prevention and management of glucocorticoid-induced side effects : A comprehensive review. J. Am. Acad. Dermatology 76, 201–207. https://doi.org/10.1016/j.jaad.2016.02.1241.

Carnahan, M.C., Goldstein, D.A., 2000. Ocular complications of topical, peri-ocular, and systemic corticosteroids. Curr. Opin. Ophtalmol. 11, 478–483. https://doi.org/10.1097/00055735-200012000-00016.

Carvajal-Vidal, P., F´abrega, M.J., Espina, M., Calpena, A.C., García, M.L., 2019. Development of Halobetasol-loaded nanostructured lipid carrier for dermal administration: Optimization, physicochemical and biopharmaceutical behavior, and therapeutic efficacy. Nanomedicine Nanotechnology. Biol. Med. 20, 1–10. https://doi.org/10.1016/j.nano.2019.102026.

Celia, C., Trapasso, E., Cosco, D., Paolino, D., Fresta, M., 2009. Turbiscan Lab® Expert analysis of the stability of ethosomes® and ultradeformable liposomes containing a bilayer fluidizing agent. Colloids Surfaces B Biointerfaces 72, 155–160. https://doi.org/10.1016/j.colsurfb.2009.03.007.

Chen, J., Zhou, J., Kelly, M., Holbein, B.E., Lehmann, C., 2017. Iron chelation for the treatment of uveitis. Med. Hypotheses 103, 1–4. https://doi.org/10.1016/j.mehy.2017.03.029.

Chen, X., Aqrawi, L.A., Utheim, T.P., Tashbayev, B., Utheim, Ø.A., Reppe, S., Hove, L.H., Herlofson, B.B., Singh, P.B., Palm, Ø., Galtung, H.K., Jensen, J.C.L., 2019. Elevated cytokine levels in tears and saliva of patients with primary Sjo¨gren's syndrome correlate with clinical ocular and oral manifestations. Sci. Rep. 9, 1–10. https://doi.org/10.1038/s41598-019-43714-5.

Derouiche, M.T.T., Abdennour, S., 2017. HET-CAM test. Application to shampoos in developing countries. Toxicol. Vitr. 45, 393–396. https://doi.org/10.1016/j.tiv.2017.05.024.

Diaz-Garrido, N., F´abrega, M.J., Vera, R., Gim´enez, R., Badia, J., Baldoma`, L., 2019. Membrane vesicles from the probiotic Nissle 1917 and gut resident Escherichia coli strains distinctly modulate human dendritic cells and subsequent T cell responses. J. Funct. Foods 61, 1–12. https://doi.org/10.1016/j.jff.2019.103495.

European Food Safety Authority, 2012. Scientific Opinion on bovine lactoferrin. EFSA J. 10, 1–26. https://doi.org/10.2903/j.efsa.2012.2701.

Fangueiro, J.F., Calpena, A.C., Clares, B., Andreani, T., Egea, M.A., Veiga, F.J., Garcia, M.L., Silva, A.M., Souto, E.B., 2016. Biopharmaceutical evaluation of epigallocatechin gallate-loaded cationic lipid nanoparticles (EGCG-LNs): In vivo, in vitro and ex vivo studies. Int. J. Pharm. 502, 161–169. https://doi.org/10.1016/j.ijpharm.2016.02.039.

Flanagan, J.L., Willcox, M.D.P., 2009. Role of lactoferrin in the tear film. Biochimie 91, 35–43. https://doi.org/10.1016/j.biochi.2008.07.007.

Foster, C.S., Kothari, S., Anesi, S.D., Vitale, A.T., Chu, D., Metzinger, J.L., Cero, O., 2016. The Ocular Immunology and Uveitis Foundation preferred practice patterns of uveitis management. Surv. Ophtalmol. 61, 1–17. https://doi.org/10.1016/j.survophthal.2015.07.001.

Fu, Y., Kao, W.J., 2010. Drug release kinetics and transport mechanisms of non-degradable and degradable polymeric delivery systems. Expert Opin. Drug Deliv. 7, 429–444. https://doi.org/10.1517/17425241003602259.

Ghasemi, H., 2018. Roles of IL-6 in Ocular Inflammation: A Review. Ocul. Immunol. Inflamm. 26, 37–50. https://doi.org/10.1080/09273948.2016.1277247.

Go´mez-Segura, L., Parra, A., Calpena-Campmany, A.C., Gimeno, A´., de Aranda, I.G., Boix-Montan˜es, A., 2020. Ex vivo permeation of carprofen vehiculated by PLGA nanoparticles through porcine mucous membranes and ophthalmic tissues. Nanomaterials 10, 16. https://doi.org/10.3390/nano10020355.

Gonza´lez-ch´avez, S.A., Ár´evalo-Gallegos, S., Rasco´n-Cruz, Q., 2009. Lactoferrin : structure, function and applications. Int. J. Antimicrob. Agents 33, 301–308. https://doi.org/10.1016/j.ijantimicag.2008.07.020.

Gonzalez-pizarro, R., Carvajal-vidal, P., Halbault, L., Cristina, A., Espina, M., Luisa, M., 2019. In-situ forming gels containing fluorometholone-loaded polymeric nanoparticles for ocular inflammatory conditions. Colloids Surfaces B Biointerfaces 175, 365–374. https://doi.org/10.1016/j.colsurfb.2018.11.065.

Gonzalez-Pizarro, R., Parrotta, G., Vera, R., Sa´nchez-Lo´pez, E., Galindo, R., Kjeldsen, F., Badia, J., Baldoma, L., Espina, M., García, M.L., 2019. Ocular penetration of fluorometholone-loaded PEG-PLGA nanoparticles functionalized with cell-penetrating peptides. Nanomedicine 14, 3089–3104. https://doi.org/10.2217/nnm-2019-0201.

Gonzalez-Pizarro, R., Silva-Abreu, M., Calpena, A.C., Egea, M.A., Espina, M., García, M.L., 2018. Development of fluorometholone-loaded PLGA nanoparticles for treatment of inflammatory disorders of anterior and posterior segments of the eye. Int. J. Pharm. 547, 338–346. https://doi.org/10.1016/j.ijpharm.2018.05.050.

Gu, Y., Wu, J., 2016. Bovine lactoferrin-derived ACE inhibitory tripeptide LRP also shows antioxidative and anti-inflammatory activities in endothelial cells. J. Funct. Foods 25, 375–384. https://doi.org/10.1016/j.jff.2016.06.013.

Han, F.Y., Thurecht, K.J., Whittaker, A.K., Smith, M.T., 2016. Bioerodable PLGA-based microparticles for producing sustained-release drug formulations and strategies for improving drug loading. Front. Pharmacol. 7, 1–11. https://doi.org/10.3389/fphar.2016.00185.

Hanstock, H.G., Edwards, J.P., Walsh, N.P., 2019. Tear lactoferrin and lysozyme as clinically relevant biomarkers of mucosal immune competence. Front. Immunol. 10, 1–11. https://doi.org/10.3389/fimmu.2019.01178.

Håversen, L., Ohlsson, B.G., Hahn-Zoric, M., Hanson, L.Å., Mattsby-Baltzer, I., 2002. Lactoferrin down-regulates the LPS-induced cytokine production in monocytic cells via NF-κB. Cell. Immunol. 220, 83–95. https://doi.org/10.1016/S0008-8749(03)00006-6.

Higuchi, A., Inoue, H., Kaneko, Y., Oonishi, E., Tsubota, K., 2016. Selenium-binding lactoferrin is taken into corneal epithelial cells by a receptor and prevents corneal damage in dry eye model animals. Sci. Rep. 6, 1–8. https://doi.org/10.1038/srep36903.

Iqbal, M., Zafar, N., Fessi, H., Elaissari, A., 2015. Double emulsion solvent evaporation techniques used for drug encapsulation. Intrnational J. Pharm. 496, 173–190. https://doi.org/10.1016/j.ijpharm.2015.10.057.

Kanwar, J.R., Roy, K., Patel, Y., Zhou, S., Singh, M.R., Singh, D., Nasir, M., Sehgal, R., Sehgal, A., Singh, R.S., Garg, S., Kanwar, R.K., 2015. Multifunctional Iron Bound Lactoferrin and Nanomedicinal Approaches to Enhance Its Bioactive Functions. Molecules 20, 9703–9731. https://doi.org/10.3390/molecules20069703.

Kanyshkova, T.G., Buneva, V.N., Nevinsky, G.A., 2001. Lactoferrin and Its Biological Functions. Biochem. 66, 5–13. https://doi.org/10.1023/a:1002817226110.

Kruzel, M.L., Zimecki, M., Actor, J.K., 2017. Lactoferrin in a context of inflammation-induced pathology. Front. Immunol. 8, 1–15. https://doi.org/10.3389/fimmu.2017.01438.

Lamprecht, A., Ubrich, N., Hombreiro P´erez, M., Lehr, C.-M., Hoffman, M., Maincent, P., 2000. Influences of process parameters on nanoparticle preparation performed by a double emulsion ultrasonication technique. Int. J. Pharm. 196, 177–182. https://doi.org/10.1016/S0378-5173(99)00422-6.

Lawrenson, J. G., 2018. Anterior Eye, in: Contact Lens Practice. Elsevier, pp. 10-27.e2. Doi: 10.1016/b978-0-7020-6660-3.00002-2.

Lee, J., Lee, J., Lee, S., Ahmad, T., Perikamana, S.K.M., Kim, E.M., Lee, S.W., Shin, H., 2020. Bioactive membrane immobilized with lactoferrin for modulation of bone regeneration and inflammation. Tissue Eng. - Part A 26, 1243–1258. https://doi.org/10.1089/ten.tea.2020.0015.

Li, P.C., Chen, S.C., Hsueh, Y.J., Shen, Y.C., Tsai, M.Y., Hsu, L.W., Yeh, C.K., Chen, H.C., Huang, C.C., 2021. Gelatin scaffold with multifunctional curcumin-loaded lipid-PLGA hybrid microparticles for regenerating corneal endothelium. Mater. Sci. Eng. C 120, 1–10. https://doi.org/10.1016/j.msec.2020.111753.

Liu, S., Chang, C.N., Verma, M.S., Hileeto, D., Muntz, A., Stahl, U., Woods, J., Jones, L. W., Gu, F.X., 2015. Phenylboronic acid modified mucoadhesive nanoparticle drug carriers facilitate weekly treatment of experimentallyinduced dry eye syndrome. Nano Res. 8, 621–635. https://doi.org/10.1007/s12274-014-0547-3.

Masoudipour, E., Kashanian, S., Hemati, A., Omidfar, K., Bazyar, E., 2017. Surfactant effects on the particle size, zeta potential, and stability of starch nanoparticles and their use in a pH- responsive manner. Cellulose 24, 4217–4234. https://doi.org/10.1007/s10570-017-1426-3.

Mazet, R., Yam´eogo, J.B.G., Wouessidjewe, D., Choisnard, L., G`eze, A., 2020. Recent advances in the design of topical ophthalmic delivery systems in the treatment of ocular surface inflammation and their biopharmaceutical evaluation. Pharmaceutics 12, 1–55. https://doi.org/10.3390/pharmaceutics12060570.

Nekkanti, V., Marwah, A., Pillai, R., 2015. Media milling process optimization for manufacture of drug nanoparticles using design of experiments (DOE). Drug Dev. Ind. Pharm. 41, 124–130. https://doi.org/10.3109/03639045.2013.850709.

Pearlman, E., Sun, Y., Roy, S., Karmakar, M., Hise, A.G., Szczotka-Flynn, L., Ghannoum, M., Chinnery, H.R., McMenamin, P.G., Rietsch, A., 2013. Host defense at the ocular surface. Int. Rev. Immunol. 32, 4–18. https://doi.org/10.3109/08830185.2012.749400.

Pillai-Kastoori, L., Schutz-Geschwender, A.R., Harford, J.A., 2020. A systematic approach to quantitative Western blot analysis. Anal. Biochem. 593, 1–16. https://doi.org/10.1016/j.ab.2020.113608.

Ponzini, E., Scotti, L., Grandori, R., Tavazzi, S., Zambon, A., 2020. Lactoferrin concentration in human tears and ocular diseases: A meta-Analysis. Investig. Ophthalmol. Vis. Sci. 61, 10. https://doi.org/10.1167/IOVS.61.12.9.

Qaddoumi, M.G., Ueda, H., Yang, J., Davda, J., Labhasetwar, V., Lee, V.H.L., 2004. The characteristics and mechanisms of uptake of PLGA nanoparticles in rabbit conjunctival epithelial cell layers. Pharm. Res. 21, 641–648. https://doi.org/10.1023/B:PHAM.0000022411.47059.76.

Rageh, A.A., Ferrington, D.A., Roehrich, H., Yuan, C., Terluk, R., Nelson, E.F., Montezuma, S.R., 2016. Lactoferrin Expression in Human and Murine Ocular Tissue. Curr. Eye Res. 41, 883–889. https://doi.org/10.3109/02713683.2015.1075220.

Ramos Yacasi, G.R., García Lo´pez, M.L., Espina García, M., Parra Coca, A., Calpena Campmany, A.C., 2016. Influence of freeze-drying and γ-irradiation in preclinical studies of flurbiprofen polymeric nanoparticles for ocular delivery using d-(+)-trehalose and polyethylene glycol. Int. J. Nanomedicine 11, 4093–4106. https://doi.org/10.2147/IJN.S105606.

Retamal Marín, R.R., Babick, F., Hillemann, L., 2017. Zeta potential measurements for non-spherical colloidal particles – Practical issues of characterisation of interfacial properties of nanoparticles. Colloids Surfaces A 532, 516–521. https://doi.org/10.1016/j.colsurfa.2017.04.010.

Rosa, L., Cutone, A., Lepanto, M.S., Paesano, R., Valenti, P., 2017. Lactoferrin : A Natural Glycoprotein Involved in Iron and Inflammatory Homeostasis. Int. J. Mol. Sci. 18, 1–26. https://doi.org/10.3390/ijms18091985.

Sah, A.K., Suresh, P.K., Verma, V.K., 2017. PLGA nanoparticles for ocular delivery of loteprednol etabonate: a corneal penetration study. Artif. Cells, Nanomedicine Biotechnol. 45, 1156–1164. https://doi.org/10.1080/21691401.2016.1203794.

Sa´nchez-Lo´pez, E., Egea, M.A., Cano, A., Espina, M., Calpena, A.C., Ettcheto, M., Camins, A., Souto, E.B., Silva, A.M., García, M.L., 2016. PEGylated PLGA nanospheres optimized by design of experiments for ocular administration of dexibuprofen-in vitro, ex vivo and in vivo characterization. Colloids Surfaces B Biointerfaces 145, 241–250. https://doi.org/10.1016/j.colsurfb.2016.04.054.

Sa´nchez-Lo´pez, E., Ettcheto, M., Egea, M.A., Espina, M., Calpena, A.C., Folch, J., Camins, A., García, M.L., 2017. New potential strategies for Alzheimer's disease prevention: pegylated biodegradable dexibuprofen nanospheres administration to APPswe/PS1dE9. Nanomedicine Nanotechnology. Biol. Med. 13, 1171–1182. https://doi.org/10.1016/j.nano.2016.12.003.

Sa´nchez-Lo´pez, E., Ettcheto, M., Egea, M.A., Espina, M., Cano, A., Calpena, A.C., Camins, A., Carmona, N., Silva, A.M., Souto, E.B., García, M.L., 2018. Memantine loaded PLGA PEGylated nanoparticles for Alzheimer's disease: In vitro and in vivo characterization. J. Nanobiotechnology 16, 1–16. https://doi.org/10.1186/s12951-018-0356-z.

Schultz, C., 2018. Ocular Inflammation. Gen. Intern. Med. Clin. Innov. 3, 1–3. https://doi.org/10.15761/gimci.1000163.

Seen, S., Tong, L., 2018. Dry eye disease and oxidative stress. Acta Ophthalmol. 96, e412–e420. https://doi.org/10.1111/aos.13526.

Shalom, Y., Perelshtein, I., Perkas, N., Gedanken, A., Banin, E., 2017. Catheters coated with Zn-doped CuO nanoparticles delay the onset of catheter-associated urinary tract infections. Nano Res. 10, 520–533. https://doi.org/10.1007/s12274-016-1310-8.

Sharma, S., Parmar, A., Kori, S., Sandhir, R., 2016. Trends in Analytical Chemistry PLGA-based nanoparticles : A new paradigm in biomedical applications 80, 30–40. https://doi.org/10.1016/j.trac.2015.06.014.

Shi, J., Votruba, A.R., Farokhzad, O.C., Langer, R., 2010. Nanotechnology in Drug Delivery and Tissue Engineering : From Discovery to Applications 3223–3230. Doi: 10.1021/nl102184c.

Smith, P.K., Krohn, R.I., Hermanson, G.T., Mallia, A.K., Gartner, F.H., Provenzano, M.D., Fujimoto, E.K., Goeke, N.M., Olson, B.J., Klenk, D.C., 1985. Measurement of protein using bicinchoninic acid. Anal. Biochem. 150, 76–85. https://doi.org/10.1016/0003-2697(85)90442-7.

Soni, V., Pandey, V., Tiwari, R., Asati, S., Tekade, R.K., 2019. Design and evaluation of ophthalmic delivery formulations, in: Basic Fundamentals of Drug Delivery. Elsevier Inc., pp. 473–538. Doi: 10.1016/B978-0-12-817909-3.00013-3.

Suzuki, Y., Wong, H., Ashida, K., Schryvers, A.B., Lo¨nnerdal, B., 2009. The N1 Domain of Human Lactoferrin is Required For Internalization By Caco-2 Cells and Targeting to the Nucleus. Biochemistry 47, 10915–10920. https://doi.org/10.1021/bi8012164. The.

Talluri, R.S., Hariharan, S., Karla, P.K., Mitra, A.K., 2010. Drug delivery to cornea and conjunctiva: Esterase- and protease-directed prodrug design, in: Encyclopedia of the Eye. Elsevier, Kansas City, pp. 42–53. Doi: 10.1016/B978-0-12-374203-2.00080-4.

Tamhane, M., Cabrera-Ghayouri, S., Abelian, G., Viswanath, V., 2019. Review of Biomarkers in Ocular Matrices: Challenges and Opportunities. Pharm. Res. 36, 1–35. https://doi.org/10.1007/s11095-019-2569-8.

Tao Meng, F., Hui Ma, G., Qiu, W., Guo Su, Z., 2003. W/O/W double emulsion technique using ethyl acetate as organic solvent: effects of its diffusion rate on the characteristics of microparticles. J. Control. Release 91, 407–416. Doi: 10.1016/s0168-3659(03)00273-6.

Tapia-Guerrero, Y.S., Del Prado-Audelo, M.L., Borbolla-Jim´enez, F.V., Giraldo Gomez, D. M., García-Aguirre, I., Colín-Castro, C.A., Morales-Gonza´lez, J.A., Leyva-Go´mez, G., Magan˜a, J.J., 2020. Effect of UV and gamma irradiation sterilization processes in the properties of different polymeric nanoparticles for biomedical applications. Materials (Basel). 13, 1–19. https://doi.org/10.3390/ma13051090.

Varela-Fern´andez, R., García-Otero, X., Díaz-Tom´e, V., Regueiro, U., Lo´pez-Lo´pez, M., Gonza´lez-Barcia, M., Lema, M.I., Otero-Espinar, F.J., 2021. Design, Optimization, and Characterization of Lactoferrin-Loaded Chitosan/TPP and Chitosan/Sulfobutylether-β-cyclodextrin Nanoparticles as a Pharmacological Alternative for Keratoconus Treatment. ACS Appl. Mater. Interfaces 13, 3559–3575. https://doi.org/10.1021/acsami.0c18926.

Vega, E., Egea, M.A., Calpena, A.C., Espina, M., García, M.L., 2012. Role of hydroxypropyl- β -cyclodextrin on freeze-dried and gamma-irradiated PLGA and PLGA – PEG diblock copolymer nanospheres for ophthalmic flurbiprofen delivery. Int. J. Nanomedicine 7, 1357–1371. https://doi.org/10.2147/IJN.S28481.

Wadhwa, S., Paliwal, R., Paliwal, S., Vyas, S., 2009. Nanocarriers in Ocular Drug Delivery: An Update Review. Curr. Pharm. Des. 15, 2724–2750. https://doi.org/10.2174/138161209788923886.

Wang, B., Timilsena, Y.P., Blanch, E., Adhikari, B., 2019a. Lactoferrin: Structure, function, denaturation and digestion. Crit. Rev. Food Sci. Nutr. 59, 580–596. https://doi.org/10.1080/10408398.2017.1381583.

Wang, B., Timilsena, Y.P., Blanch, E., Adhikari, B., 2017. Characteristics of bovine lactoferrin powders produced through spray and freeze drying processes. Int. J. Biol. Macromol. 95, 985–994. https://doi.org/10.1016/j.ijbiomac.2016.10.087.

Wang, T., Markham, A., Thomas, S.J., Wang, N., Huang, L., Clemens, M., Rajagopalan, N., 2019b. Solution Stability of Poloxamer 188 Under Stress Conditions. J. Pharm. Sci. 108, 1264–1271. https://doi.org/10.1016/j.xphs.2018.10.057.

Ward, P.P., Paz, E., Conneely, O.M., 2005. Multifunctional roles of lactoferrin : a critical overview. Cell. Mol. Life Sci. 62, 2540–2548. https://doi.org/10.1007/s00018-005-5369-8.

Yan, F., Zhang, C., Zheng, Y., Mei, L., Tang, L., Song, C., Sun, H., Huang, L., 2010. The effect of poloxamer 188 on nanoparticle morphology, size, cancer cell uptake, and cytotoxicity. Nanomedicine Nanotechnology. Biol. Med. 6, 170–178. https://doi.org/10.1016/j.nano.2009.05.004.

Yao, X., Bunt, C., Cornish, J., Quek, S.Y., Wen, J., 2014. Preparation, optimization and characterization of bovine lactoferrin-loaded liposomes and solid lipid particles modified by hydrophilic polymers using factorial design. Chem. Biol. Drug Des. 83, 560–575. https://doi.org/10.1111/cbdd.12269.

You, J., Yu, Y., Cai, K., Zhou, D., Zhu, H., Wang, R., Zhang, Q., Liu, H., Cai, Y., Lu, D., Kim, J.K., Gan, L., Zhai, T., Luo, Z., 2020. Enhancement of MoTe2 near-infrared absorption with gold hollow nanorods for photodetection. Nano Res. 13, 1636–1643. https://doi.org/10.1007/s12274-020-2786-9.

Yousry, C., Elkheshen, S.A., El-laithy, H.M., Essam, T., Fahmy, R.H., 2017. Studying the influence of formulation and process variables on Vancomycin-loaded polymeric nanoparticles as potential carrier for enhanced ophthalmic delivery. Eur. J. Pharm. Sci. 100, 142–154. https://doi.org/10.1016/j.ejps.2017.01.013.

3.2. Development of lactoferrin-loaded liposomes for the management of dry eye disease and ocular inflammation.

Ana López-Machado, Natalia Díaz, Amanda Cano, Marta Espina, Josefa Badía, Laura Baldomà, Ana Cristina Calpena, Eliana B. Souto, María Luisa García, Elena Sánchez-López.

Pharmaceutics

Año: 2021

ISSN: 10.3390/pharmaceutics13101698

Factor de impacto: 6,525

Resumen Gráfico

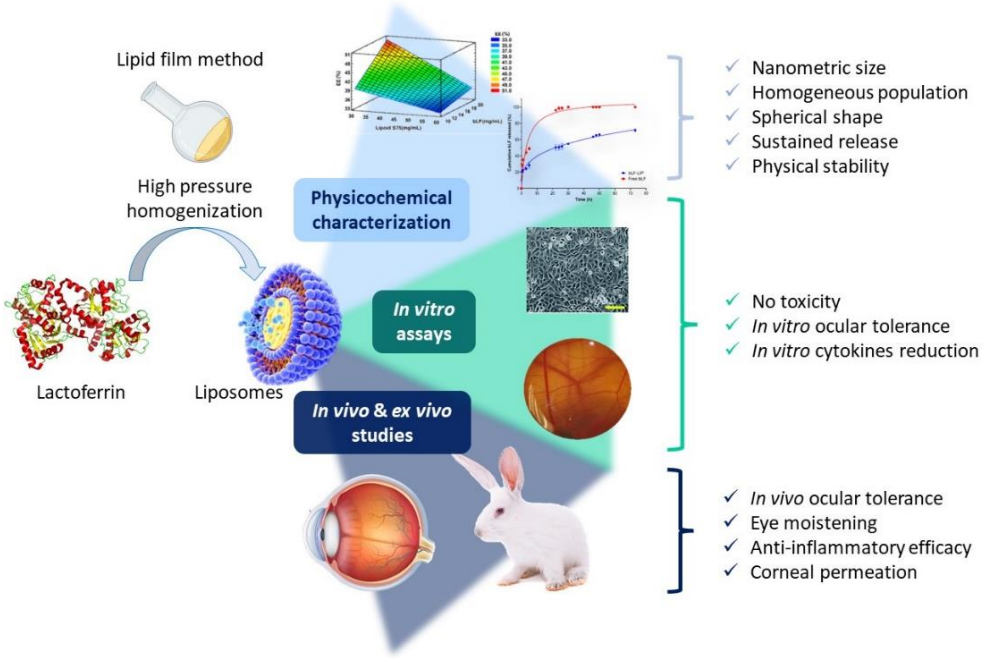

pharmaceutics

MDPI

Article

Development of Lactoferrin-Loaded Liposomes for the Management of Dry Eye Disease and Ocular Inflammation

Ana López-Machado [1,2], Natalia Díaz-Garrido [3,4,5], Amanda Cano [1,2,6], Marta Espina [1,2], Josefa Badia [3,4,5], Laura Baldomà [3,4,5], Ana Cristina Calpena [1,2], Eliana B. Souto [7], María Luisa García [1,2,*,†] and Elena Sánchez-López [1,2,6,*,†]

1 Department of Pharmacy and Pharmaceutical Technology and Physical Chemistry, Faculty of Pharmacy and Food Sciences, University of Barcelona, 08028 Barcelona, Spain; alopezmachado@ub.edu (A.L.-M.); acanofernandez@ub.edu (A.C.); m.espina@ub.edu (M.E.); anacalpena@ub.edu (A.C.C.)
2 Institute of Nanoscience and Nanotechnology (IN2UB), University of Barcelona, 08028 Barcelona, Spain
3 Department of Biochemistry & Physiology, Faculty of Pharmacy & Food Sciences, University of Barcelona, 08028 Barcelona, Spain; ndiazgarrido@ub.edu (N.D.-G.); josefabadia@ub.edu (J.B.); lbaldoma@ub.edu (L.B.)
4 Institute of Biomedicine (IBUB), University of Barcelona, 08028 Barcelona, Spain
5 Sant Joan de Déu Research Institute (IR-SJD), 08950 Barcelona, Spain
6 Biomedical Research Networking Centre in Neurodegenerative Diseases (CIBERNED), 28031 Madrid, Spain
7 Centre of Biological Engineering (CEB), Campus de Gualtar, University of Minho, 4710-057 Braga, Portugal; eliana.souto@ceb.uminho.pt
* Correspondence: marisagarcia@ub.edu (M.L.G.); esanchezlopez@ub.edu (E.S.-L.)
† Both authors have equally contributed.

check for updates

Citation: López-Machado, A.; Díaz-Garrido, N.; Cano, A.; Espina, M.; Badia, J.; Baldomà, L.; Calpena, A.C.; Souto, E.B.; García, M.L.; Sánchez-López, E. Development of Lactoferrin-Loaded Liposomes for the Management of Dry Eye Disease and Ocular Inflammation. *Pharmaceutics* **2021**, *13*, 1698. https://doi.org/10.3390/pharmaceutics13101698

Academic Editor: Christian Celia

Received: 27 September 2021
Accepted: 12 October 2021
Published: 15 October 2021

Publisher's Note: MDPI stays neutral with regard to jurisdictional claims in published maps and institutional affiliations.

Abstract: Dry eye disease (DED) is a high prevalent multifactorial disease characterized by a lack of homeostasis of the tear film which causes ocular surface inflammation, soreness, and visual disturbance. Conventional ophthalmic treatments present limitations such as low bioavailability and side effects. Lactoferrin (LF) constitutes a promising therapeutic tool, but its poor aqueous stability and high nasolacrimal duct drainage hinder its potential efficacy. In this study, we incorporate lactoferrin into hyaluronic acid coated liposomes by the lipid film method, followed by high pressure homogenization. Pharmacokinetic and pharmacodynamic profiles were evaluated in vitro and ex vivo. Cytotoxicity and ocular tolerance were assayed both in vitro and in vivo using New Zealand rabbits, as well as dry eye and anti-inflammatory treatments. LF loaded liposomes showed an average size of 90 nm, monomodal population, positive surface charge and a high molecular weight protein encapsulation of 53%. Biopharmaceutical behaviour was enhanced by the nanocarrier, and any cytotoxic effect was studied in human corneal epithelial cells. Developed liposomes revealed the ability to reverse dry eye symptoms and possess anti-inflammatory efficacy, without inducing ocular irritation. Hence, lactoferrin loaded liposomes could offer an innovative nanotechnological tool as suitable approach in the treatment of DED.

Keywords: lactoferrin; liposomes; dry eye disease; ocular anti-inflammatory; drug delivery

1. Introduction

Dry eye disease (DED) or keratoconjunctivitis sicca is considered a chronic multifactorial pathology of the ocular surface characterized by a loss of homeostasis of the tear film, associated with characteristic ocular symptoms, such as tear film instability and hyperosmolarity, ocular surface inflammation and damage. Moreover, neurosensory abnormalities play etiological roles, according to the TFOS DEWS II [1].

DED is one of the most frequent ocular surface conditions, affecting millions of patients globally, with a prevalence ranging from 5 to 50% [2,3]. Numerous risk factors are identified, including advanced age, female gender, Sjögren syndrome, androgen deficiency, several medications such as antihistamines, antidepressants, anxiolytics, or oral contraceptives, thyroid disease, menopause and smoking, among others [4]. Moreover, the continuous use

of contact lenses, certain environmental conditions as elevated pollution or low humidity, and the excessive smartphone and computer use has led to an increase in DED incidence especially among the younger population [4].

This osmotic and cellular stress at the ocular surface leads to irritation, ocular surface inflammation, soreness, blurred vision, and visual disturbance, resulting in a considerable decline in quality of life [3]. The elevated tear osmolarity, oxidative and mechanical stress-associated trigger a pro-inflammatory environment [5]. It is characterized by a broad release of pro-inflammatory mediators, cytokines, chemokines, and immune cells, leading to the extracellular matrix degradation and disruption of tight junctions between corneal epithelial cells. These conditions damage the ocular surface and favour inflammatory cell recruitment [6,7]. Thus, generating a self-inflammatory feedback loop that affects ocular function and integrity [4].

Topical administration is the preferred route to treat DED because it is painless and easy to handle. Artificial tears in the form of eyedrops, gel or ointment are used to lubricate dry eyes maintaining moisture of the eye's surface and often constitute the first line of therapy. They instantly relieve symptoms by lowering osmolarity and diluting inflammatory markers. However, artificial tears have no anti-inflammatory properties and do not deal with the fundamental pathogenesis of the disease [4]. Moreover, usual treatments for ocular inflammation comprises corticosteroids and non-steroidal anti-inflammatory drugs (NSAIDs), but its prolonged use involves severe side effects [8–10].

To overcome these drawbacks, lactoferrin (LF), an iron-binding glycoprotein with anti-inflammatory, antiviral, antibacterial, antifungal, antiparasitic, and immunomodulatory properties, has been investigated to address various ocular disorders [11–14].

LF has two highly homologous lobes with stable and reversible iron-binding capacity. LF is secreted by neutrophils and exocrine glands and it is found in colostrum and milk, tears, saliva, or gastrointestinal secretions [15]. At ocular level, LF amount is around 20–30% in basal and reflex tears and is also present in vitreous humour and a variety of ocular tissues, such as cornea, iris, and retinal pigment epithelium [16,17]. Moreover, recent studies have confirmed that the concentration of LF in tear fluids is considerably lower in patients with DED [18].

Most of the in vitro and in vivo studies have been assayed using bovine LF (bLF) since presents high sequence homology and has analogous functions to human LF [19]. bLF is generally recognized as safe substance (GRAS) by the Food and Drug Administration (FDA) and the European Food Safety Authority (EFSA) [19,20]. bLF is internalized by corneal epithelial cells and exerts its anti-inflammatory activity by attenuating the nuclear transcription factor kappa B (NF-κB)-induced transcription of genes for several inflammatory mediators [19,21–23].

Furthermore, reactive oxygen species (ROS) also play a major role in inflammatory processes. It has been reported that redox reactions are triggered by the presence of free iron, as it can easily accept or donate electrons, favouring the formation of ROS [18]. bLF can scavenge oxygen free radicals and hydroxyl, presenting a potential approach to treat DED [24,25].

However, one of the major challenges of ocular treatment, is the fast elimination via conjunctiva and nasolacrimal duct. It results in a pre-corneal drug half-life of 1–3 min and the need for frequent administrations [26]. In consideration of that, during the last years, drug administration using nanotechnological carriers for controlled release has attracted great interest, owing to improved stability, permeability, and bioavailability, offering advantages over traditional pharmaceutical forms [27,28].

Liposomes, since discovery by Bangham [29], have been widely used as delivery system for therapeutic and diagnostic compounds such as drugs, imaging agents, genes, or proteins [30]. Liposomes enhance the active corneal permeability due to their ability to come in close contact with cornea and conjunctiva as well as increase the extent of corneal uptake by prolonging the corneal contact time [31].

Therefore, bLF encapsulation into biocompatible and biodegradable liposomes has been carried out to overcome its compromised stability and increase therapeutic activity and half-life in the ocular surface, granting its prolonged release [31,32].

Moreover, one of the most utilised viscosity-building macromolecules in ocular delivery devices is hyaluronic acid (HA), an anionic polysaccharide with ocular mucomimetic properties, that exhibits the capacity of prolonging the precorneal residence time and reducing surface desiccation [3,33].

Therefore, the aim of this study was the development of a nanostructured drug delivery system based on HA-coated bLF-loaded liposomes for the treatment of DED. This study has focused on the incorporation of a high molecular weight protein within a lipidic nanocarrier. Likewise, different in vitro and in vivo studies have been carried out to assess their biocompatibility, capability to reverse DED symptoms, and anti-inflammatory efficacy. Moreover, achievement of sustained drug release and corneal permeability is essential for improving the pharmacokinetic and pharmacodynamic profile of bLF.

2. Materials and Methods

1. *Materials*

bLF was purchased from Azienda Chimica e Farmaceutica (Fiorenzuola d'Arda, Italy); fat-free soybean phospholipids with 70% phosphatidylcholine (lipoid S75) from Lipoid Gmbh (Ludwigshafen am Rhein, Germany); cholesterol and polysorbate 80 were purchased from Sigma Aldrich (Madrid, Spain); and Sodium hyaluronate was kindly donated by Bloomage Freda Biopharm (Jinan, China). Water filtered through a Millipore® MilliQ system was used for all the experiments and all the other reagents used were of analytical grade.

2. *Lactoferrin Loaded Liposomes Production*

bLF loaded liposomes (bLF-LIP) were produced using lipid film hydration method [34]. Briefly, the oil phase was formed dissolving a predetermined amount of lipids (lipoid S75) and cholesterol in 2 mL of ethanol (0.002% tocopherol). Aqueous phase was obtained by dissolving bLF (20 mg × mL^{-1}) and polysorbate 80 (P80) (3 mg·mL^{-1}) in 10 mL of deionized water. The lipid film was achieved by removing the organic solvent of the oil phase, under reduced pressure, using the rotary evaporation method (Rotavapor® R-210/215 Buchi, Flawil, Switzerland). To ensure complete solvent evaporation, the obtained film was subjected to a nitrogen flow for 10 min. Then, the aqueous phase was added to the lipid film and the mixture was homogenized using an ultrasonic bath (Transsonic Digitals, Elma Schmidbauer GmbH, Singen, Germany). Subsequently, the liposomes undergo a high-pressure homogenization process at 800 mbar at room temperature (2 cycles) by Stansted-pressure cell homogeniser-FPG12800 (Stansted Fluid Power, Harlow, UK). Finally, sodium hyaluronate was added under magnetic stirring to obtain a hyaluronic acid (HA) concentration of 0.1 mg·mL^{-1}.

3. *Optimization of Lactoferrin Loaded Liposomes*

A factorial 2^3 design matrix was employed to obtain the optimal formulation using StatGraphics Centurion XVI.I. This design was established to evaluate the effects of the independents variables (bLF, lipoid S75 and P80 concentrations) on the dependent parameters (average particle size (Z_{av}), polydispersity index (PI), zeta potential (ZP) and encapsulation efficiency (EE)) [35]. Each factor was examined at two levels and the responses were modelled through the first-order equation.

4. *Physicochemical Characterization*

Physicochemical parameters such as Z_{av} and PI or ZP were acquired by dynamic light scattering (DLS) and electrophoresis laser doppler, respectively, using a ZetaSizer NanoZS (Malvern Instruments, Malvern, UK). Samples were diluted (1:20) and measurements were carried out by triplicate at 25 °C [36].

EE was determined indirectly by quantifying the non-loaded bLF in the dispersion medium. bLF-LIP were ultracentrifugated at 4 °C and 45000 rpm for 60 min and the non-entrapped drug was isolated (Optima® Beckman Coulter, Brea, CA, USA). Then, supernatant was used to evaluate the EE according to the following equation [37]:

$$EE(\%) = \frac{\text{Total amount of bLF} - \text{Free amount of bLF}}{\text{Total amount of bLF}} \times 100 \quad (1)$$

The amount of the bLF in the aqueous phase was quantified by a reverse-phase high-performance liquid chromatography (RP-HPLC) method described elsewhere [38]. The methodology was validated in accordance with the international guidelines (EMEA, 2011), involving the evaluation of linearity, sensitivity, accuracy, and precision. Concisely, samples were quantified employing HPLC Waters 2695 separation module (Waters, Milford, MA, USA) and a Europa® Protein 300 C_8 column (5 µm, 250 × 4.6 mm) (Teknokroma Analítica, Barcelona, Spain). Mobile phase was constituted by a water phase containing 0.1% trifluoro acetic acid (TFA) and an organic phase consisting on acetonitrile/water/TFA (95:5:0.1), applying a gradient (from 95% to 25% of water phase and back in 8 min, keeping this ratio up to 25 min) at 0.75 mL·min^{-1}. Concentrations ranged from 0.1 to 1 mg·mL^{-1} were used in calibration curve. A diode array detector Waters® 2996 (Waters, Milford, MA, USA) at a wavelength of 219 nm was utilized to identify the bLF and data were handled using Empower 3® Software.

5. Morphological Characterization and Interaction Studies of Optimized Liposomes

The morphological evaluation of bLF-LIP was done using a Tecnai® G2 F20 TWIN cryogenic transmission electron microscopy (Cryo-TEM) (FEI Company, Hillsboro, OR, USA). Interaction studies were carried out through Differential Scanning Calorimetry (DSC). Thermograms were acquired on a Mettler TA 4000 system (Mettler, Greifensee, Switzerland) equipped with a DSC-25 cell. Samples were weighted in perforated aluminium pans (Mettler M3 Microbalance, Mettler, Greifensee, Switzerland) and heated under nitrogen flow at rate of 10 °C/min. An empty pan with similar attributes was utilized as reference [26].

6. Stability Studies

The stability of bLF-LIP stored at 4 and 25 °C was studied analysing light backscattering (BS) using Turbiscan® Lab (Formulaction, Toulouse, France). Twenty millilitres of sample were introduced into a glass measurement cell. The light source was a pulsed near infrared light source (λ = 880 nm) and it was detected by a BS detector at an angle of 45° from the incident beam. BS data were obtained at 1, 15, 30 and 60 days for 24 h at periods of 1 h. Likewise, measures of Z_{av}, PI, ZP, and EE were assayed.

7. Biopharmaceutical Behaviour

Direct dialysis bag technique was applied to examine the in vitro release profile due to the hydrophilicity of bLF [39]. bLF-LIP were placed in 1 mL dialysis bags (Float-A-Lyzer® dialysis device, 1000 kDa) (Repligen Corporation, Waltham, MA, USA) and phosphate buffer saline (PBS) 0.1 M buffer solution (pH 7.4) was employed as release medium and maintained under magnetic stirring at 37 °C. At various time intervals, 1 mL of release medium was removed and replaced with fresh buffer solution. RP-HPLC method previously described was used to analyse and data were adjusted to the most frequent pharmacokinetic models [40].

The ex vivo bLF permeation study from bLF-LIP was carried out using isolated corneas from New Zealand rabbits (2.5 kg males), according to the Ethics Committee of Animal Experimentation from the University of Barcelona (CEEA-UB), using a method described elsewhere [26]. Briefly, corneas were placed in a Franz-type cell between donor and receptor compartments. The receptor compartment was filled with PBS at 32 °C, under magnetic stirring. At pre-selected times, 300 µL of sample were withdrawn and replaced

by PBS. Samples were directly quantified by RP-HPLC [11,41]. Tests were carried out by triplicate and values were registered as the mean ± SD.

8. Cytotoxicity

Human corneal epithelial cells (HCE-2) (LGC Standards, Barcelona, Spain) were used to perform in vitro MTT cytotoxicity assay, previously described [42]. To elucidate the possible cytotoxicity of the formulation, cells were exposed to bLF-LIP and free bLF at different drug concentrations (0.2–2 $mg \cdot mL^{-1}$) for 24 h of incubation. The absorbance was read at λ = 560 nm by an automatic Modulus® Microplate Photometer (Turner BioSystems, Sunnyvale, CA, USA). Viability was expressed as percentage of negative control (untreated cells).

9. Ocular Tolerance

To assess ocular tolerance, in vitro HET-CAM test was carried out to guarantee that bLF-LIP was non-irritating after topical administration [43]. Irritation, coagulation, and haemorrhage phenomena in the chorioallantoic membrane of a fertilized chicken egg were evaluated by applying 300 µL of samples. The effects were checked during the first 5 min after the application. Test was performed according to the guidelines of ICCVAM (The Interagency Coordinating Committee on the Validation of Alternative Methods). Eggs (purchased from the farm G.A.L.L.S.A, Tarragona, Spain) were kept at 12 ± 1 °C for at least 24 h before putting them in the incubator with monitored temperature (37.8 °C) and humidity (50–60%) during the incubation days. At day 9 of incubation, 3 eggs were used for each group (free bLF, bLF-LIP, positive control (NaOH 0.1 M) and negative control (0.9% NaCl). Ocular irritation index (OII) was determined by the sum of the scores of each damage parameter according to the expression:

$$OII = \frac{(301 - H) \times 5}{300} + \frac{(301 - V) \times 7}{300} + \frac{(301 - C) \times 9}{300} \quad (2)$$

where H, V, and C are times (s) up to the start of haemorrhage (*H*), vasoconstriction (*V*), and coagulation (*C*), respectively. The formulations were categorized according to the following classification: OII ≤ 0.9 non-irritating; 0.9 < OII ≤ 4.9 weakly irritating; 4.9 < OII ≤ 8.9 moderately irritating; 8.9 < OII ≤ 21 irritating [43,44].

To confirm the results acquired from the HEM-CAM test, in vivo Draize test was carried out to evaluate primary ocular irritation [26]. New Zealand male albino rabbits of 2.0–2.5 kg were maintained under monitored ambient conditions with food and water ad libitum. For the experiment, 50 µL of bLF-LIP suspension were applied in the ocular conjunctival sac followed by a slight massage (n = 3/group). The appearance of irritation signs was evaluated at the time of instillation and following 1 h. If necessary, evaluation was also carried out at predefined intervals: 24 h, 48 h, 72 h, and 7 days. Draize test score was established by examining the ocular anterior segment and alterations in the structures of the cornea (turbidity or opacity), iris, and conjunctiva (congestion, chemosis, and swelling) (for detailed punctuation see Table A1 of Appendix A).

2.10. Induction and Treatment of Dry Eye

Induction of moderate dry eye was performed in male New Zealand albino rabbits (2.5 kg). The animals were treated for two weeks with two drops per day of 0.1% benzalkonium chloride in the right eye. Afterwards, the tear level was evaluated throughout Schirmer's test and the animals were treated for 5 days, either with bLF- LIP or with NaCl 0.9% (positive controls) [45].

Measurement of aqueous tear secretion was carried out using tear strips of Care Group® (Gujrat, India). General anaesthesia was induced to the rabbits using intramuscular ketamine/xylazine (35/5 mg/kg). Subsequently, 0.5% proparacaine (local anaesthetic) was administered topically. The lower eyelid was pulled down slightly and placed the test paper strip on the palpebral conjunctival vesica, which is near the junction of the middle

and outer third of the lower lid. The soaked length (in millimeters) of the paper strip was read 5 min later. The procedure was performed by triplicate [45].

11. Anti-Inflammatory Efficacy Assays

In vitro proinflammatory cytokines determination was assessed to evaluate the anti-inflammatory activity of the bLF-LIP and free bLF in HCE-2 cells. Samples were added to the culture medium at 2 mg·mL^{-1} of bLF and inflammation was induced with LPS (1 µg·mL^{-1}). Cells stimulated only with LPS were set as a positive control and untreated cells as a negative control. After 24 h incubation, supernatants were collected and pro-inflammatory cytokine levels (IL-8 and TNF-α) were quantified using the enzyme-linked immunosorbent assay (ELISA) according to manufacturer's instructions.

In vivo anti-inflammatory effectiveness was carried out throughout the evaluation test for the inflammation prevention ability and the anti-inflammatory efficacy. Assays were carried out using New Zealand male albino rabbits (n = 3/group), described previously. The activity of bLF-LIP in comparison with free bLF and NaCl 0.9% (control group) was measured. The inflammation prevention study consisted of the ocular application of 50 µL of each formulation. After 30 min of exposure, an inflammatory stimulus, 50 µL of 0.5% sodium arachidonate (SA) dissolved in PBS, was instilled in the right eye and the left eye was used as a control. In the anti-inflammatory treatment study, the inflammatory stimulus was applied 30 min before than the application of each formulation tested. The evaluation of prevention and treatment of each formulation were carried out from the first application up to 210 min, according to the Draize modified test scoring system (Table A1 of Appendix A) [26].

12. Statistical Analysis

Two-way ANOVA followed by Tukey post hoc test was performed for multi-group comparison. Student's t-test was used for two-group comparisons. All the data are presented as the mean ± S.D. Statistical significance was set at $p < 0.05$ by using GraphPad Prism 8.4.3. ImageJ was used to analyse images.

3. Results and Discussion

1. Optimization Study

Aiming to achieve the optimal formulation, the effect of independent variables such as concentrations of bLF, lipoid S75 and P80 on the physicochemical properties of the liposomes was evaluated by 2^3 factorial design. Table 1 shows the results obtained in the optimization study and the corresponding surface responses are showed in Figure 1.

Table 1. Values of the 2^{3+} star central composite rotatable factorial design, parameters and measured responses. Results presented as mean ± standard deviation.

	Independent Variables						Dependent Variables			
	cP80		cbLF		cLipoid-S75		Z_{av}	PI	ZP	EE
	(mg·mL^{-1})		(mg·mL^{-1})		(mg·mL^{-1})		(nm)		(mV)	(%)
1	−1	2.0	−1	10.0	−1	30.0	253.6 ± 2.2	0.121 ± 0.024	21.9 ± 0.6	49.2 ± 0.9
2	1	3.0	−1	10.0	−1	30.0	378.2 ± 1.4	0.317 ± 0.064	16.3 ± 0.3	40.6 ± 0.3
3	−1	2.0	1	20.0	−1	30.0	160.0 ± 3.9	0.179 ± 0.021	22.9 ± 0.2	55.4 ± 1.7
4	1	3.0	1	20.0	−1	30.0	85.0 ± 2.4	0.165 ± 0.033	22.7 ± 0.3	50.0 ± 2.5
5	−1	2.0	−1	10.0	1	60.0	471.7 ± 2.3	0.383 ± 0.046	24.3 ± 1.9	39.6 ± 4.0
6	1	3.0	−1	10.0	1	60.0	133.7 ± 1.4	0.292 ± 0.036	25.4 ± 0.6	33.1 ± 1.5
7	−1	2.0	1	20.0	1	60.0	602.8 ± 6.2	0.282 ± 0.016	26.0 ± 1.2	35.3 ± 0.4
8	1	3.0	1	20.0	1	60.0	242.1 ± 2.3	0.484 ± 0.031	26.2 ± 0.3	37.4 ± 0.3

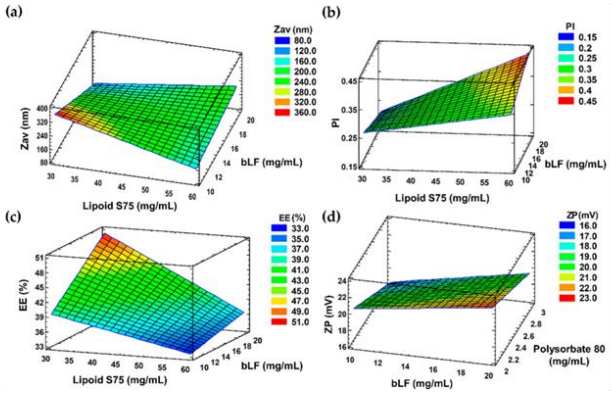

Figure 1. (**a**) Z_{av}, (**b**) PI, and (**c**) EE (%) surface response at a fixed P80 concentration (3 mg·mL^{-1}). (**d**) ZP surface response at a lipid concentration (30 mg·mL^{-1}).

Concerning Z_{av}, PI, and EE, lower lipids concentrations (30 mg·mL^{-1}) and higher protein concentrations (20 mg·mL^{-1}) favoured smaller particle size, lower PI values, and greater drug encapsulation. Regarding EE and ZP, the most influential variable was lipoid S75 concentration. bLF-LIP obtained had an average size of 85 nm, + 23 mV of ZP, and PI around 0.165, characteristic of a monomodal system, so they are suitable for ocular administration [46]. The PI is a measure of size distribution, agreeing with the literature, liposomal formulation is considered to be heterogeneous if the value is > 0.3 [47]. Cationic liposome formulation improves ocular surface adherence since ocular mucosa depicts slightly negative charge over its isoelectric point, thus increasing ocular bioavailability and prevent tear washout, prolonging corneal residence time [48]. P80 surfactant concentrations showed a slight effect on ZP, being inversely proportional. Increasing the concentration of surfactant resulted in significant particle size reduction. Results are in accordance with those obtained by other authors [49,50]. During the last years, the use of surfactants has been researched for the application in liposomal formulations. P80 is a biodegradable, non-ionic surfactant with great emulsifying properties, generally recommended as safe (GRAS) excipient with established safety profile, without causing ocular irritation [51]. It has reported to be well tolerated in ocular administration up to concentrations of 10% [52]. According to FDA GRAS list, the maximum allowable limit for its use in ophthalmic emulsions is 4% w/w, thus, in the factorial design we have chosen concentration in the range of 0.02–0.03% *w*/*w* to minimize adverse effects [53]. The addition of P80 decreases the interfacial tension and form smaller emulsion droplets by stabilizing oil/water interface [54].

From the factorial design outcomes, an optimized formulation (F4) was selected. As it can be noted in Table 1, the optimized bLF concentration was 20.00 mg·mL^{-1}, 30.00 mg·mL^{-1} of lipoid S75 and 3.00 mg·mL^{-1} of surfactant. The morphometry and surface charge (Z_{av}, PI and ZP) were established by photon correlation spectroscopy.

Final optimized formulation, obtained by adding hyaluronic acid (HA) 0.1 mg·mL^{-1} to formulation 4 of factorial design, retained suitable physicochemical properties for ocular administration (Table 2). Z_{av} and PI of the HA coated liposomes increased slightly after HA addition, whereas ZP became less positive. This is due to the fact that HA molecules possess a negatively charged carboxylic acid groups in their chemical structure which are able to interact with cationic liposomes (F4) by electrostatic forces. This caused a decrease in ZP and also led to a tiny increase in Z_{av} and PI [55].

Table 2. Physicochemical parameters of bLF-LIP after adding HA.

Z_{av}	PI	ZP	EE
(nm)		(mV)	(%)
90.5 ± 0.6	0.201 ± 0.070	20.5 ± 0.4	50.0 ± 3.0

Values are expressed as mean ± standard deviation.

2. *Morphological Characterization*

The addition of HA produced a slight increase in average size and PI and a slight ZP reduction, maintaining a strongly positive potential that favours the stability of the system through repulsion by electrostatic forces between particles [56]. Optimized bLF-LIP were characterized morphologically by imaging using cryo-TEM (Figure 2a). Images revealed a spherical and homogenous shape of bLF-LIP, without aggregation events and average particle dispersion similar to the obtained by DLS. According to other authors, the addition of P80 surfactant could contribute to the morphology improvement [54].

3. *Interaction Studies*

A factor that considerably influences the pharmacokinetics of the active substance is the physical state of the drug inside the nanosystem. DSC study was carried out to determine the physical state of bLF and the components of the formulation (Figure 2b). The bLF thermogram presents a severe endothermic accident related to its fusion, with a maximum temperature (T_{max}) of 170.41 °C which was not found in bLF-LIP. The cholesterol melting peak (T_{max} 150 °C) was also missing. The HA thermogram showed a wide and slight endothermic event around 100 °C, which appeared smoothed in the bLF-LIP thermogram compared with the lipoid S75 one, may be due to the melting of the polymer [57]. Typically, HA presents an exothermic peak at around 240 °C, attributed to the degradation of the polysaccharide. However, it is not observed since it is out of the temperature range, being not relevant to the study [57,58]. Likewise, the lipoid S75 thermogram did not exhibit any thermal events in the range, as a consequence of its low melting point [59]. Empty liposomes showed a similar thermogram to bLF-LIP. Data suggest the adequate incorporation of the formulation components within the bLF-LIP structure.

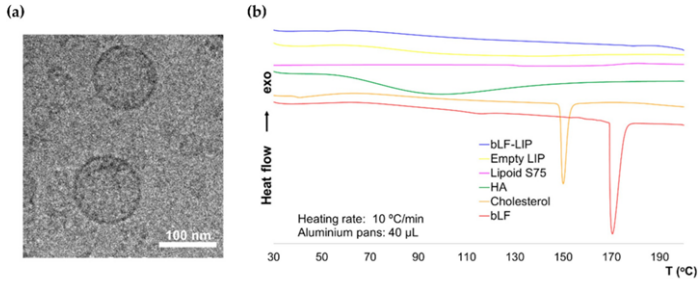

Figure 2. (**a**) Cryo-TEM image of bLF-LIP. (**b**) DSC thermograms of bLF-LIP.

3.4. *Stability of Lactoferrin Loaded Liposomes*

The BS profile of bLF-LIP was analysed over 60 days (Figure 3). This technique identifies the different destabilization phenomena of the colloidal suspension such as creaming, sedimentation and flocculation or coalescence [60]. The optimized formulation was stored at 4 and 25 °C. BS profile did not show any process of destabilization or migration of particles through the time or fluctuations greater than 5%, which indicates that bLF-LIP remain stable stored at both temperatures. This technique allows predicting the instability courses of liposomes earlier than detected by other methods [28]. Furthermore, several authors have reported that liposomal particle size bellow 90 nm allows for better

stability of the colloidal dispersion because gravitational phase partition is avoided by Brownian motion [56]. Moreover, the high value of ZP, over +20 mV, avoids electrostatic interaction between particles and the consequent phenomena of instability [61].

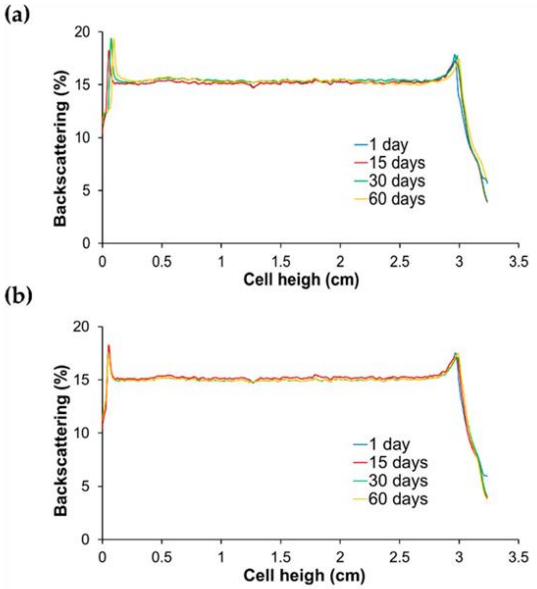

Figure 3. Backscattering profiles of bLF-LIP stored at: (**a**) 4 °C and (**b**) 25 °C.

3.5. Biopharmaceutical Behaviour of bLF-LIP

The in vitro release of bLF from bLF-LIP and free bLF exhibited a controlled and prolonged release of bLF from nanosystems. The release from liposomes arises as a function of physical and chemical processes that compromise membrane stability carrying out to a few or complete leakage of the liposomal content [62]. Drug release is highly dependent on the composition of the liposomal formulation, including amount of cholesterol, charge, side chains or acyl chain length; and also on the pharmacokinetic properties of the drug itself [62]. Free bLF showed an earlier release, reaching 98% after 24 h, adjusted to hyperbola equation release profile (AIC = 90.60, r^2 = 0.96), characterized by a rapid release followed by a prolonged release [63]. However, bLF-LIP formulation exhibited a more sustained release. Characterized by a faster bLF release stage, during the first 24 h, up to 50.53%, and afterward, the release speed of bLF-LIP decreased significantly, leading to a prolonged release up to 71.44% after 72 h, without reaching a plateau (Figure 4a).

The non-linear regression models such as Higuchi or Korsmeyer–Peppas are the two most utilized mathematical models to interpret non-linear diffusion profiles [64]. This biphasic release profile was probably caused by the drug diffusion through the bilayer and HA coating [65]. The Korsmeyer–Peppas release kinetics was the most accurate model to fit the experimental data, showing a minimum Akaike Information Criterion (AIC) value and a maximum r^2 value (AIC = 67.83, r^2 = 0.98). Data were adjusted to the most common kinetic models to obtain the best fit for bLF release (Table 3).

Table 3. Parameters for kinetic models of bLF-NPs and free bLF solution.

Models	bLF-NPs		Free bLF	
	AIC	R^2	AIC	R^2
Zero Order	94.76	0.84	115.87	0.64
First Order	94.33	0.84	93.67	0.94
Higuchi	77.93	0.96	104.86	0.86
Hyperbola	89.26	0.90	90.60	0.96
Korsmeyer–Peppas	n = 0.014		n = 0.022	
	67.83	0.98	93.91	0.94

Ex vivo corneal permeation of bLF-LIP and free bLF were performed to study their behaviour and compare different permeation parameters (Figure 4a). Permeation parameters were obtained by plotting the cumulative bLF permeated versus time, determining the x-intercept by linear regression analysis (Figure 4b) [66]. Table 4 shows that bLF-LIP formulation presents statistically significant differences ($p < 0.05$) against free bLF in all examined permeation parameters. According to the steady-state flux (J) value is twice higher in bLF-LIP, therefore bLF from LIPs infused the cornea faster than free bLF. All permeation parameters follow similar ratios, with the permeability coefficient (K_P) and the quantity permeated at 24 h (Q24) greater in bLF-LIP than free bLF. Otherwise, the opposite ratio is observed in the case of QR, being twice longer the bLF quantity retained in the cornea from free bLF sample. Owing to their high lipophilicity, the epithelium layer of the cornea, composed of lipid, favoured the release of bLF-LIP and prevents the entry of hydrophilic substances, such as free bLF solution, thus retaining a significant part of the protein in the cornea [67]. Furthermore, particles below 100 nm, particles with deformable nature and positively charged liposomes could potentially facilitate their permeability and absorption through the corneal membrane, leading to an enhance in all pharmacokinetic parameters [31,47]. Therefore, bLF-LIP may efficiently release bLF to the specified area by delivering bLF slowly across the corneal tissue, which would be helpful for the management of DED and the derived ocular inflammation.

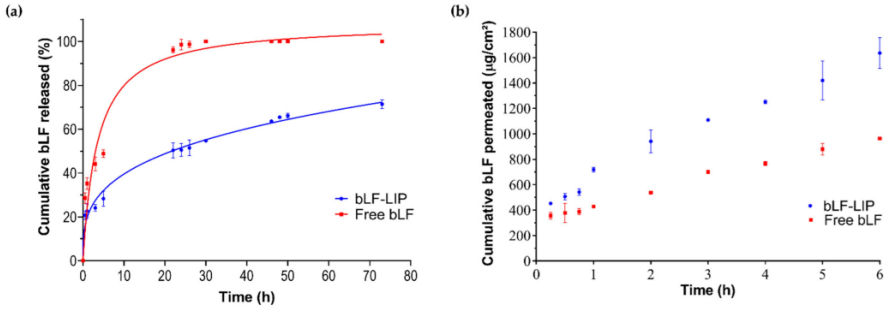

Figure 4. Biopharmaceutical behaviour. (**a**) In vitro release profile of bLF-LIP (Korsmeyer–Peppas equation) against free bLF (hyperbola equation). (**b**) Ex vivo corneal permeation profile of bLF-LIP compared with free bLF and permeation parameters.

Table 4. Pharmacokinetic parameters adjusted to linear regression of the ex vivo corneal permeation of bLF-LIP against bLF.

Parameters	Free bLF	bLF-LIP
J ($\mu g \cdot h^{-1} \cdot cm^{-2}$)	171.79 ± 9.83	317.50 ± 67.84 *
Kp · 10^3 ($cm \cdot h^{-1}$)	8.59 ± 0.49	15.88 ± 3.39 *
Q24 (μg)	2635.83 ± 151.49	4874.52 ± 1042.71 *
QR ($\mu g \cdot g^{-1} \cdot cm^{-2}$)	1.12 ± 0.01	0.55 ± 0.02 **

Statistical significance: * $p < 0.05$, ** $p < 0.0001$. J, steady-state flux; Kp, permeability coefficient; Q24, permeated amount at 24 h; QR, retained amount.

3.6. Cytotoxicity

To settle liposomes ocular administration suitability, in vitro MTT cytotoxicity assay was evaluated in HCE-2 cells (Figure 5). Results showed that after 24 h incubation both bLF-LIP and free bLF did not cause relevant cytotoxic effects. Cell viability was higher than 80% at all concentrations tested.

LF is one of the most abundant components in the healthy tear fluid, representing 20–30% of the total proteins, varying between 0.63–2.9 $mg \cdot mL^{-1}$, depending on gender and age [68,69]. The basal tear flow (1 $\mu L \cdot min^{-1}$) is considerably increased upon acute stimulation, the expression of LF is upregulated to inhibit the production of inflammatory cytokines [18]. Moreover, LF contributes to antimicrobial activity via inhibiting the growth of bacteria and mitigates oxidative stress via iron retention mechanism [5,16]. However, current research has proved that these activities are inactive in DED patients [70]. It is due to the fact that there is a reduced LF amount at ocular level, since tear volumes have positive correlation with LF concentration [18]. Hence bLF-LIP could provide a sustained release of protein and improve its bioavailability, for cases in which LF tear concentration is compromised.

Regarding other formulation components, it has been reported that lipoid s75 (soybean phospholipids with 70% phosphatidylcholine) is non-immunogenic, biocompatible, biodegradable and a safe substance used for the development of lipid vehicles for delivering pharmacological substances with a broad range of solubilities at ocular level [62,71].

HA is widely used in the management of DED. Is a naturally occurring, endogenous, glycosaminoglycan polymer present in various tissue fluids in human body, mainly in the extracellular matrix [72]. In particular, high molecular weight HA (>1000 kDa) was reported to have some immunosuppressive, antioxidant, anti-inflammatory, anti-angiogenic effect, and wound repair capacity [73].

These outcomes verify the biocompatibility of the developed bLF-LIP with corneal cells, matching with the generally recognized as safe (GRAS) designation of the formulation components [71].

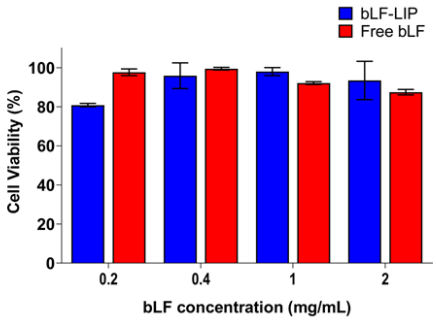

Figure 5. Effect of bLF-LIP on the viability of HCE-2 cells. The 100% cell viability corresponds with the average of MTT reduction values of untreated cells.

3.7. Ocular Tolerance

In vitro ocular tolerance was studied by HET-CAM test. bLF-LIP and free bLF were proved to verify the potential instant irritation response in the CAM of 3 eggs. The addition of free bLF solution or bLF-LIP did not reveal any sign of damage or vascular alteration. Likewise, negative control (0.9% NaCl) did not produce any response over the time tested. In contrast, the addition of positive control (1M NaOH) generated a severe vasoconstriction and haemorrhage [74]. As shown in Figure 6, the suitability for ocular administration is confirmed. The outcome showed that, at the ocular level, bLF-LIP are classified as a non-irritating substance (Table 5). These results agree to those obtained by in vitro HCE-2 cytotoxicity assays.

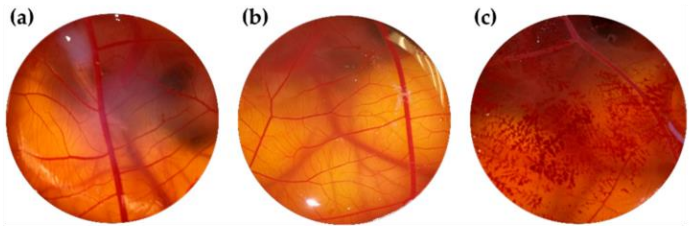

Figure 6. HET-CAM test assessed with different formulations: (**a**) bLF-LIP; (**b**) free bLF and (**c**) positive control.

Table 5. Ocular tolerance: in vitro (HET-CAM) and in vivo (Draize test).

Formulation	Medium Score		Classification
	HET-CAM	Draize	
bLF-LIP	0.07 ± 0.00	0.00 ± 0.00	Non-irritant
Free bLF (20 mg·mL^{-1})	0.07 ± 0.00	0.00 ± 0.00	Non-irritant

In vivo ocular tolerance Draize test or primary irritation test was assessed to verify the irritation potential of the optimized liposomes formulation [75]. Rabbit model is commonly chosen to perform these experiments because its ocular physiology is well known and implies easy manipulation. Moreover, rabbit eye is usually more susceptible to irritation than the human eye [76]. Due to the high sensibility of the ocular surface, it was essential to check possible irritating effects or ocular damage caused [26].

The in vivo test was assessed considering taking into account that each of the formulation compounds was safe and biocompatible, based on the previously performed in vitro HET-CAM test and analysed by other authors [48,77].

Results showed no signs of redness, ocular inflammation, or increased tear production following instillation of bLF-LIP, being the total score for each rabbit zero (Table 5). Therefore, bLF-LIP could be classified as non-irritant substance.

3.8. Therapeutic Efficacy against Dry Eye Disease

Aiming to verify the therapeutic efficacy of the developed bLF-LIP in the treatment of dry eye, the Schirmer's test was carried out. A severe decrease in the aqueous tear secretion was achieved after the application of benzalkonium chloride for 2 weeks. Figure 7 showed a considerable difference between the tear volume secreted by the dry eye of positive control and by the group treated with liposomes. There were statistically significant differences on days 0 and 5 in bLF-LIP group, being 6.25-fold higher after 5 days of treatment, and 4.5-fold greater than the eye treated with physiological saline. These results matched with the result obtained by other authors. One of these studies reported an ameliorated dry eye symptoms and tear film stability in patients supplemented with oral LF [78]. Furthermore,

these results are supported by other authors that studied the ocular instillation of LF in a rabbit dry eye model, resulting in a restoration of corneal epithelial integrity, suggesting its potential use for treating DED [77]. In the case of the developed bLF-LIP formulation, improved drug pharmacokinetics and pharmacodynamics were observed thanks to its encapsulation within biocompatible lipidic nanosystem.

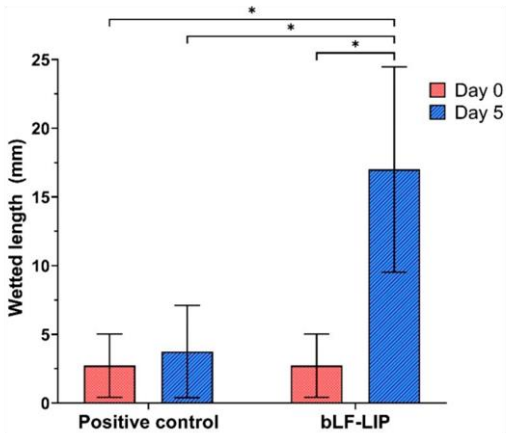

Figure 7. Schirmer's test results. Values are expressed as mean ± SD; * $p < 0.05$ significantly higher than the secreted tear by non-treated with bLF-LIP eye for 5 days.

9. Anti-Inflammatory Efficacy

1. In Vitro Assays: IL-8 and TNF-α Determination

There is evidence that in the dry eye syndrome and chronic inflammation-associated, tears present overexpression of different inflammatory mediators, specially IL-8 and TNF-α cytokines [79]. Hence, the in vitro cytokines determination was carried out in HCE-2 cells to assess the ability of bLF-LIP to inhibit the inflammatory response caused by LPS (Figure 8a,b) [80].

Various authors have studied the influence of DED on the presence of different inflammation markers at ocular level. It has been reported that there is a significant increase of inflammation, doubling the concentration of IL-8 in patients with DED compared with healthy controls [2,81]. This high concentration of IL-8 at the tear level leads to the migration of different immune cells towards the eye, triggering the aggravation of the ocular inflammation symptoms present in the disease [15]. At the same time, higher tear concentration of another inflammatory cytokine, TNF-α, had been detected, keeping the inflammatory environment in patients with different ophthalmopathies-associated [79,81,82].

In Figure 8 it can be observed that the highest levels of cytokines induced by LPS were obtained in the absence of bLF-LIP (positive control). Administration of bLF-LIP considerably diminished the expression of IL-8 and TNF-α, reaching similar levels to those obtained with free bLF ($p < 0.05$). This fact indicated that an anti-inflammatory effect was achieved with the administration of bLF-LIP in corneal cells.

The findings are in accordance with what has been described for LF, which has the capacity to modulate the expression of various cytokines through different mechanisms [77]. Including the interaction with cell surface receptors involved in the inflammatory response, by binding to CD14 receptor, thus diminishing NF-κB-induced transcription of various genes encoding inflammatory mediators [13,21,83]. Regarding to its iron-chelating ability, LF can manage the oxidative burst produced by neutrophils and macrophages, by oxygen free radical and hydroxyl scavenging activities, thus mitigating the inflammatory response and tissue damage caused by ROS [19].

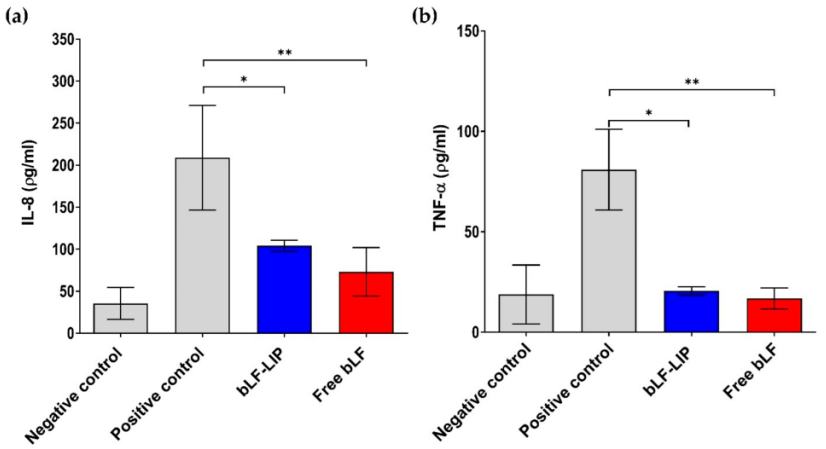

Figure 8. (**a**) Quantification of secreted IL-8 proinflammatory cytokine in LPS-stimulated HCE-2 cells; (**b**) quantification of secreted TNF-α. Negative control: no treatment; Positive control: LPS. Values are expressed as the mean ± SD; * $p < 0.05$; ** $p < 0.01$ significantly lower than LPS-induced cytokine concentration.

3.9.2. In Vivo Assays

In vivo anti-inflammatory efficacy was assayed to confirm the capacity of the liposomes to prevent and treat ocular inflammation through two different tests.

In vivo inflammatory prevention test showed significant differences between the degree of inflammation treated with bLF formulations or physiological serum during all the timepoints tested. Nevertheless, eyes treated with bLF-LIP presented a faster swelling reduction rather than free bLF, mainly owing to tear clearance in case of free bLF and the improved ocular surface adherence of liposomes, thus presenting longer residence time in the cornea [26]. bLF-LIP exhibited significant differences regarding positive control over the time. Thus, bLF-LIP exhibited a preventive effect of inflammation caused by the sustained release of bLF to the corneal cells (Figure 9a).

In addition, the in vivo inflammation treatment was assessed. Liposomes and free bLF were applied after 30 min of SA exposure, and the degree of inflammation was quantified.

Figure 9b revealed that the degree of inflammation was significantly reduced after the first hour post-administration of bLF-LIP. This fact confirms its controlled bLF release from liposomes, providing a longer anti-inflammatory activity and enhancing its bioavailability. The presence of a cationic surface charge in the lipidic nanocarrier, may increase the residence time by interaction with the negatively charged corneal epithelium and the mucins from tears fluid and conjunctiva [56]. Moreover, statistically significant differences were observed between the positive inflammation control and the group treated with free bLF, displaying its anti-inflammatory activity [19]. After 90 min of contact, both bLF formulations were effective in treating inflammation symptoms. However, a greater and faster reduction was observed in the case of bLF-LIP during the assay. Hence, it can be concluded that the controlled release system based on bLF-LIP has ocular anti-inflammatory activity, both for prevention level and inflammation treatment.

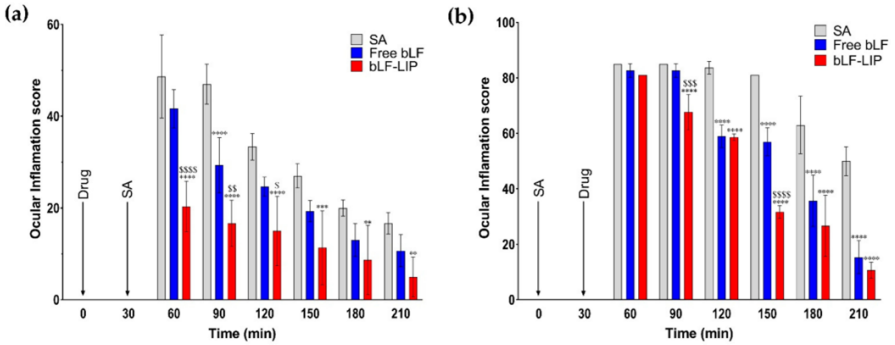

Figure 9. (**a**) Ocular inflammation prevention. (**b**) Ocular inflammation treatment test. Values are expressed as mean ± SD; * $p < 0.05$, ** $p < 0.01$ and *** $p < 0.001$ and **** $p < 0.0001$ significantly lower than the inflammatory effect induced by SA; $ $p < 0.05$, $$ $p < 0.01$ and $$$ $p < 0.001$ and $$$$ p <0.0001 significantly lower than the inflammatory effect induced by free bLF.

4. Conclusions

In summary, a novel nanotechnological tool has been developed for the management of DED and its ocular complications. It is based on the encapsulation of bLF, an anti-inflammatory and antioxidant high molecular weight protein, into hyaluronic acid coated liposomes. This nanosystem has been proven to be physically stable with a prolonged bLF release as well as high corneal permeability, thus improving biopharmaceutical bLF behaviour. In addition, in vitro and in vivo tests corroborate that the developed formulation is biocompatible without any sign of ocular irritation or cytotoxicity. Furthermore, bLF-LIP exert the ability to revert DED symptoms by restoring physiological tear levels. At the same time, bLF-LIP were able to decrease inflammation both in vitro and in vivo. Hence, hyaluronic acid coated bLF-loaded liposomes constitute a suitable system to treat and prevent DED and ocular inflammation.

5. Patents

Liposomes described in this work have been patented under the reference EP 3603621 A1 and this patent has recently been extended to the US under the reference US 10,835,494 B2.

Author Contributions: Conceptualization, E.S.-L., M.E., and M.L.G.; methodology, A.L.-M., N.D.-G., M.E., A.C.C., J.B. and L.B.; formal analysis, A.L.-M., A.C., A.C.C., E.B.S., E.S.-L. and M.L.G.; investigation, A.L.-M., N.D.-G. and M.E.; resources, E.S.-L. and M.L.G.; writing—original draft preparation, A.L.-M., A.C., M.E. and E.S.-L. writing—review and editing, E.S.-L., J.B., L.B., E.B.S., and M.L.G., funding acquisition, J.B., L.B. and M.L.G. All authors have read and agreed to the published version of the manuscript.

Funding: This work was supported by Portuguese Science and Technology Foundation (FCT/MCT) and from European Funds (PRODER/COMPETE) under the project reference UIDB/04469/2020 (strategic found), co-financed by FEDER, under the Partnership Agreement PT2020: UIDB/04469/2020.

Institutional Review Board Statement: The study was conducted according to the guidelines of the Declaration of Helsinki and approved by the Institutional Review Board (or Ethics Committee) of the University of Barcelona (protocol code 454/18 approved on the 12 of July of 2021).

Informed Consent Statement: Not applicable.

Acknowledgments: The authors A.L.-M., E.S.-L., M.L.G., and M.E. would like to acknowledge 2017SGR1477.

Conflicts of Interest: The authors declare no conflict of interest.

Appendix A

Table A1. Rating scale to evaluate the degree of ocular irritation (Draize test).

Structure	Injury	Evaluation	Score
CORNEA	(A) Degree of cloudiness or opacity		Corneal score: A × B × 5 Maximum score: 80
	-Absence of ulceration	0	
	-Diffuse areas	1	
	-Translucent areas	2	
	-Opalescent areas	3	
	-Full opacity	4	
	(B) Affected areas		
	-None	0	
	-A quarter or less	1	
	-More than a quarter but without means	2	
	-More than three quarters up a whole plane	3	
	-More than half but less than three quarters	4	
IRIS	(A) Iris injury score		Iris score: A·× 5 Maximum score: 10
	-Normal	0	
	-Deep folds, congestion, swelling, moderate circumcorneal injection	1	
	-No reaction to light, haemorrhage, great destruction	2	
CONJUNCTIVA	(A) Redness		Conjunctival score: (A + B + C) × 2 Maximum score: 20
	-Normal glasses	0	
	-Some clearly injected vessels	1	
	-Diffuse redness	2	
	-Big diffuse redness	3	
	(B) Chemosis or Inflammation		
	-None	0	
	-Some	1	
	-Marked with partial disorder of the eyelids	2	
	-Eyelid more or less closed	3	
	-Semi eyelids	4	
	(C) Sweat		
	-None	0	
	-Any amount anomalous	1	
	-Wetting and eyelid hairs	2	
	-Periocular wetting	3	
Calculation of the Ocular Irritation Index		OII	Classification
OII = Cornea (A·× B·× 5) + Iris (A × 5) + Conjunctiva ((A + B + C) × 2)		0	Non-irritant
		0–15	Weakly irritant
		>15–30	Moderately irritant
		>30–50	Irritant
		>50	Extremely irritant

References

1. Craig, J.P.; Nelson, J.D.; Azar, D.T.; Belmonte, C.; Bron, A.J.; Chauhan, S.K.; de Paiva, C.S.; Gomes, J.A.P.; Hammitt, K.M.; Jones, L.; et al. TFOS DEWS II Report Executive Summary. *Ocul. Surf.* **2017**, *15*, 802–812. [CrossRef] [PubMed]
2. Roda, M.; Corazza, I.; Reggiani, M.L.B.; Pellegrini, M.; Taroni, L.; Giannaccare, G.; Versura, P. Dry Eye Disease and Tear Cytokine Levels—A Meta-Analysis. *Int. J. Mol. Sci.* **2020**, *21*, 3111. [CrossRef] [PubMed]
3. Agarwal, P.; Craig, J.; Rupenthal, I. Formulation Considerations for the Management of Dry Eye Disease. *Pharmaceutics* **2021**, *13*, 207. [CrossRef]
4. Joossen, C.; Baán, A.; Moreno-Cinos, C.; Joossens, J.; Cools, N.; Lanckacker, E.; Moons, L.; Lemmens, K.; Lambeir, A.-M.; Fransen, E.; et al. A novel serine protease inhibitor as potential treatment for dry eye syndrome and ocular inflammation. *Sci. Rep.* **2020**, *10*, 1–14. [CrossRef]
5. Seen, S.; Tong, L. Dry eye disease and oxidative stress. *Acta Ophthalmol.* **2018**, *96*, e412–e420. [CrossRef]

6. Mazet, R.; Yaméogo, J.B.G.; Wouessidjewe, D.; Choisnard, L.; Gèze, A. Recent Advances in the Design of Topical Ophthalmic Delivery Systems in the Treatment of Ocular Surface Inflammation and Their Biopharmaceutical Evaluation. *Pharmaceutics* **2020**, *12*, 570. [CrossRef] [PubMed]
7. Anfuso, C.D.; Olivieri, M.; Fidilio, A.; Lupo, G.; Rusciano, D.; Pezzino, S.; Gagliano, C.; Drago, F.; Bucolo, C. Gabapentin Attenuates Ocular Inflammation: In vitro and In vivo Studies. *Front. Pharmacol.* **2017**, *8*, 173. [CrossRef]
8. Foster, C.S.; Kothari, S.; Anesi, S.D.; Vitale, A.T.; Chu, D.; Metzinger, J.L.; Cerón, O. The Ocular Immunology and Uveitis Foundation preferred practice patterns of uveitis management. *Surv. Ophthalmol.* **2016**, *61*, 1–17. [CrossRef] [PubMed]
9. Caplan, A.; Fett, N.; Rosenbach, M.; Werth, V.P.; Micheletti, R.G. Prevention and management of glucocorticoid-induced side effects: A comprehensive review. *J. Am. Acad. Dermatol.* **2017**, *76*, 201–207. [CrossRef] [PubMed]
10. Carnahan, M.C.; Goldstein, D.A. Ocular complications of topical, peri-ocular, and systemic corticosteroids. *Curr. Opin. Ophthalmol.* **2000**, *11*, 478–483. [CrossRef] [PubMed]
11. Wang, B.; Timilsena, Y.; Blanch, E.; Adhikari, B. Characteristics of bovine lactoferrin powders produced through spray and freeze drying processes. *Int. J. Biol. Macromol.* **2017**, *95*, 985–994. [CrossRef] [PubMed]
12. González-Chávez, S.A.; Arévalo-Gallegos, S.; Rascon-Cruz, Q. Lactoferrin: Structure, function and applications. *Int. J. Antimicrob. Agents* **2009**, *33*, 301.e1–301.e8. [CrossRef]
13. Lee, J.; Lee, J.; Lee, S.; Ahmad, T.; Perikamana, S.K.M.; Kim, E.M.; Lee, S.W.; Shin, H. Bioactive Membrane Immobilized with Lactoferrin for Modulation of Bone Regeneration and Inflammation. *Tissue Eng. Part A* **2020**, *26*, 1243–1258. [CrossRef]
14. Kanyshkova, T.G.; Buneva, V.N.; Nevinsky, G.A. Lactoferrin and Its biological functions. *Biochemestry* **2001**, *66*, 1–7. [CrossRef]
15. Tamhane, M.; Cabrera-Ghayouri, S.; Abelian, G.; Viswanath, V. Review of Biomarkers in Ocular Matrices: Challenges and Opportunities. *Pharm. Res.* **2019**, *36*, 1–35. [CrossRef]
16. Hanstock, H.G.; Edwards, J.P.; Walsh, N.P. Tear Lactoferrin and Lysozyme as Clinically Relevant Biomarkers of Mucosal Immune Competence. *Front. Immunol.* **2019**, *10*, 1178. [CrossRef] [PubMed]
17. Rageh, A.A.; Ferrington, D.; Roehrich, H.; Yuan, C.; Terluk, M.R.; Nelson, E.F.; Montezuma, S.R. Lactoferrin Expression in Human and Murine Ocular Tissue. *Curr. Eye Res.* **2016**, *41*, 883–889. [CrossRef]
18. Zhang, Y.; Lu, C.; Zhang, J. Lactoferrin and Its Detection Methods: A Review. *Nutrients* **2021**, *13*, 2492. [CrossRef]
19. Rosa, L.; Cutone, A.; Lepanto, M.S.; Paesano, R.; Valenti, P. Lactoferrin: A Natural Glycoprotein Involved in Iron and Inflammatory Homeostasis. *Int. J. Mol. Sci.* **2017**, *18*, 1985. [CrossRef]
20. EFSA Panel on Dietetic Products, Nutrition and Allergies (NDA). Scientific Opinion on bovine lactoferrin. *EFSA J.* **2012**, *10*, 1–26. [CrossRef]
21. Håversen, L.; Ohlsson, B.G.; Hahn-Zoric, M.; Hanson, L. Å; Mattsby-Baltzer, I. Lactoferrin down-regulates the LPS-induced cytokine production in monocytic cells via NF-κB. *Cell. Immunol.* **2002**, *220*, 83–95. [CrossRef]
22. Suzuki, Y.A.; Wong, H.; Ashida, K.-Y.; Schryvers, A.B.; Lönnerdal, B. The N1 Domain of Human Lactoferrin Is Required for Internalization by Caco-2 Cells and Targeting to the Nucleus. *Biochemistry* **2008**, *47*, 10915–10920. [CrossRef]
23. Gu, Y.; Wu, J. Bovine lactoferrin-derived ACE inhibitory tripeptide LRP also shows antioxidative and anti-inflammatory activities in endothelial cells. *J. Funct. Foods* **2016**, *25*, 375–384. [CrossRef]
24. Chen, J.; Zhou, J.; Kelly, M.; Holbein, B.E.; Lehmann, C. Iron chelation for the treatment of uveitis. *Med. Hypotheses* **2017**, *103*, 1–4. [CrossRef] [PubMed]
25. Kanwar, J.R.; Roy, K.; Patel, Y.; Zhou, S.-F.; Singh, M.R.; Singh, D.; Nasir, M.; Sehgal, R.; Sehgal, A.; Singh, R.S.; et al. Multifunctional Iron Bound Lactoferrin and Nanomedicinal Approaches to Enhance Its Bioactive Functions. *Molecules* **2015**, *20*, 9703–9731. [CrossRef]
26. López, E.S.; Egea, M.; Cano, A.; Espina, M.; Calpena, A.C.; Ettcheto, M.; Camins, A.; Souto, E.; Silva, A.; García, M. PEGylated PLGA nanospheres optimized by design of experiments for ocular administration of dexibuprofen—In vitro, ex vivo and in vivo characterization. *Colloids Surfaces B: Biointerfaces* **2016**, *145*, 241–250. [CrossRef] [PubMed]
27. Kumari, S.; Dandamudi, M.; Rani, S.; Behaeghel, E.; Behl, G.; Kent, D.; O'Reilly, N.; O'Donovan, O.; McLoughlin, P.; Fitzhenry, L. Dexamethasone-Loaded Nanostructured Lipid Carriers for the Treatment of Dry Eye Disease. *Pharmaceutics* **2021**, *13*, 905. [CrossRef] [PubMed]
28. Cano, A.; Sánchez-López, E.; Espina, M.; Egea, M.A.; García, M.L. Polymeric nanoparticles of (-)-epigallocatechin gallate: A new formulation for the treatment of ocular diseases. *J. Control. Release* **2017**, *259*, e7. [CrossRef]
29. Bangham, A.D.; Standish, M.M.; Watkins, J.C. Diffusion of univalent ions across the lamellae of swollen phospholipids. *J. Mol. Biol.* **1965**, *13*, 238–252. [CrossRef]
30. Lebrón, J.A.; López-López, M.; García-Calderón, C.B.; Rosado, I.V.; Balestra, F.R.; Huertas, P.; Rodik, R.V.; Kalchenko, V.I.; Bernal, E.; Moyá, M.L.; et al. Multivalent Calixarene-Based Liposomes as Platforms for Gene and Drug Delivery. *Pharmaceutics* **2021**, *13*, 1250. [CrossRef]
31. Navarro-Partida, J.; Castro-Castaneda, C.; Cruz-Pavlovich, F.S.; Aceves-Franco, L.; Guy, T.; Santos, A. Lipid-Based Nanocarriers as Topical Drug Delivery Systems for Intraocular Diseases. *Pharmaceutics* **2021**, *13*, 678. [CrossRef]
32. Shi, J.; Votruba, A.R.; Farokhzad, O.; Langer, R. Nanotechnology in Drug Delivery and Tissue Engineering: From Discovery to Applications. *Nano Lett.* **2010**, *10*, 3223–3230. [CrossRef] [PubMed]
33. Rao, N.; Rho, J.G.; Um, W.; Ek, P.K.; Nguyen, V.Q.; Oh, B.H.; Kim, W.; Park, J.H. Hyaluronic Acid Nanoparticles as Nanomedicine for Treatment of Inflammatory Diseases. *Pharmaceutics* **2020**, *12*, 931. [CrossRef]

34. Xiang, B.; Cao, D.-Y. Preparation of Drug Liposomes by Thin-Film Hydration and Homogenization. In *Liposome-Based Drug Delivery Systems*; Lu, W.-L., Qi, X.-R., Eds.; Springer: Berlin/Heidelberg, Germany, 2021; pp. 25–35.
35. Nekkanti, V.; Marwah, A.; Pillai, R. Media milling process optimization for manufacture of drug nanoparticles using design of experiments (DOE). *Drug Dev. Ind. Pharm.* **2013**, *41*, 124–130. [CrossRef] [PubMed]
36. Anaraki, N.I.; Sadeghpour, A.; Iranshahi, K.; Toncelli, C.; Cendrowska, U.; Stellacci, F.; Dommann, A.; Wick, P.; Neels, A. New approach for time-resolved and dynamic investigations on nanoparticles agglomeration. *Nano Res.* **2020**, *13*, 2847–2856. [CrossRef]
37. Gonzalez-Pizarro, R.; Silva-Abreu, M.; Calpena, A.C.; Egea, M.A.; Espina, M.; García, M.L. Development of fluorometholone-loaded PLGA nanoparticles for treatment of inflammatory disorders of anterior and posterior segments of the eye. *Int. J. Pharm.* **2018**, *547*, 338–346. [CrossRef]
38. Aguilar, M.-I. *HPLC of Peptides and Proteins. Methods and Protocols*, 1st ed.; Humana Press: Totowa, NJ, USA, 2004.
39. Cano, A.; Ettcheto, M.; Espina, M.; Auladell, C.; Calpena, A.C.; Folch, J.; Barenys, M.; López, E.S.; Camins, A.; García, M.L. Epigallocatechin-3-gallate loaded PEGylated-PLGA nanoparticles: A new anti-seizure strategy for temporal lobe epilepsy. *Nanomed. Nanotechnol. Biol. Med.* **2018**, *14*, 1073–1085. [CrossRef]
40. Cano, A.; Ettcheto, M.; Chang, J.-H.; Barroso, E.; Espina, M.; Kühne, B.A.; Barenys, M.; Auladell, C.; Folch, J.; Souto, E.B.; et al. Dual-drug loaded nanoparticles of Epigallocatechin-3-gallate (EGCG)/Ascorbic acid enhance therapeutic efficacy of EGCG in a APPswe/PS1dE9 Alzheimer's disease mice model. *J. Control. Release* **2019**, *301*, 62–75. [CrossRef]
41. Smith, P.K.; Krohn, R.I.; Hermanson, G.T.; Mallia, A.K.; Gartner, F.H.; Provenzano, M.D. Measurement of protein using bicinchoninic acid. *Anal. Biochem.* **1985**, *150*, 76–85. [CrossRef]
42. Gonzalez-Pizarro, R.; Parrotta, G.; Vera, R.; Sánchez-López, E.; Galindo, R.; Kjeldsen, F.; Badia, J.; Baldoma, L.; Espina, M.; García, M.L. Ocular penetration of fluorometholone-loaded PEG-PLGA nanoparticles functionalized with cell-penetrating peptides. *Nanomedicine* **2019**, *14*, 3089–3104. [CrossRef]
43. Derouiche, M.T.T.; Abdennour, S. HET-CAM test. Application to shampoos in developing countries. *Toxicol. Vitr.* **2017**, *45*, 393–396. [CrossRef]
44. Shalom, Y.; Perelshtein, I.; Perkas, N.; Gedanken, A.; Banin, E. Catheters coated with Zn-doped CuO nanoparticles delay the onset of catheter-associated urinary tract infections. *Nano Res.* **2016**, *10*, 520–533. [CrossRef]
45. Li, C.; Song, Y.; Luan, S.; Wan, P.; Li, N.; Tang, J.; Han, Y.; Xiong, C.; Wang, Z. Research on the Stability of a Rabbit Dry Eye Model Induced by Topical Application of the Preservative Benzalkonium Chloride. *PLOS ONE* **2012**, *7*, e33688. [CrossRef]
46. Wadhwa, S.; Paliwal, R.; Paliwal, S.; Vyas, S. Nanocarriers in Ocular Drug Delivery: An Update Review. *Curr. Pharm. Des.* **2009**, *15*, 2724–2750. [CrossRef] [PubMed]
47. Kandzija, N.; Khutoryanskiy, V.V. Delivery of Riboflavin-5′-Monophosphate Into the Cornea: Can Liposomes Provide Any Enhancement Effects? *J. Pharm. Sci.* **2017**, *106*, 3041–3049. [CrossRef]
48. Fangueiro, J.; Andreani, T.; Egea, M.A.; Garcia, M.L.; Souto, S.B.; Silva, A.; Souto, E.B. Design of cationic lipid nanoparticles for ocular delivery: Development, characterization and cytotoxicity. *Int. J. Pharm.* **2014**, *461*, 64–73. [CrossRef] [PubMed]
49. Aboali, F.A.; Habib, D.A.; Elbedaiwy, H.M.; Farid, R.M. Curcumin-loaded proniosomal gel as a biofreindly alternative for treatment of ocular inflammation: In-vitro and in-vivo assessment. *Int. J. Pharm.* **2020**, *589*, 119835. [CrossRef]
50. Yi, X.; Zheng, Q.; Pan, M.-H.; Chiou, Y.-S.; Li, Z.; Li, L.; Chen, Y.; Hu, J.; Duan, S.; Wei, S.; et al. Liposomal vesicles-protein interaction: Influences of iron liposomes on emulsifying properties of whey protein. *Food Hydrocoll.* **2019**, *89*, 602–612. [CrossRef]
51. Mazyed, E.A.; Abdelaziz, A.E. Fabrication of Transgelosomes for Enhancing the Ocular Delivery of Acetazolamide: Statistical Optimization, In Vitro Characterization, and In Vivo Study. *Pharmaceutics* **2020**, *12*, 465. [CrossRef]
52. Ibrahim, S.S. The Role of Surface Active Agents in Ophthalmic Drug Delivery: A Comprehensive Review. *J. Pharm. Sci.* **2019**, *108*, 1923–1933. [CrossRef]
53. Ismail, A.; Nasr, M.; Sammour, O. Nanoemulsion as a feasible and biocompatible carrier for ocular delivery of travoprost: Improved pharmacokinetic/pharmacodynamic properties. *Int. J. Pharm.* **2020**, *583*, 119402. [CrossRef]
54. Youshia, J.; Kamel, A.O.; El Shamy, A.; Mansour, S. Gamma sterilization and in vivo evaluation of cationic nanostructured lipid carriers as potential ocular delivery systems for antiglaucoma drugs. *Eur. J. Pharm. Sci.* **2021**, *163*, 105887. [CrossRef] [PubMed]
55. Lee, S.-E.; Lee, C.D.; Bin Ahn, J.; Kim, D.-H.; Lee, J.K.; Lee, J.-Y.; Choi, J.-S.; Park, J.-S. Hyaluronic acid-coated solid lipid nanoparticles to overcome drug-resistance in tumor cells. *J. Drug Deliv. Sci. Technol.* **2019**, *50*, 365–371. [CrossRef]
56. González-Fernández, F.; Bianchera, A.; Gasco, P.; Nicoli, S.; Pescina, S. Lipid-Based Nanocarriers for Ophthalmic Administration: Towards Experimental Design Implementation. *Pharmaceutics* **2021**, *13*, 447. [CrossRef] [PubMed]
57. Sadeghi-Ghadi, Z.; Ebrahimnejad, P.; Amiri, F.T.; Nokhodchi, A. Improved oral delivery of quercetin with hyaluronic acid containing niosomes as a promising formulation. *J. Drug Target.* **2021**, *29*, 225–234. [CrossRef] [PubMed]
58. Larrañeta, E.; Henry, M.; Irwin, N.J.; Trotter, J.; Perminova, A.A.; Donnelly, R. Synthesis and characterization of hyaluronic acid hydrogels crosslinked using a solvent-free process for potential biomedical applications. *Carbohydr. Polym.* **2018**, *181*, 1194–1205. [CrossRef]
59. Abdelkader, H.; Longman, M.R.; Alany, R.G.; Pierscionek, B. Phytosome-hyaluronic acid systems for ocular delivery of L-carnosine. *Int. J. Nanomed.* **2016**, *11*, 2815–2827. [CrossRef]

60. Carvajal-Vidal, P.; Fábrega, M.-J.; Espina, M.; Calpena, A.C.; García, M.L. Development of Halobetasol-loaded nanostructured lipid carrier for dermal administration: Optimization, physicochemical and biopharmaceutical behavior, and therapeutic efficacy. *Nanomed. Nanotechnol. Biol. Med.* **2019**, *20*, 102026. [CrossRef]
61. Marín, R.R.; Babick, F.; Hillemann, L. Zeta potential measurements for non-spherical colloidal particles – Practical issues of characterisation of interfacial properties of nanoparticles. *Colloids Surfaces A Physicochem. Eng. Asp.* **2017**, *532*, 516–521. [CrossRef]
62. Maritim, S.; Boulas, P.; Lin, Y. Comprehensive analysis of liposome formulation parameters and their influence on encapsulation, stability and drug release in glibenclamide liposomes. *Int. J. Pharm.* **2021**, *592*, 120051. [CrossRef]
63. Fangueiro, J.; Calpena, A.C.; Clares, B.; Andreani, T.; Egea, M.A.; Veiga, F.; Garcia, M.L.; Silva, A.; Souto, E.B. Biopharmaceutical evaluation of epigallocatechin gallate-loaded cationic lipid nanoparticles (EGCG-LNs): In vivo, in vitro and ex vivo studies. *Int. J. Pharm.* **2016**, *502*, 161–169. [CrossRef] [PubMed]
64. Wu, I.Y.; Bala, S.; Škalko-Basnet, N.; di Cagno, M.P. Interpreting non-linear drug diffusion data: Utilizing Korsmeyer-Peppas model to study drug release from liposomes. *Eur. J. Pharm. Sci.* **2019**, *138*, 105026. [CrossRef] [PubMed]
65. Fernández-Romero, A.-M.; Maestrelli, F.; Mura, P.A.; Rabasco, A.M.; González-Rodríguez, M.L. Novel Findings about Double-Loaded Curcumin-in-HPβcyclodextrin-in Liposomes: Effects on the Lipid Bilayer and Drug Release. *Pharmaceutics* **2018**, *10*, 256. [CrossRef] [PubMed]
66. Gómez-Segura, L.; Parra, A.; Calpena-Campmany, A.C.; Gimeno, Á.; De Aranda, I.G.; Boix-Montañes, A. Ex Vivo Permeation of Carprofen Vehiculated by PLGA Nanoparticles through Porcine Mucous Membranes and Ophthalmic Tissues. *Nanomaterials* **2020**, *10*, 355. [CrossRef]
67. Soni, V.; Pandey, V.; Tiwari, R.; Asati, S.; Tekade, R.K. Design and Evaluation of Ophthalmic Delivery Formulations. In *Basic Fundamentals of Drug Delivery*; Elsevier BV: Amsterdam, The Netherlands, 2019; pp. 473–538.
68. Flanagan, J.; Willcox, M. Role of lactoferrin in the tear film. *Biochimie* **2009**, *91*, 35–43. [CrossRef]
69. Lawrenson, J.G. Anterior Eye. In *Contact Lens Practice*; Elsevier: Amsterdam, The Netherlands, 2018; pp. 10–27.e2.
70. Ponzini, E.; Scotti, L.; Grandori, R.; Tavazzi, S.; Zambon, A. Lactoferrin Concentration in Human Tears and Ocular Diseases: A Meta-Analysis. *Investig. Opthalmology Vis. Sci.* **2020**, *61*, 9. [CrossRef]
71. Han, F.Y.; Thurecht, K.J.; Whittaker, A.K.; Smith, M.T. Bioerodable PLGA-Based Microparticles for Producing Sustained-Release Drug Formulations and Strategies for Improving Drug Loading. *Front. Pharmacol.* **2016**, *7*, 185. [CrossRef]
72. Li, Y.; Ruan, S.; Wang, Z.; Feng, N.; Zhang, Y. Hyaluronic Acid Coating Reduces the Leakage of Melittin Encapsulated in Liposomes and Increases Targeted Delivery to Melanoma Cells. *Pharmaceutics* **2021**, *13*, 1235. [CrossRef]
73. Kim, D.J.; Jung, M.-Y.; Pak, H.-J.; Park, J.-H.; Kim, M.; Chuck, R.S.; Park, C.Y. Development of a novel hyaluronic acid membrane for the treatment of ocular surface diseases. *Sci. Rep.* **2021**, *11*, 1–16. [CrossRef]
74. Gonzalez-Pizarro, R.; Carvajal-Vidal, P.; Bellowa, L.H.; Calpena, A.C.; Espina, M.; García, M.L. In-situ forming gels containing fluorometholone-loaded polymeric nanoparticles for ocular inflammatory conditions. *Colloids Surfaces B Biointerfaces* **2019**, *175*, 365–374. [CrossRef]
75. Eldesouky, L.; El-Moslemany, R.; Ramadan, A.; Morsi, M.; Khalafallah, N. Cyclosporine Lipid Nanocapsules as Thermoresponsive Gel for Dry Eye Management: Promising Corneal Mucoadhesion, Biodistribution and Preclinical Efficacy in Rabbits. *Pharmaceutics* **2021**, *13*, 360. [CrossRef]
76. Yousry, C.; Elkheshen, S.A.; El Laithy, H.; Essam, T.; Fahmy, R.H. Studying the influence of formulation and process variables on Vancomycin-loaded polymeric nanoparticles as potential carrier for enhanced ophthalmic delivery. *Eur. J. Pharm. Sci.* **2017**, *100*, 142–154. [CrossRef] [PubMed]
77. Vagge, A.; Senni, C.; Bernabei, F.; Pellegrini, M.; Scorcia, V.; E Traverso, C.; Giannaccare, G. Therapeutic Effects of Lactoferrin in Ocular Diseases: From Dry Eye Disease to Infections. *Int. J. Mol. Sci.* **2020**, *21*, 6668. [CrossRef] [PubMed]
78. Devendra, J. Effect of Oral Lactoferrin on Cataract Surgery Induced Dry Eye: A Randomised Controlled Trial. *J. Clin. Diagn. Res.* **2015**, *9*, NC06–NC09. [CrossRef] [PubMed]
79. Chen, X.; Aqrawi, L.A.; Utheim, T.P.; Tashbayev, B.; Utheim, Ø.A.; Reppe, S.; Hove, L.H.; Herlofson, B.B.; Singh, P.B.; Palm, Ø.; et al. Elevated cytokine levels in tears and saliva of patients with primary Sjögren's syndrome correlate with clinical ocular and oral manifestations. *Sci. Rep.* **2019**, *9*, 7319. [CrossRef] [PubMed]
80. Diaz-Garrido, N.; Fabrega, M.J.; Vera, R.; Giménez, R.; Badia, J.; Baldomà, L. Membrane vesicles from the probiotic Nissle 1917 and gut resident Escherichia coli strains distinctly modulate human dendritic cells and subsequent T cell responses. *J. Funct. Foods* **2019**, *61*, 1–12. [CrossRef]
81. Shih, K.C.; Fong, P.Y.; Lam, P.Y.; Chan, T.C.Y.; Jhanji, V.; Tong, L. Role of tear film biomarkers in the diagnosis and management of dry eye disease. *Taiwan J. Ophthalmol.* **2019**, *9*, 150–159. [CrossRef]
82. Ghasemi, H. Roles of IL-6 in Ocular Inflammation: A Review. *Ocul. Immunol. Inflamm.* **2018**, *26*, 37–50. [CrossRef]
83. Kruzel, M.L.; Zimecki, M.; Actor, J.K. Lactoferrin in a Context of Inflammation-Induced Pathology. *Front. Immunol.* **2017**, *8*, 1438. [CrossRef]

4.

DISCUSIÓN

DISCUSIÓN

Las enfermedades que cursan con inflamación ocular, entre las que se incluye el síndrome del ojo seco, por lo general, son patologías multifactoriales y de etiología muy diversa, que afectan a millones de pacientes en todo el mundo. Su prevalencia e incidencia es elevada, especialmente en los países desarrollados y están relacionadas con incremento de la esperanza de vida, el uso de ciertos fármacos, la contaminación del aire y el incremento masivo del uso de pantallas de visualización de datos. El proceso inflamatorio presente en la mayoría de las afecciones oculares se presenta inicialmente como mecanismo de defensa del organismo y su objetivo es el de eliminar al patógeno o causante de la lesión y favorecer la reparación tisular. Este se torna peligroso cuando se cronifica y desencadena un entorno proinflamatorio caracterizado por la presencia de diferentes mediadores proinflamatorios junto con un alto grado de estrés oxidativo, lo cual favorece el reclutamiento de más células inmunitarias generando una situación de retroalimentación autoinflamatoria, pudiendo verse afectada la función y la integridad ocular.

El objeto principal de la presente investigación consistió en el desarrollo y evaluación de dos sistemas nanoestructurados de diferente naturaleza para el transporte y la liberación, a nivel ocular, de una proteína (LF) con actividad farmacológica, capaces de aumentar su estabilidad y biodisponibilidad, a fin de ejercer un efecto terapéutico tanto en la prevención como en el tratamiento de la inflamación y la sequedad ocular.

Por lo tanto, se desarrolló un sistema basado en NPs poliméricas de PLGA y otro de naturaleza lipídica mediante la formulación de liposomas, ambos conteniendo la proteína. Una vez se optimizaron ambas

formulaciones haciendo uso de diseños de experimentos (DoE), se llevaron a cabo estudios de caracterización fisicoquímica, esterilización y estabilidad en estado líquido a diferentes temperaturas, así como la evaluación de sus propiedades biofarmacéuticas, su seguridad y eficacia antinflamatoria *in vitro* e *in vivo* y en el tratamiento de la sequedad ocular *in vivo*.

Previo al desarrollo de las formulaciones, se llevó a cabo el diseño y validación de un método instrumental, basado en la cromatografía liquida de alta resolución (HPLC), que permitiese la correcta determinación y cuantificación de la proteína presente en las formulaciones y posterior a su interacción y paso a través de diferentes membranas sintéticas u oculares.

La optimización de ambos nanovehículos se realizó mediante el desarrollo de dos diseños de experimentos factoriales compuestos, para estudiar qué factores afectaban y en qué medida en las síntesis de los nanosistemas. La fabricación de las bLF-NPs se llevó a cabo mediante el método de la doble emulsión, teniendo en cuenta la hidrosolubilidad del activo (Tao Meng et al., 2003). En el caso de los bLF-LIP, fueron elaborados mediante la técnica de hidratación del film lipídico y su posterior homogenización a alta presión, con el fin de obtener liposomas pequeños y unilamelares (Xiang and Cao, 2021). En los diseños de experimentos se establecieron como variables independientes la concentración de principio activo (bLF), el componente mayoritario del vehículo (siendo este el polímero en el caso de las NPs y el lípido en los liposomas) y el tensioactivo para cada una de las formulaciones. Las variables dependientes evaluadas, en ambos casos, fueron: el tamaño medio de partícula, el índice de polidispersión, la carga superficial de las partículas (determinada en base al

potencial Z) y la eficiencia de encapsulación de la proteína en el vehículo. Los componentes que conformaban los nanosistemas fueron escogidos en base a su seguridad para uso humano y ocular y su compatibilidad con el principio activo y entre sí (Cano et al., 2019).

La formulación de NPs poliméricas optimizada presentó un tamaño medio de partículas de aproximadamente 130 nm, carga superficial positiva de alrededor + 30 mV, población monodispersa y una capacidad de encapsulación de proteína de aproximadamente el 60 %. Paralelamente, se confirmó a través de microscopía electrónica de transmisión (TEM) y de fuerzas atómicas (AFM) que las NPs presentaban una morfología esférica, sin evidencia de agregación entre partículas y un tamaño similar a lo observado mediante la técnica de dispersión dinámica de la luz (DLS).

Por otro lado, la formulación optimizada de liposomas (bLF-LIP), tras la adición de ácido hialurónico, mostró un tamaño medio de partícula de 90 nm, siendo este ligeramente inferior al de las NPs poliméricas, carga superficial positiva de alrededor de + 20 mV, población monomodal y una encapsulación de la proteína de alto peso molecular del 53 %. En este caso, con el fin de conservar la estructura de la bicapa lipídica, se llevó a cabo el análisis por microscopía electrónica de baja temperatura (cryo-TEM) para su caracterización morfológica (Ghitman et al., 2020). Las imágenes revelaron la forma esférica y homogénea de los bLF-LIP, así como su conseguida estructura unilamelar.

Estas características hacen que los dos sistemas desarrollados sean adecuados para la administración por vía ocular, sin inducir irritación corneal. Además, la carga altamente positiva consigue que el tiempo de

residencia de las NPs y los liposomas en la película lagrimal, adyacente al epitelio corneal, sea prolongado, debido a sus interacciones electrostáticas con las proteínas presentes cargadas negativamente, como mucinas y lisozimas, lo cual facilita la penetración del activo y favorece su liberación sostenida en el tiempo (Daull et al., 2020).

Además, las bLF-NPs demostraron ser estables en suspensión a temperaturas bajas, durante 30 días, sin variaciones significativas en sus características fisicoquímicas. Así mismo, la formulación lipídica, bLF-LIP tampoco mostró ningún proceso de desestabilización o migración de partículas durante un periodo de tiempo de 60 días, almacenada tanto a temperatura ambiente como a 4 ^{o}C. La estabilidad prolongada que presentaron las formulaciones optimizadas fue debida, entre otros factores, a los valores elevados de potencial Z presentes, indicativo de una carga superficial elevada, que evitarían la interacción electrostática entre las partículas y los consiguientes fenómenos de desestabilización de las suspensiones coloidales por formación de agregados (Retamal Marín et al., 2017).

Previamente, las bLF-NPs fueron sometidas a un proceso de esterilización mediante su exposición a radiación gamma (Youshia et al., 2021). Esta irradiación se caracteriza por una penetración profunda y a dosis bajas capaz de acabar de manera efectiva con los microorganismos que puedan estar presentes en las formulaciones farmacéuticas o en sus envases. Es un método registrado en la Farmacopea Europea y aceptado para su uso en productos farmacéuticos, mayoritariamente termolábiles (EMA, 2015). Su posterior caracterización reveló que la estructura y los parámetros

fisicoquímicos del sistema no se veían afectados. No se observaron diferencias significativas entre las NPs antes y después de irradiar, por lo que no se vieron afectadas tampoco sus propiedades farmacológicas. Sin embargo, en el caso de bLF-LIP, no fue posible llevar a cabo este tipo de esterilización. Como es bien sabido, los liposomas o partículas lipídicas, al ser esterilizados mediante la aplicación de radiación gamma en medio acuoso, pueden sufrir diferentes procesos químicos (peroxidación, oxidación, hidrólisis y/o agregación) debido a la formación de radicales libres procedentes de la radiólisis del agua (radicales hidroxilo, electrones hidratados y/o átomos de hidrógeno) o al efecto directo de la radiación gamma sobre los fosfolípidos. Además, el colesterol también genera una gran cantidad de productos de oxidación cuando se expone a dosis bajas de irradiación, responsable de un incremento en la permeabilidad de la membrana de los liposomas y, por consiguiente, la pérdida del activo encapsulado, así como variaciones notables en la mayoría de los parámetros fisicoquímicos (Delma et al., 2021; Toh and Chiu, 2013).

Con el objetivo de conocer el estado físico de la proteína en el interior de los nanovehículos, condicionante en gran medida de su farmacocinética, se llevaron a cabo diferentes estudios de interacción entre los componentes de las formulaciones desarrolladas. En el caso de las bLF-NPs, los resultados obtenidos mediante calorimetría diferencial de barrido (DSC) y espectroscopía de infrarrojo con transformada de Fourier (FTIR) demostraron que la bLF estaba dispersada perfectamente en la matriz polimérica y que no existían enlaces covalentes entre ellas. Este hecho indicaría que el activo es capaz de liberarse de forma adecuada desde el interior de la NP, fenómeno confirmado con el estudio de liberación *in vitro*.

DISCUSIÓN

Las bLF-NPs presentaron una liberación inicial brusca del principio activo característica de este tipo de matrices poliméricas, seguida de un perfil de liberación sostenida hasta el final del ensayo (Cano et al., 2018; Fu and Kao, 2010). Así mismo, los resultados del estudio de interacción entre la bLF y el vehículo lipídico, mediante DSC, sugirieron la incorporación adecuada de todos los componentes de la formulación dentro de la estructura del liposoma. Esto fue corroborado con el estudio de comportamiento biofarmacéutico *in vitro*, donde se observó un perfil de liberación de la proteína desde el vehículo, prolongado en el tiempo y caracterizado por una etapa inicial de liberación más aguda. Este evento depende en gran medida de la composición de la formulación liposomal, incluida la cantidad de colesterol, de tensioactivo, la longitud de las cadenas de acilo o la carga del sistema, además de las características farmacocinéticas del propio fármaco (Maritim et al., 2021).

Las NPs polimérica liberaron en torno al 70 % del activo encapsulado en las primeras 24 h, mientras que los liposomas alcanzaron únicamente un 50 % en el mismo periodo de tiempo, por lo que se observa una liberación más sostenida en el caso de bLF-LIP. Con ambos nanosistemas, el estudio de liberación *in vitro* se realizó comparándolos con una muestra de principio activo libre (bLF) de su misma concentración y se obtuvieron resultados similares (Gonzalez-Pizarro et al., 2019). Se observó que, a las 24 horas desde el inicio del ensayo, el 100 % de bLF libre había sido liberado de la membrana de diálisis al medio receptor, a diferencia de los sistemas poliméricos y lipídicos.

Los estudios de comportamiento biofarmacéutico incluyeron también la permeación corneal *ex vivo* de ambos sistemas respecto al principio activo en solución (Carvajal-Vidal et al., 2017). Los resultados evidenciaron que la concentración de bLF procedente de las NPs que logró permear la córnea fue significativamente más elevada que en caso de la proteína libre. Este mismo fenómeno ocurrió durante la permeación de bLF-LIP. En ambos ensayos, todos los parámetros de permeación examinados presentaron diferencias estadísticamente significativas ($p<0,05$) frente a los obtenidos con la bLF libre, excepto en el caso de la cantidad retenida en la córnea (QR) procedente del ensayo con las NPs poliméricas. Tanto el flujo en estado estacionario (J), como el coeficiente de permeabilidad (K_p) y la cantidad permeada a las 24 h (Q_{24}) presentaron valores superiores en la permeación de los nanovehículos que en la del activo libre. Este hecho se debe a la mayor lipofilicidad que presentan tanto el vehículo polimérico como el lipídico, en relación con la proteína libre. Debido a que el epitelio corneal restringe el paso de sustancias hidrofílicas, actúa como factor limitante en la entrada y velocidad de administración de estos fármacos a nivel ocular. Por lo tanto, las dos formulaciones desarrolladas consiguieron la administración del principio activo de manera efectiva, ya que fueron capaces de liberarlo lentamente a través del tejido corneal, por lo que confirmaron su potencial como medicamentos de uso ocular.

Los ensayos de citotoxicidad *in vitro,* llevados a cabo en células de córnea humana HCE-2, demostraron que las formulaciones optimizadas, bLF-NPs y bLF-LIP, no afectaban en la viabilidad celular. Estos resultados confirmaron que los nanosistemas son biocompatibles y no tóxicos, aptos para su administración por vía ocular.

Adicionalmente, las bLF-NPs fueron sintetizadas paralelamente con un polímero al que previamente se le había incorporado un agente fluoróforo, la rodamina 110 (Rho). Diferentes concentraciones de Rho-bLF-NPs fueron incubadas, durante 48 horas, en presencia de células HCE-2. Posteriormente se tiñó el núcleo celular con DAPI y se llevó a cabo su observación mediante microscopía confocal. En las imágenes obtenidas se pudo observar que las NPs poliméricas penetraron al citoplasma celular. Los resultados obtenidos concuerdan con los de otros autores que demuestran la internalización celular de NPs de PLGA en las células corneales (Gonzalez-Pizarro et al., 2019; Li et al., 2021; Sah et al., 2017; Sánchez-López et al., 2016). Además, en el caso de la lactoferrina, las células del epitelio corneal poseen un receptor especifico de membrana (LRP1) para su internalización, por lo que podría participar otro mecanismo de entrada celular posible, además de la endocitosis mediada por receptor, común a todas las NPs de aproximadamente 100 nm de tamaño medio (Higuchi et al., 2016).

La evaluación de la tolerancia ocular de ambas formulaciones optimizadas en estudios *in vitro* e *in vivo,* HET-CAM y Test de Draize respectivamente, puso de manifiesto su inocuidad en el tratamiento de patologías inflamatorias oculares. Ambos estudios clasificaron a las NPs poliméricas y a los liposomas como agentes no irritantes y seguros para su uso por vía ocular, lo cual fue un resultado previsible dado que todos los componentes de la formulación están aceptados para su uso en humanos (Yousry et al., 2017).

Dada la evidencia de que el síndrome del ojo seco y la inflamación crónica asociada conlleva la sobreexpresión de ciertos mediadores

inflamatorios a nivel corneal, como la IL-8 o el TNF-α, se analizó la actividad antiinflamatoria de las NPs poliméricas y los liposomas mediante la determinación de estos dos mediadores en células HCE-2 tras ser estimuladas con lipopolisacárido. El tratamiento con ambos sistemas tras el estímulo con el agente inflamatorio demostró, en todos los casos, su eficacia antiinflamatoria. Las concentraciones detectadas de los mediadores inflamatorios fueron significativamente menores en el caso de las células tratadas con respecto al control positivo de inflamación, en cuyo caso no se aplicó tratamiento posterior. En ambos casos se observaron diferencias estadísticamente no significativas entre la aplicación de los nanosistemas y de la proteína libre, siendo las concentraciones obtenidas, tras la aplicación de esta última, ligeramente menores, lo cual podría explicarse por la liberación sostenida del fármaco, pudiendo este no liberar el 100% del activo durante el transcurso del experimento. Los valores obtenidos confirmarían el papel de la lactoferrina en la modulación de la expresión de diversas citoquinas proinflamatorias, posiblemente mediante la inhibición de la transcripción inducida por NF-κB (Kruzel et al., 2017).

Así mismo, los resultados adquiridos en los ensayos *in vivo* de prevención y tratamiento de la inflamación ocular en conejo evidenciaron que, en el caso de las NPs poliméricas, tanto la capacidad de prevención como el tratamiento de la inflamación ocular fue satisfactorio. Se observaron diferencias notables entre controles y tratados, con una recuperación ligeramente más rápida en el caso de las bLF-NPs que en el tratamiento con la proteína libre a lo largo del tiempo, probablemente debido a la eliminación por el reflejo nasolacrimal.

Los liposomas también demostraron ejercer actividad antiinflamatoria tras su administración en la profilaxis y tratamiento de procesos inflamatorios oculares. Se observaron diferencias significativas entre la disminución de los signos oculares de inflamación, en ambos estudios, con respecto al control positivo y a la proteína libre. Los resultados obtenidos para bLF-LIP pusieron de manifiesto su capacidad de adherencia en la superficie corneal y la liberación prolongada de la proteína (González-Fernández et al., 2021).

En el caso de la prevención de la inflamación ambos sistemas demostraron ejercer un efecto similar, favorecido por la cesión sostenida del activo aplicado previo al estímulo inflamatorio (González-Fernández et al., 2021). En cambio, en relación con los valores obtenidos en el tratamiento de la inflamación y, por ende, la aplicación de los nanosistemas posterior al estímulo inflamatorio se observó que bLF-NPs ejerció un efecto antiinflamatorio mayor que bLF-LIP. Este hecho concuerda con los resultados de liberación *in vitro*, donde se observó que la liberación de activo procedente de los liposomas era más sostenida que en el caso de las NPs poliméricas, además, esto podría entenderse ya que el liposoma tiene en su superficie un recubrimiento polimérico basado en ácido hialurónico, además del propio vehículo lipídico, por lo tanto, la cesión de la proteína se podría ver ralentizada con respecto a las NPs de PLGA. Sin embargo, ambos sistemas demostraron ser agentes antiinflamatorios eficaces, disminuyendo significativamente los signos de irritación e inflamación ocular con respecto a los controles positivos de inflamación (conejos tratados con suero fisiológico).

DISCUSIÓN

Con el objetivo de comprobar la eficacia terapéutica de los nanosistemas desarrollados en el tratamiento del síndrome de ojo seco *in vivo* se realizó el test de Schirmer. Se evaluó el nivel de lágrima producida por un ojo diagnosticado con SOS y tras 5 días de tratamiento. En este estudio, solo los animales tratados con liposomas respondieron de manera satisfactoria. El tratamiento con bLF-LIP logró una diferencia estadísticamente significativa en el volumen de lagrima secretado con respecto al obtenido del control positivo no tratado. Se observan diferencias considerables entre el día 0 y 5, el volumen de lagrima secretado en el grupo tratado con liposomas es 6,25 veces superior el quinto día del tratamiento y 4,5 veces mayor que el ojo tratado con suero fisiológico. Estos resultados corroboran la información proporcionada por otro autores, que sugieren el uso de la lactoferrina en el tratamiento del síndrome del ojo seco (Devendra and Singh, 2015; Vagge et al., 2020). Además, no se debe pasar por alto la presencia del ácido hialurónico como agente de recubrimiento del liposoma, ampliamente utilizado en el tratamiento de esta patología ocular por sus propiedades mucomiméticas oculares, que, además, tiende a formar una capa protectora en la superficie ocular que reduce la desecación, la fricción y el daño celular (Agarwal et al., 2021).

5.

CONCLUSIONES

CONCLUSIONES

Two controlled release nanostructured systems, based on polymeric and lipidic carriers, containing bLF have been developed for the treatment of ocular inflammation and dry eye disease. In this context, the conclusions of the present doctoral thesis are:

1. bLF-NPs (prepared by double emulsion method) and bLF-LIP (prepared by lipid film hydration technique and posterior high pressure homogenization method) exhibit physicochemical properties that allow them to perform sustained protein release and are suitable for ocular administration as eye drops.
2. Polymeric NPs are shown to be stable when stored at 4 ^{o}C for 1 month and liposomes stored at 4 and 25 ^{o}C for 2 months without any physicochemical changes.
3. Gamma-ray sterilisation maintains the physicochemical properties of bLF-NPs.
4. Biopharmaceutical studies indicate that the incorporation of bLF into both nanocarriers results in its prolonged release and promotes its permeation through the cornea, increasing its pharmacological effectiveness and decreasing the number of daily doses required.
5. *In vitro* cytotoxicity and *in vivo* tolerance assays demonstrate that bLF-NPs and bLF-LIP formulations are safe and well-tolerated at the cellular and histological level.
6. Both nanosystems developed reduce the production of pro-inflammatory cytokines in HCE-2 corneal cells, an *in vitro* method that supports the anti-inflammatory efficacy *in vivo*.

7. *In vivo* anti-inflammatory efficacy studies show that both formulations developed are effective and exhibit higher activity than free protein at the ocular level.
8. bLF-LIP demonstrates efficacy in the treatment of dry eye syndrome, achieving an increase in the volume of tears produced after 5 days of treatment.

In summary, these studies demonstrate that nanostructured systems with bLF, an anti-inflammatory and antioxidant high molecular weight protein, possess optimal properties to become in an innovative, promising, suitable, and safe strategy for the treatment of these diseases and other pathologies affecting the eyeball associated with inflammation.

6.

BIBLIOGRAFÍA

BIBLIOGRAFÍA

Agarwal, P., Craig, J.P., Rupenthal, I.D., 2021. Formulation considerations for the management of dry eye disease. Pharmaceutics 13, 19. https://doi.org/10.3390/pharmaceutics13020207

Alfonso, S.A., Fawley, J.D., Lu, X.A., 2015. Conjunctivitis. Prim. Care - Clin. Off. Pract. 42, 20. https://doi.org/10.1016/j.pop.2015.05.001

Anfuso, C.D., Olivieri, M., Fidilio, A., Lupo, G., Rusciano, D., Pezzino, S., Gagliano, C., Drago, F., Bucolo, C., 2017. Gabapentin attenuates ocular inflammation: In vitro and in vivo studies. Front. Pharmacol. 8, 1–10. https://doi.org/10.3389/fphar.2017.00173

Antimisiaris, S.G., Marazioti, A., Kannavou, M., Natsaridis, E., Gkartziou, F., Kogkos, G., Mourtas, S., 2021. Overcoming barriers by local drug delivery with liposomes. Adv. Drug Deliv. Rev. 174, 53–86. https://doi.org/10.1016/j.addr.2021.01.019

Bachu, R.D., Chowdhury, P., Al-Saedi, Z.H.F., Karla, P.K., Boddu, S.H.S., 2018. Ocular drug delivery barriers—role of nanocarriers in the treatment of anterior segment ocular diseases. Pharmaceutics 10, 1–31. https://doi.org/10.3390/pharmaceutics10010028

Bangham, A.D., De Gier, J., Greville, G.D., 1967. Osmotic properties and water permeability of phospholipid liquid crystals. Chem. Phys. Lipids 1, 225–246. https://doi.org/10.1016/0009-3084(67)90030-8

Bangham, A.D., Horne, R.W., 1964. Negative staining of phospholipids and their structural modification by surface-active agents as observed in the electron microscope. J. Mol. Biol. 8, 660–668. https://doi.org/10.1016/S0022-2836(64)80115-7

BIBLIOGRAFÍA

Begines, B., Ortiz, T., Pérez-Aranda, M., Martínez, G., Merinero, M., Argüelles-Arias, F., Alcudia, A., 2020. Polymeric nanoparticles for drug delivery: Recent developments and future prospects. Nanomaterials 10, 1–38. https://doi.org/10.3390/nano10071403

Brandl, M., Bachmann, D., Drechsler, M., Bauer, K.H., 1990. Liposome Preparation by a New High Pressure Homogenizer Gaulin Micron Lab 40. Drug Dev. Ind. Pharm. 16, 2167–2191. https://doi.org/10.3109/03639049009023648

Cano, A., Ettcheto, M., Chang, J.H., Barroso, E., Espina, M., Kühne, B.A., Barenys, M., Auladell, C., Folch, J., Souto, E.B., Camins, A., Turowski, P., García, M.L., 2019. Dual-drug loaded nanoparticles of Epigallocatechin-3-gallate (EGCG)/Ascorbic acid enhance therapeutic efficacy of EGCG in a APPswe/PS1dE9 Alzheimer's disease mice model. J. Control. Release 301, 62–75. https://doi.org/10.1016/j.jconrel.2019.03.010

Cano, A., Ettcheto, M., Espina, M., Auladell, C., Calpena, A.C., Folch, J., Barenys, M., Sánchez-López, E., Camins, A., García, M.L., 2018. Epigallocatechin-3-gallate loaded PEGylated-PLGA nanoparticles: A new anti-seizure strategy for temporal lobe epilepsy. Nanomedicine Nanotechnology, Biol. Med. 14, 1073–1085. https://doi.org/10.1016/j.nano.2018.01.019

Carvajal-Vidal, P., Mallandrich, M., García, M.L., Calpena, A.C., 2017. Effect of different skin penetration promoters in halobetasol propionate permeation and retention in human skin. Int. J. Mol. Sci. 18, 16. https://doi.org/10.3390/ijms18112475

Chen, J., Zhou, J., Kelly, M., Holbein, B.E., Lehmann, C., 2017. Iron chelation for the treatment of uveitis. Med. Hypotheses 103, 1–4. https://doi.org/10.1016/j.mehy.2017.03.029

Cholkar, K., Dassari, S., Pal, D., Mitra, A.K., 2012. Eye: anatomy, pgisiology and barrier to drug delivery, in: Ocular Transporters and Receptors: Their Role in Drug Delivery. Elsevier, pp. 2–28.

Conneely, O.M., Conneely, O.M., 2013. Antiinflammatory Activities of Lactoferrin Antiinflammatory Activities of Lactoferrin 5724. https://doi.org/10.1080/07315724.2001.10719173

Connell, S., Kawashima, M., Nakamura, S., Imada, T., Yamamoto, H., Tsubota, K., Fukuda, S., 2021. Lactoferrin Ameliorates Dry Eye Disease Potentially through Enhancement of Short-Chain Fatty Acid Production by Gut Microbiota in Mice. Int. J. Mol. Sci. 22, 1–18. https://doi.org/10.3390/ijms222212384

Craig, J.P., Nelson, J.D., Azar, D.T., Belmonte, C., Bron, A.J., Chauhan, S.K., de Paiva, C.S., Gomes, J.A.P., Hammitt, K.M., Jones, L., Nichols, J.J., Nichols, K.K., Novack, G.D., Stapleton, F.J., Willcox, M.D.P., Wolffsohn, J.S., Sullivan, D.A., 2017. TFOS DEWS II Report Executive Summary. Ocul. Surf. 15, 802–812.

Crucho, C.I.C., Barros, M.T., 2017. Polymeric nanoparticles: A study on the preparation variables and characterization methods. Mater. Sci. Eng. C 80, 771–784. https://doi.org/10.1016/j.msec.2017.06.004

Daull, P., Amrane, M., Ismail, D., Georgiev, G., Cwiklik, L., Baudouin, C., Leonardi, A., Garhofer, G., Garrigue, J.S., 2020. Cationic Emulsion-

Based Artificial Tears as a Mimic of Functional Healthy Tear Film for Restoration of Ocular Surface Homeostasis in Dry Eye Disease. J. Ocul. Pharmacol. Ther. 36, 355–365. https://doi.org/10.1089/jop.2020.0011

Degobert, G., Aydin, D., 2021. Lyophilization of Nanocapsules: Instability Sources, Formulation and Process Parameters. Pharmaceutics 13, 1–26. https://doi.org/10.3390/pharmaceutics13081112

Delma, K.L., Lechanteur, A., Evrard, B., Semdé, R., Piel, G., 2021. Sterilization methods of liposomes: Drawbacks of conventional methods and perspectives. Int. J. Pharm. 597, 1–13. https://doi.org/10.1016/j.ijpharm.2021.120271

Dennis, E.A., Norries, P.C., 2015. Eicosanoid stomrm in infaction and inflammation. Nat. Rev. Immunol. 11, 511–523. https://doi.org/10.1038/nri3859.Eicosanoid

Devendra, J., Singh, S., 2015. Effect of oral lactoferrin on cataract surgery induced dry eye: A randomised controlled trial. J. Clin. Diagnostic Res. 9, 6–9. https://doi.org/10.7860/JCDR/2015/15797.6670

Diebold, Y., Calonge, M., 2010. Applications of nanoparticles in ophthalmology. Prog. Retin. Eye Res. 29, 596–609. https://doi.org/10.1016/j.preteyeres.2010.08.002

Downie, L.E., Bandlitz, S., Bergmanson, J.P.G., Craig, J.P., Dutta, D., Maldonado-Codina, C., Ngo, W., Siddireddy, J.S., Wolffsohn, J.S., 2021. BCLA CLEAR - Anatomy and physiology of the anterior eye. Contact Lens Anterior Eye 44, 132–156.

https://doi.org/10.1016/J.CLAE.2021.02.009

Drago-Serrano, M.E., Campos-Rodríguez, R., Carrero, J.C., De La Garza, M., Andrade, P., Valentão, P., 2017. Lactoferrin: Balancing Ups and Downs of Inflammation Due to Microbial Infections. Int. J. Mol. Sci. 18, 1–25. https://doi.org/10.3390/ijms18030501

Dua, H.S., Faraj, L.A., Said, D.G., Gray, T., Lowe, J., 2013. Human corneal anatomy redefined: A novel pre-descemet's layer (Dua's Layer). Ophthalmology 120, 1778–1785. https://doi.org/10.1016/j.ophtha.2013.01.018

Elizabeth Childs, C., Vlasova, A.N., Figueroa-Lozano, S., van Leeuwen, S.S., Dijkhuizen, L., Valk-Weeber, R.L., Akkerman, R., Abdulahad, W., de Vos, P., 2020. Inhibitory Effects of Dietary N-Glycans From Bovine Lactoferrin on Toll-Like Receptor 8; Comparing Efficacy With Chloroquine. Front. Immunol. 11, 1–12. https://doi.org/10.3389/fimmu.2020.00790

Elzoghby, A.O., Abdelmoneem, M.A., Hassanin, I.A., Abd Elwakil, M.M., Elnaggar, M.A., Mokhtar, S., Fang, J.Y., Elkhodairy, K.A., 2020. Lactoferrin, a multi-functional glycoprotein: Active therapeutic, drug nanocarrier & targeting ligand. Biomaterials 263, 1–21. https://doi.org/10.1016/j.biomaterials.2020.120355

EMA, 2015. EMA 2015. Guideline on the sterilisation of the medicinal product , active substance , excipient and primary container.

European Food Safety Authority, 2012. Scientific Opinion on bovine lactoferrin. EFSA J. 10, 1–26. https://doi.org/10.2903/j.efsa.2012.2701

BIBLIOGRAFÍA

Fessi, H., Puisieux, F., Devissaguet, J.P., Ammoury, N., Benita, S., 1989. Nanocapsule formation by interfacial polymer deposition following solvent displacement. Int. J. Pharm. 55, 1–4. https://doi.org/10.1016/0378-5173(89)90281-0

Flanagan, J.L., Willcox, M.D.P., 2009. Role of lactoferrin in the tear film. Biochimie 91, 35–43. https://doi.org/10.1016/j.biochi.2008.07.007

Fonte, P., Reis, S., Sarmento, B., 2016. Facts and evidences on the lyophilization of polymeric nanoparticles for drug delivery. J. Control. Release 225, 75–86. https://doi.org/10.1016/j.jconrel.2016.01.034

Forrester, J. V., Dick, A.D., McMenamin, P.G., Roberts, F., Pearlman, E., 2016. Anatomy of the eye and orbit, in: The Eye. pp. 1-102.e2. https://doi.org/10.1016/b978-0-7020-5554-6.00001-0

Foster, C.S., Kothari, S., Anesi, S.D., Vitale, A.T., Chu, D., Metzinger, J.L., Cero, O., 2016. The Ocular Immunology and Uveitis Foundation preferred practice patterns of uveitis management. Surv. Ophtalmol. 61, 1–17. https://doi.org/10.1016/j.survophthal.2015.07.001

Fu, Y., Kao, W.J., 2010. Drug release kinetics and transport mechanisms of non-degradable and degradable polymeric delivery systems. Expert Opin. Drug Deliv. 7, 429–444. https://doi.org/10.1517/17425241003602259

Gallo, J., Raska, M., Kriegova, E., Goodman, S.B., 2017. Inflammation and its resolution and the musculoskeletal system. J. Orthop. Transl. 10, 52–67. https://doi.org/10.1016/j.jot.2017.05.007

Galloway, N.R., Amoaku, W.M.K., Galloway, P.H., Browning, A.C., 2016.

Basic Anatomy and Physiology of the Eye, in: Common Eye Diseases and Their Management. Springer, pp. 8–16. https://doi.org/10.1007/978-3-319-32869-0_2

Gaudana, R., Ananthula, H.K., Parenky, A., Mitra, A.K., 2010. Ocular Drug Delivery. AAPS J. 12, 348–360.

Georgiev, G.A., Eftimov, P., Yokoi, N., 2017. Structure-function relationship of tear film lipid layer: A contemporary perspective. Exp. Eye Res. 163, 17–28. https://doi.org/10.1016/J.EXER.2017.03.013

Ghitman, J., Biru, E.I., Stan, R., Iovu, H., 2020. Review of hybrid PLGA nanoparticles: Future of smart drug delivery and theranostics medicine. Mater. Des. 193, 1–20. https://doi.org/10.1016/j.matdes.2020.108805

González-Chávez, S.A., Arévalo-Gallegos, S., Rascón-Cruz, Q., 2009. Lactoferrin: structure, function and applications. Int. J. Antimicrob. Agents 33, 301.e1-301.e8. https://doi.org/10.1016/j.ijantimicag.2008.07.020

González-Fernández, F.M., Bianchera, A., Gasco, P., Nicoli, S., Pescina, S., 2021. Lipid-based nanocarriers for ophthalmic administration: Towards experimental design implementation. Pharmaceutics 13, 30. https://doi.org/10.3390/pharmaceutics13040447

Gonzalez-Pizarro, R., Parrotta, G., Vera, R., Sánchez-López, E., Galindo, R., Kjeldsen, F., Badia, J., Baldoma, L., Espina, M., García, M.L., 2019. Ocular penetration of fluorometholone-loaded PEG-PLGA nanoparticles functionalized with cell-penetrating peptides. Nanomedicine 14, 3089–3104. https://doi.org/10.2217/nnm-2019-

0201

Gote, V., Sikder, S., Sicotte, J., Pal, D., 2019. Ocular drug delivery: Present innovations and future challenges. J. Pharmacol. Exp. Ther. 370, 602–624. https://doi.org/10.1124/jpet.119.256933

Groef, L. De, Cordeiro, M.F., 2018. Is the Eye an Extension of the Brain in Central Nervous System Disease? J. Ocul. Pharmacol. Ther. 34, 129–133.

Gu, Y., Wu, J., 2016. Bovine lactoferrin-derived ACE inhibitory tripeptide LRP also shows antioxidative and anti-inflammatory activities in endothelial cells. J. Funct. Foods 25, 375–384. https://doi.org/10.1016/j.jff.2016.06.013

Guimarães, D., Cavaco-Paulo, A., Nogueira, E., 2021. Design of liposomes as drug delivery system for therapeutic applications. Int. J. Pharm. 601, 1–15. https://doi.org/10.1016/j.ijpharm.2021.120571

Hanstock, H.G., Edwards, J.P., Walsh, N.P., 2019. Tear lactoferrin and lysozyme as clinically relevant biomarkers of mucosal immune competence. Front. Immunol. 10, 1–11. https://doi.org/10.3389/fimmu.2019.01178

Has, C., Sunthar, P., 2020. A comprehensive review on recent preparation techniques of liposomes. J. Liposome Res. 30, 336–365. https://doi.org/10.1080/08982104.2019.1668010

Håversen, L., Ohlsson, B.G., Hahn-Zoric, M., Hanson, L.Å., Mattsby-Baltzer, I., 2002. Lactoferrin down-regulates the LPS-induced cytokine production in monocytic cells via NF-κB. Cell. Immunol. 220, 83–95.

https://doi.org/10.1016/S0008-8749(03)00006-6

Hazare, S., Yang, R., Chavan, S., Menon, M.D., Chougule, M.B., 2016. Aging Disorders of the Eye: Challenges and Approaches for Their Treatment, in: Pathak, Y., Sutariya, V., Hirani, A.A. (Eds.), Nano-Biomaterials For Ophthalmic Drug Delivery. Springer International Publishing, Cham, pp. 277–320. https://doi.org/10.1007/978-3-319-29346-2_14

Higuchi, A., Inoue, H., Kaneko, Y., Oonishi, E., Tsubota, K., 2016. Selenium-binding lactoferrin is taken into corneal epithelial cells by a receptor and prevents corneal damage in dry eye model animals. Sci. Rep. 6, 1–8. https://doi.org/10.1038/srep36903

Hussain, M.T., Forbes, N., Perrie, Y., Malik, K.P., Duru, C., Matejtschuk, P., 2020. Freeze-drying cycle optimization for the rapid preservation of protein-loaded liposomal formulations. Int. J. Pharm. 573, 1–10. https://doi.org/10.1016/J.IJPHARM.2019.118722

Jain, R.A., 2000. The manufacturing techniques of various drug loaded biodegradable poly(lactide-co-glycolide) (PLGA) devices. Biomaterials 21, 2475–2490. https://doi.org/10.1016/S0142-9612(00)00115-0

Javier López-Cano, J., Ana González-Cela-Casamayor, M., Andrés-Guerrero, V., Herrero-Vanrell, R., Molina-Martínez, I.T., López-Cano, J.J., 2021. Liposomes as vehicles for topical ophthalmic drug delivery and ocular surface protection. Expert Opin. Drug Deliv. 18, 819–847. https://doi.org/10.1080/17425247.2021.1872542

BIBLIOGRAFÍA

Jeon, H.J., Jeong, Y. Il, Jang, M.K., Park, Y.H., Nah, J.W., 2000. Effect of solvent on the preparation of surfactant-free poly(dl-lactide-co-glycolide) nanoparticles and norfloxacin release characteristics. Int. J. Pharm. 207, 99–108. https://doi.org/10.1016/S0378-5173(00)00537-8

Joossen, C., Baán, A., Moreno-Cinos, C., Joossens, J., Cools, N., Lanckacker, E., Moons, L., Lemmens, K., Lambeir, A.M., Fransen, E., Delputte, P., Caljon, G., Van Der Veken, P., Maes, L., De Meester, I., Kiekens, F., Augustyns, K., Cos, P., 2020. A novel serine protease inhibitor as potential treatment for dry eye syndrome and ocular inflammation. Sci. Rep. 10, 14. https://doi.org/10.1038/s41598-020-74159-w

Kanwar, J.R., Roy, K., Patel, Y., Zhou, S., Singh, M.R., Singh, D., Nasir, M., Sehgal, R., Sehgal, A., Singh, R.S., Garg, S., Kanwar, R.K., 2015. Multifunctional Iron Bound Lactoferrin and Nanomedicinal Approaches to Enhance Its Bioactive Functions. Molecules 20, 9703–9731. https://doi.org/10.3390/molecules20069703

Kanyshkova, T.G., Buneva, V.N., Nevinsky, G.A., 2001. Lactoferrin and Its Biological Functions. Biochem. 66, 5–13. https://doi.org/10.1023/a:1002817226110

Kaur, I.P., Kanwar, M., 2002. Ocular Preparations: The Formulation Approach. Drug Dev. Ind. Pharm. 28, 473–493. https://doi.org/10.1081/DDC-120003445

Kawasaki, H., Shimanouchi, T., Kimura, Y., 2019. Recent Development of Optimization of Lyophilization Process. J. Chem. 2019, 1–14.

https://doi.org/10.1155/2019/9502856

Kels, B.D., Grzybowski, A., Grant-kels, J.M., 2015. Human ocular anatomy. Clin. Dermatol. 33, 140–146.

Khiev, D., Mohamed, Z.A., Vichare, R., Paulson, R., Bhatia, S., Mohapatra, S., Lobo, G.P., Valapala, M., Kerur, N., Passaglia, C.L., Mohapatra, S.S., Biswal, M.R., Haley, J.A., 2021. Emerging Nano-Formulations and Nanomedicines Applications for Ocular Drug Delivery. Nanomaterials 11, 1–18. https://doi.org/10.3390/nano11010173

Kirby, C., Gregoriadis, G., 1984. Dehydration-Rehydration Vesicles: A Simple Method for High Yield Drug Entrapment in Liposomes. Bio/Technology 2, 979–984. https://doi.org/10.1038/nbt1184-979

Kreuter, J., 2004. Nanoparticles as drug delivery systems. Encycl. Nanosci. Nanotechnol.

Kruzel, M.L., Zimecki, M., Actor, J.K., 2017. Lactoferrin in a context of inflammation-induced pathology. Front. Immunol. 8, 1–15. https://doi.org/10.3389/fimmu.2017.01438

Kuribayashi, K., Tresset, G., Coquet, P., Fujita, H., Takeuchi, S., 2006. Electroformation of giant liposomes in microfluidic channels. Meas. Sci. Technol 17, 3121–3126.

Lakhani, P., Patil, A., Majumdar, S., 2018. Recent advances in topical nano drug-delivery systems for the anterior ocular segment. Ther. Deliv. 9, 137–153. https://doi.org/10.4155/tde-2017-0088

Lalu, L., Tambe, V., Pradhan, D., Nayak, K., Bagchi, S., Maheshwari, R.,

Kalia, K., Tekade, R.K., 2017. Novel nanosystems for the treatment of ocular inflammation: Current paradigms and future research directions. J. Control. Release 268, 19–39. https://doi.org/10.1016/j.jconrel.2017.07.035

Lawrenson, J.G., 2018. Anterior Eye, in: Contact Lens Practice. Elsevier, pp. 10-27.e2. https://doi.org/10.1016/b978-0-7020-6660-3.00002-2

Lee, Jinkyu, Lee, Jinki, Lee, S., Ahmad, T., Perikamana, S.K.M., Kim, E.M., Lee, S.W., Shin, H., 2020. Bioactive membrane immobilized with lactoferrin for modulation of bone regeneration and inflammation. Tissue Eng. - Part A 26, 1243–1258. https://doi.org/10.1089/ten.tea.2020.0015

Legrand, D., 2016. Overview of Lactoferrin as a Natural Immune Modulator. J. Pediatr. 173S, 10–15. https://doi.org/10.1016/j.jpeds.2016.02.071

Leroux, J.C., Allemann, E., Doelker, E., Gurny, R., 1995. New Approach for the Preparation of Nanoparticles by an Emulsification-Diffusion Method. Eur. J. Pharm. Biopharm. 41, 14–18.

Li, C., Deng, Y., 2004. A novel method for the preparation of liposomes: Freeze drying of monophase solutions. J. Pharm. Sci. 93, 1403–1414. https://doi.org/10.1002/jps.20055

Li, P.C., Chen, S.C., Hsueh, Y.J., Shen, Y.C., Tsai, M.Y., Hsu, L.W., Yeh, C.K., Chen, H.C., Huang, C.C., 2021. Gelatin scaffold with multifunctional curcumin-loaded lipid-PLGA hybrid microparticles for regenerating corneal endothelium. Mater. Sci. Eng. C 120, 1–10.

https://doi.org/10.1016/j.msec.2020.111753

Lim, H.Y., Puah, S.H., Ang, L.J.P.S., Teo, E.Q., Lau, S.Y., Goh, K.S., Lim, A.Y.H., Tai, D.Y.H., Abisheganaden, J., Verma, A., 2015. Subconjunctival haemorrhage from bronchoscopy: A case report. Respir. Med. Case Reports 16, 97–100. https://doi.org/10.1016/j.rmcr.2015.08.008

Lynch, C., Kondiah, P.P.D., Choonara, Y.E., Du Toit, L.C., Ally, N., Pillay, V., 2019. Advances in Biodegradable Nano-Sized Polymer-Based Ocular Drug Delivery. Polymers (Basel). 11. https://doi.org/10.3390/polym11081371

Makadia, H.K., Siegel, S.J., 2011. Poly Lactic-co-Glycolic Acid (PLGA) as Biodegradable Controlled Drug Delivery Carrier. Polymers (Basel). 3, 1377–1397. https://doi.org/10.3390/polym3031377

Maritim, S., Boulas, P., Lin, Y., 2021. Comprehensive analysis of liposome formulation parameters and their influence on encapsulation, stability and drug release in glibenclamide liposomes. Int. J. Pharm. 592, 13. https://doi.org/10.1016/j.ijpharm.2020.120051

Mazet, R., Yaméogo, J.B.G., Wouessidjewe, D., Choisnard, L., Gèze, A., 2020. Recent advances in the design of topical ophthalmic delivery systems in the treatment of ocular surface inflammation and their biopharmaceutical evaluation. Pharmaceutics 12, 1–55. https://doi.org/10.3390/pharmaceutics12060570

Nagarwal, R.C., Kant, S., Singh, P.N., Maiti, P., Pandit, J.K., 2009. Polymeric nanoparticulate system: A potential approach for ocular

drug delivery. J. Control. Release 136, 2–13. https://doi.org/10.1016/j.jconrel.2008.12.018

Parra, A., Mallandrich, M., Clares, B., Egea, M.A., Espina, M., García, M.L., Calpena, A.C., 2015. Design and elaboration of freeze-dried PLGA nanoparticles for the transcorneal permeation of carprofen : Ocular anti-inflammatory applications. Colloids Surfaces B Biointerfaces 136, 935–943.

Patel, A., Cholkar, K., Agrahari, V., Mitra, A.K., 2013. Ocular drug delivery systems: An overview. World J. Pharmacol. 2, 47–64. https://doi.org/10.5497/wjp.v2.i2.47

Patil, K.R., Mahajan, U.B., Unger, B.S., Goyal, S.N., Belemkar, S., Surana, S.J., Ojha, S., Patil, C.R., 2019. Animal Models of Inflammation for Screening of Anti-inflammatory Drugs: Implications for the Discovery and Development of Phytopharmaceuticals. Int. J. Mol. Sci 20, 1–38. https://doi.org/10.3390/ijms20184367

Pattni, B.S., Chupin, V. V., Torchilin, V.P., 2015. New Developments in Liposomal Drug Delivery. Chem. Rev. 115, 10938–10966. https://doi.org/10.1021/acs.chemrev.5b00046

Pinto Reis, C., Neufeld, R.J., Ribeiro, A.J., Veiga, F., 2006. Nanoencapsulation I. Methods for preparation of drug-loaded polymeric nanoparticles. Nanomedicine Nanotechnology, Biol. Med. 2, 8–21. https://doi.org/10.1016/J.NANO.2005.12.003

Pitts, F., Jardine, A.G., Murray, S.B., Barker, N.H., 1992. Spontaneous subconjunctival haemorrhage - a sign of hypertension? Br. J.

Ophtalmol. 76, 297–299.

Przic, D.S., Ruzic, N.L., Petrovic, S.D., 2004. Lyophilization - The process and industrial use. Chem. Ind 12, 552–562.

Rageh, A.A., Ferrintong, D.A., Roechrich, H., Yuan, C., Terluk, M.R., Nelson, E.F., Montezuma, S.R., 2017. Lactoferrin Expresion in Human and Murine Ocular Tissue. Cur Eye Res 41, 883–889. https://doi.org/10.3109/02713683.2015.1075220

Rascón-Cruz, Q., Espinoza-Sánchez, E.A., Siqueiros-Cendón, T.S., Nakamura-Bencomo, S.I., Arévalo-Gallegos, S., Iglesias-Figueroa, B.F., 2021. Lactoferrin: A Glycoprotein Involved in Immunomodulation, Anticancer, and Antimicrobial Processes. Molecules 26, 1–15. https://doi.org/10.3390/molecules26010205

Retamal Marín, R.R., Babick, F., Hillemann, L., 2017. Zeta potential measurements for non-spherical colloidal particles – Practical issues of characterisation of interfacial properties of nanoparticles. Colloids Surfaces A 532, 516–521. https://doi.org/10.1016/j.colsurfa.2017.04.010

Rhen, T., Cidlowski, J.A., 2005. Antiinflammatory Action of Glucocorticoids-New Mechanisms for Old Drugs, The New England Journal of Medicine.

Riaz, M.K., Riaz, M.A., Zhang, X., Lin, C., Wong, K.H., Chen, X., Zhang, G., Lu, A., Yang, Z., 2018. Surface functionalization and targeting strategies of liposomes in solid tumor therapy: A review. Int. J. Mol. Sci. 19, 1–27. https://doi.org/10.3390/ijms19010195

BIBLIOGRAFÍA

Roda, M., Corazza, I., Bacchi Reggiani, M.L., Pellegrini, M., Taroni, L., Giannaccare, G., Versura, P., 2020. Dry eye disease and tear cytokine levels - A meta analaysis. Int. J. Mol. Sci. 21, 17. https://doi.org/10.3390/ijms21093111

Rosa, L., Cutone, A., Lepanto, M.S., Paesano, R., Valenti, P., 2017. Lactoferrin : A Natural Glycoprotein Involved in Iron and Inflammatory Homeostasis. Int. J. Mol. Sci. 18, 1–26. https://doi.org/10.3390/ijms18091985

Sah, A.K., Suresh, P.K., Verma, V.K., 2017. PLGA nanoparticles for ocular delivery of loteprednol etabonate: a corneal penetration study. Artif. Cells, Nanomedicine Biotechnol. 45, 1156–1164. https://doi.org/10.1080/21691401.2016.1203794

Sahinoglu-Keskek, N., Cevher, S., Ergin, A., 2013. Analysis of subconjunctival hemorrhage. Pakistan J. Med. Sci. 29, 132–134. https://doi.org/10.12669/pjms.291.2802

Salama, A., Elsheikh, A., Alweis, R., 2018. Is this worrisome red eye? Episcleritis in the primary care setting. J. Community Hosp. Intern. Med. Perspect. 8, 46–48.

Sánchez-López, E., Egea, M.A., Cano, A., Espina, M., Calpena, A.C., Ettcheto, M., Camins, A., Souto, E.B., Silva, A.M., García, M.L., 2016. PEGylated PLGA nanospheres optimized by design of experiments for ocular administration of dexibuprofen-in vitro, ex vivo and in vivo characterization. Colloids Surfaces B Biointerfaces 145, 241–250. https://doi.org/10.1016/j.colsurfb.2016.04.054

Sánchez-lópez, E., Espina, M., Doktorovova, S., Souto, E.B., García, M.L., 2017. Lipid nanoparticles (SLN , NLC): Overcoming the anatomical and physiological barriers of the eye – Part I – Barriers and determining factors in ocular delivery. Eur. J. Pharm. Biopharm. 110, 70–75.

Sanli, D., Bozbag, • S E, Erkey, • C, 2012. Synthesis of nanostructured materials using supercritical CO 2 : Part I. Physical transformations. J Mater Sci 47, 2995–3025. https://doi.org/10.1007/s10853-011-6054-y

Schultz, C., 2018. Ocular Inflammation. Gen. Intern. Med. Clin. Innov. 3, 1–3. https://doi.org/10.15761/gimci.1000163

Seen, S., Tong, L., 2018. Dry eye disease and oxidative stress. Acta Ophthalmol. 96, e412–e420. https://doi.org/10.1111/aos.13526

Sharma, S., Parmar, A., Kori, S., Sandhir, R., 2016. Trends in Analytical Chemistry PLGA-based nanoparticles : A new paradigm in biomedical applications 80, 30–40. https://doi.org/10.1016/j.trac.2015.06.014

Souto, E.B., Dias-Ferreira, J., López-Machado, A., Ettcheto, M., Cano, A., Espuny, A.C., Espina, M., Garcia, M.L., Sánchez-López, E., 2019. Advanced formulation approaches for ocular drug delivery: State-of-the-art and recent patents. Pharmaceutics 11, 29. https://doi.org/10.3390/pharmaceutics11090460

Suffredini, G., East, J.E., Levy, L.M., 2014. New applications of Nanotechnology for Neuroimaging. Am. J. Neuroradiol. 35, 1246–1253. https://doi.org/10.3174/ajnr.A3543

Superti, F., 2020. Lactoferrin from Bovine Milk: A Protective Companion for Life. Nutrients 12, 1–25. https://doi.org/10.3390/nu12092562

BIBLIOGRAFÍA

Suzuki, Y., Wong, H., Ashida, K., Schryvers, A.B., Lönnerdal, B., 2009. The N1 Domain of Human Lactoferrin is Required For Internalization By Caco-2 Cells and Targeting to the Nucleus. Biochemistry 47, 10915–10920. https://doi.org/10.1021/bi8012164.The

Swetledge, S., Jung, J.P., Carter, R., Sabliov, C., 2021. Distribution of polymeric nanoparticles in the eye: implications in ocular disease therapy. J. Nanobiotechnology 19, 1–19. https://doi.org/10.1186/s12951-020-00745-9

Szoka, F., Papahadjopoulos, D., 1980. Comparative Properties and Methods of Preparation of Lipid Vesicles (Liposomes). Annu. Rev. Biophys. Bioeng. 9, 467–508. https://doi.org/10.1146/annurev.bb.09.060180.002343

Tamhane, M., Cabrera-Ghayouri, S., Abelian, G., Viswanath, V., 2019. Review of Biomarkers in Ocular Matrices: Challenges and Opportunities. Pharm. Res. 36, 1–35. https://doi.org/10.1007/s11095-019-2569-8

Tao Meng, F., Hui Ma, G., Qiu, W., Guo Su, Z., 2003. W/O/W double emulsion technique using ethyl acetate as organic solvent: effects of its diffusion rate on the characteristics of microparticles. J. Control. Release 91, 407–416. https://doi.org/10.1016/s0168-3659(03)00273-6

Tarlan, B., Kiratli, H., 2013. Subconjunctival hemorrhage: Risk factors and potential indicators. Clin. Ophthalmol. 7, 1163–1170. https://doi.org/10.2147/OPTH.S35062

Thomas, A.H., Catalá, Á., Vignoni, M., 2016. Soybean phosphatidylcholine

liposomes as model membranes to study lipid peroxidation photoinduced by pterin. Biochim. Biophys. Acta 1858, 139–145. https://doi.org/10.1016/J.BBAMEM.2015.11.002

Toh, M.-R., Chiu, G.N.C., 2013. Liposomes as esterile preparations and limitations of sterilisation techniques in liposomal manufacturing. Asian J. Pharm. Sci. 8, 88–95.

Trenkenschuh, E., Friess, W., 2021. Freeze-drying of nanoparticles: How to overcome colloidal instability by formulation and process optimization. Eur. J. Pharm. Biopharm. 165, 345–360. https://doi.org/10.1016/J.EJPB.2021.05.024

Tsai, C.-H., Wang, P.-Y., Lin, I.-C., Huang, H., Liu, G.-S., Tseng, C.-L., 2018. Ocular Drug Delivery: Role of Degradable Polymeric Nanocarriers for Ophthalmic Application. Int. J. Mol. Sci. 19, 1–20. https://doi.org/10.3390/ijms19092830

Tsubota, K., Pflugfelder, S.C., Liu, Z., Baudouin, C., Kim, H.M., Messmer, E.M., Kruse, F., Liang, L., Carreno-Galeano, J.T., Rolando, M., Yokoi, N., Kinoshita, S., Dana, R., 2020. Defining dry eye from a clinical perspective. Int. J. Mol. Sci. 21, 1–24. https://doi.org/10.3390/IJMS21239271

Vagge, A., Senni, C., Bernabei, F., Pellegrini, M., Scorcia, V., Traverso, C.E., Giannaccare, G., 2020. Therapeutic effects of lactoferrin in ocular diseases: From dry eye disease to infections. Int. J. Mol. Sci. https://doi.org/10.3390/ijms21186668

Vanderhoff, J.W., El Aasser, M.S., 1979. Polymer emulsification process.

U.S. Patent.

Vergouwen, D.P.C., Rothova, A., Berge, J.C.T., Verdijk, R.M., van Laar, J.A.M., Vingerling, J.R., Schreurs, M.W.J., 2020. Current insights in the pathogenesis of scleritis. Exp. Eye Res. 197, 108078. https://doi.org/10.1016/j.exer.2020.108078

Wang, B., Timilsena, Y.P., Blanch, E., Adhikari, B., 2019. Lactoferrin: Structure, function, denaturation and digestion. Crit. Rev. Food Sci. Nutr. 59, 580–596. https://doi.org/10.1080/10408398.2017.1381583

Wang, B., Timilsena, Y.P., Blanch, E., Adhikari, B., 2017. Characteristics of bovine lactoferrin powders produced through spray and freeze drying processes. Int. J. Biol. Macromol. 95, 985–994. https://doi.org/10.1016/j.ijbiomac.2016.10.087

White, M., 1999. Mediators of inflammation and the inflammatory process. J. Allergy Clin. Immunol. 103, 378–381. https://doi.org/10.1016/S0091-6749(99)70215-0

Willoughby, C.E., Ponzin, D., Ferrari, S., Lobo, A., Landau, K., Omidi, Y., 2010. Anatomy and physiology of the human eye: Effects of mucopolysaccharidoses disease on structure and function - a review. Clin. Exp. Ophthalmol. 38, 2–11. https://doi.org/10.1111/j.1442-9071.2010.02363.x

Xiang, B., Cao, D.-Y., 2021. Preparation of Drug Liposomes by Thin-Film Hydration and Homogenization, in: Lu, W.-L., Qi, X.-R. (Eds.), Liposome-Based Drug Delivery Systems. Springer Berlin Heidelberg, Berlin, Heidelberg, pp. 25–35. https://doi.org/10.1007/978-3-662-

49320-5_2

Yang, C., Yang, J., Lu, A., Gong, J., Yang, Y., Lin, X., Li, M., Xu, H., 2022. Nanoparticles in ocular applications and their potential toxicity. Front. Mol. Biosci. 9, 18. https://doi.org/10.3389/fmolb.2022.931759

Youshia, J., Kamel, A.O., El Shamy, A., Mansour, S., 2021. Gamma sterilization and in vivo evaluation of cationic nanostructured lipid carriers as potential ocular delivery systems for antiglaucoma drugs. Eur. J. Pharm. Sci. 163, 11. https://doi.org/10.1016/j.ejps.2021.105887

Yousry, C., Elkheshen, S.A., El-laithy, H.M., Essam, T., Fahmy, R.H., 2017. Studying the influence of formulation and process variables on Vancomycin-loaded polymeric nanoparticles as potential carrier for enhanced ophthalmic delivery. Eur. J. Pharm. Sci. 100, 142–154. https://doi.org/10.1016/j.ejps.2017.01.013

Zhang, Y., Lu, C., Zhang, J., 2021. Lactoferrin and its detection methods: A review. Nutrients 13, 18. https://doi.org/10.3390/nu13082492

Zuhaila García-Rubio, Y., Lima-Gómez, V., 2014. Las bases: retinopatía diabética y edema macular. Rev Hosp Jua Mex 81, 231–234.

ANEXO

(19) Europäisches Patentamt
European Patent Office
Office européen des brevets

(11) EP 3 603 621 A1

(12) **EUROPEAN PATENT APPLICATION**

(43) Date of publication:
05.02.2020 Bulletin 2020/06

(21) Application number: **19189078.9**

(22) Date of filing: **30.07.2019**

(51) Int Cl.:
A61K 9/127 *(2006.01)* ***A61K 38/40*** *(2006.01)*
A61K 47/36 *(2006.01)* ***A61K 31/722*** *(2006.01)*
A61K 31/728 *(2006.01)*

(84) Designated Contracting States:
AL AT BE BG CH CY CZ DE DK EE ES FI FR GB GR HR HU IE IS IT LI LT LU LV MC MK MT NL NO PL PT RO RS SE SI SK SM TR
Designated Extension States:
BA ME
Designated Validation States:
KH MA MD TN

(30) Priority: **31.07.2018 IT 201800007677**

(71) Applicant: **TDC Technology Dedicated to Care S.r.l.**
20125 Milano (IT)

(72) Inventors:
- **LÓPEZ MACHADO, Ana Laura**
  38416 Santa Cruz de Tenerife (ES)
- **SÁNCHEZ LÓPEZ, Elena**
  08024 Barcelona (ES)
- **GARCIA LOPEZ, Maria Luisa**
  08028 Barcelona (ES)
- **BIANCARDI, Martina**
  08012 Barcelona (ES)

(74) Representative: **Trupiano, Federica**
Marietti, Gislon e Trupiano S.r.l.
Via Larga, 16
20122 Milano (IT)

(54) **LIPOSOMES FOR THE TREATMENT OF OCULAR DISEASES**

(57) The invention refers to a product made of liposomes which comprises lactoferrin and a component selected from hyaluronic acid or chitosan, as active ingredients, as well as to compositions comprising it and their use in the prevention and/or treatment of diseases related to the eye, such as for example the ocular diseases characterized by the presence of an inflammatory condition.

EP 3 603 621 A1

Printed by Jouve, 75001 PARIS (FR)

ANEXO

Description

STATE OF THE ART

[0001] Ocular diseases are diseases concerning one or more eye structures.

[0002] Among them, there are more or less severe diseases, such as for example the inflammatory diseases, hyposphagma and the dry eye syndrome (or more simply, dry eye).

[0003] The ocular inflammatory diseases are pathologies characterized by the inflammation of one or more eye structures. They can occur at the level of internal and/or external structures at the eyeball. In particular, the ocular inflammatory diseases are characterized by the presence of an inflammatory process arising in different areas of the eye. Some of the main ocular inflammatory diseases are, for example, conjunctivitis, chalazion, stye, blepharoconjunctivitis and keratitis.

[0004] Hyposphagma, or subconjunctival hemorrhage, is characterized by bleeding under the conjunctiva.

[0005] The dry eye syndrome is a disease characterized by the quantitative and/or qualitative reduction of tear film.

[0006] The therapy for the treatment of the ocular diseases varies according to the type of pathology, e.g. depending on the type and severity of the inflammation. The most used drugs for the treatment of such kind of pathologies and their complications are mainly antibiotics for topical use, ocular lubricants, steroidal anti-inflammatory drugs and, in the most severe cases, orally taken drugs.

[0007] However, the use of the above mentioned drugs has some disadvantages. For example, the prolonged use of some antibiotics for topical use can limit or cure the ocular microbiological infection, but at the same time can involve an acute inflammation of the external tunic (fibrous tunic) of the eye, with redness and itch symptoms. Moreover, a prolonged use of the antibiotic can favor the occurrence of bacterial strains resistant to the active ingredient used (antimicrobial resistance event). Moreover, the drugs containing steroidal anti-inflammatory drugs have notoriously typical side-effects, which involve, for example, the glucidic, protein, lipid and bone metabolisms, the kidney excretion of sodium and potassium, the gastric acid excretion, the blood crasis and the mood. Finally, the orally taken drugs usually require a higher dose with respect to the topically taken drugs, in order to provide the same concentrations in the area of interest. Moreover, the orally taken drugs are more prone to provide side-effects at the systemic level, since they are absorbed at the gastrointestinal level and are delivered in all the organism districts through the systemic circulation.

[0008] In view of the disadvantages of the above stated conventional drugs, novel ocular compositions which allow to overcome such disadvantages and that show efficacy capable of preventing, alleviating and/or solving such diseases are nowadays required.

OBJECTS OF THE INVENTION

[0009] Object of the present invention is to provide a product which can prevent, alleviate and/or treat the ocular diseases, in particular hyposphagma, dry eye syndrome, inflammatory ocular diseases and their related complications.

[0010] Further object of the present invention is to provide a pharmaceutical composition, preferably for topical use, more preferably for ocular topical use, which comprises the above product and which is used for the prevention and/or treatment of the ocular diseases.

DESCRIPTION OF THE INVENTION

[0011] The objects stated above, as well as other objects, are achieved by means of the object of the present invention, i.e. a product constituted by liposomes that comprises lactoferrin and a component selected from hyaluronic acid or chitosan, as active ingredients. As it will be shown in the experimental section, the product of the invention is useful for the treatment of ocular diseases.

[0012] In the present invention, with the term "liposome" it is meant a vesicle consisting of at least one lipid bilayer and one core of aqueous solution encapsulated within the lipid bilayer. The lipids constituting the liposome bilayer (or liposome-forming lipids) can comprise mixtures composed essentially of phospholipids, such as for example phosphatidylcholine, and cholesterol in a lower amount. By way of example, lipids useful to constitute the lipid bilayer of liposome are a mixture of cholesterol and sodium lecithin comprising 70% phosphatidylcholine (such as for example the commercial product Lipoid S75, or the commercial product Lipoid S80, currently commercialized by the Lipoid Kosmetik AG Company, DE). The liposome can also comprise, in its lipid bilayer, further compounds of non-lipid nature, e.g. other organic compounds (such as tocopherol).

[0013] Lactoferrin comprised in the liposomes according to the invention is preferably encapsulated inside the lipid bilayer, and more preferably it is solubilized in the core of aqueous solution which is typically inside the lipid bilayer.

[0014] The product of the invention, constituted by liposomes, can comprise, in addition to lactoferrin, a component selected from hyaluronic acid or chitosan.

[0015] According to a particular aspect of the invention, when the product comprises hyaluronic acid as component, chitosan can also be comprised, and vice versa. In other words, the products of the invention can comprise lactoferrin and hyaluronic acid in combination with chitosan; or alternatively the products of the invention can comprise lactoferrin and chitosan in combination with hyaluronic acid.

[0016] When the product of the invention comprises hyaluronic acid, the hyaluronic acid can also be outside the lipid bilayer of liposomes.

[0017] According to another embodiment, when the product of the invention comprises hyaluronic acid, the hyaluronic acid is encapsulated inside the lipid bilayer and solubilized in the core of aqueous solution inside the liposome lipid bilayer.

[0018] When the products of the invention comprise chitosan, such chitosan preferably forms a coating of the lipid bilayer of the liposomes.

[0019] As already mentioned, the product of the invention, as well as the compositions comprising it, has prophylactic and therapeutic properties towards diseases, and in particular towards ocular diseases.

[0020] It has been surprisingly found that the products of the invention show therapeutic and prophylactic effects against inflammation, and in particular ocular inflammation. Such effects are demonstrated in the experimental section. Still as demonstrated in the experimental section, it was surprisingly observed that the therapeutic and prophylactic effects against the ocular inflammation characterizing the products according to the invention, are not obtained instead by comparative solutions comprising free lactoferrin, i.e. lactoferrin not encapsulated into the lipid bilayer of the liposomes.

[0021] It was also surprisingly found that the products of the invention are particularly effective in alleviating and/or curing the symptoms of hyposphagma and dry eye syndrome.

[0022] The product of the invention has in addition various advantages which makes it particularly stable and effective for its use in the eye. For example, lactoferrin, which is a glycoprotein belonging to the ferritin family, is stabilized thanks to its incorporation into the liposomes, according to the invention, and is therefore protected against a possible denaturation.

[0023] Hyaluronic acid, which is comprised in the product of the invention, effectively lubricates the ocular surface and favors the regeneration of the corneal epithelium.

[0024] Also, the liposomes assist and favor the ocular adhesion process, thus favoring the topic permanence and the delivery of lactoferrin and of the other components comprised in it.

[0025] It was also found that chitosan, which preferably coats the lipid bilayer of the liposomes, favors a sustained release of the components encapsulated into the lipid bilayer of the liposomes, such as for example of lactoferrin.

[0026] It was also observed, by means of ocular tolerance tests, that the product of the invention is biocompatibile when topically applied at ocular level, as it is demonstrated in the experimental section. As a matter of fact it does not cause undesired inflammatory effects. For this reason, the product of the invention, consisting of liposomes as described above, can be formulated in compositions which can be topically administered, which allow lactoferrin and the other components comprised in it to be vehiculated, such as for example hyaluronic acid, directly to the area of interest, i.e. the eye. This provides to the product of the invention all the typical advantages of the topical formulations.

[0027] Preferably, the lipids constituting the bilayer confer to the liposomes a positive surface electrical charge. Such electrical charge is advantageous for the ocular topical administration, since it is responsible of the adhesion of the liposome to the eye by electrostatic attraction. Therefore, the liposome-forming lipids advantageously have such a positive charge to confer positive surface electrical charge to the liposomes according to the invention. An indicator of such positive charge is the Z-potential. Advantageously, the Z-potential charge of the liposomes according to the invention, when suspended in an aqueous medium, can be greater than 0 mV, preferably can be greater than or equal to 10 mV, more preferably can be greater than or equal to 15 mV, still more preferably can be greater than or equal to 20 mV. For example, the Z-potential charge of the liposomes can be in the range from 25 to 30 mV. The Z-potential values as described above can be advantageously measured by using a particle analyzer by means of the laser Doppler electrophoresis technique, e.g. by means of the Zetasizer Nano ZS instrument by Malvern Panalytical.

[0028] The liposomes according to the invention have preferably a size lower than or equal to 200 nm, more preferably lower than or equal to 150 nm, still more preferably lower than or equal to 100 nm, still more preferably in the range from 70 nm to 100 nm. The sizes as described above can be advantageously measured by using a particle analyzer by means of the dynamics light scattering technique (DLS), e.g. by means of the Zetasizer Nano ZS instrument by Malvern Panalytical. Such measurements can be carried out after appropriately diluting the liposomes, e.g. with a 1:10 dilution with distilled water. The sizes described above allow a composition comprising the product according to the invention, being it as well object of the present invention, not to cause irritation or other unfavorable effects to the ocular microenvironment when it is administered by ophthalmic topical route.

[0029] According to the present invention, preferred hyaluronic acids are those with a low/intermediate/high molecular weight, e.g. those with a molecular weight in the range from 20 kDa to 1500 kDa, or those with a molecular weight in the range from 800 kDa to 2000 kDa, preferably from 100 kDa to 1000 kDa, or preferably in the range from 1500 kDa to 2000 kDa, more preferably it is about 290 kDa, or more preferably it is about 1600 kDa. The hyaluronic acids having the molecular weight above are commercially available. The molecular weight of such hyaluronic acids can be determined

ANEXO

by means of conventional methods, e.g. by means of gel permeation chromatography. Gel permeation chromatography (GPC) is a type of size exclusion chromatography (SEC). It was found that the use of hyaluronic acid with molecular weight as described above allows higher encapsulation efficiency of the protein (lactoferrin) inside the liposome to be obtained.

[0030] The hyaluronic acid can be also comprised in the product of the invention in the form of a pharmaceutically acceptable salt thereof.

[0031] The product according to the invention can comprise, in its base formulation, agents suitable to modulate its viscosity and/or preservatives and/or stabilizing agents and/or agents suitable to modulate its osmolarity.

[0032] The liposomes can also incorporate pharmaceutically suitable functional agents, such as for example cryoprotectants, osmolarity modulators, surfactants and buffers.

[0033] The cryoprotectants allow to maintain unaltered the chemical-physical characteristics of the liposomes, as well as of the compositions comprising them. Indeed, cryoprotectants are useful, e.g., if the liposomes have to be freeze-dried to be long-term stored. Cryoprotectants useful in the present invention can be, for example, mannitol, trehalose and cyclodextrin, and preferably are trehalose and cyclodextrin. According to the present invention, a particularly advantageous cyclodextrin is hydroxypropyl-β-cyclodextrin.

[0034] Osmolarity modulators allow to the core of aqueous solution, once it has been released, to avoid osmotic stresses to the ocular microenvironment. Advantageously, the osmolarity modulators confer to the core of aqueous solution such an osmolarity to be hypotonic or isotonic relative to the ocular microenvironment. Osmolarity modulators useful in the present invention can be cationic electrolytes, among which Na, K, Ca, Mg, and sugars and/or polyalcohols, such as for example mannitol, trehalose and cyclodextrin, trehalose and cyclodextrin being preferred.

[0035] Advantageously, the cryoprotectants can also be osmolarity modulating agents, such as for example mannitol, trehalose and cyclodextrin.

[0036] Cyclodextrin is a particularly useful functional agent according to the present invention, both incorporated inside the liposomes and comprised in a composition comprising the product of the invention. Cyclodextrin assists the protein solubilization and stabilization, such as for example of lactoferrin, and contributes to the osmolarity of the core of aqueous solution of the liposomes and/or composition of the invention. Moreover, cyclodextrin allows to favor the freeze-drying process, as it is a cryoprotectant, and protects and increases the stability of lactoferrin incorporated in the liposome.

[0037] Advantageously, the core of aqueous solution inside liposomes can have an osmolarity comprised in a range from 200 to 500 mOsm/Kg, preferably from 250 to 450 mOsm/Kg, and more preferably it is about 310 mOsm/Kg. Alternatively, the osmolarity can be about 275 mOsm/Kg for the liposomes comprising hyaluronic acid, and about 420 mOsm/Kg for the liposomes comprising chitosan. Such osmolarity values can be measured by means of conventional instruments, such as for example Advanced® Model 3320 Micro-Osmometer (Advanced® Instruments, Inc., Norwood, MA, USA). The liposomes comprising a core of aqueous solution that have the above osmolarity, avoid to cause osmotic stresses to the ocular microenvironment once they are administered by ocular topical route. Such osmolarity can be adjusted by osmolarity modulators as described above, e.g. to make the liposomes and/or the composition of the invention suitable for the ophthalmic administration and compliant with Phrmacopoeia requirements.

[0038] Further functional agents useful in the present invention, in particular for the preparation of the liposomes, are the surfactants. Advantageously, surfactants according to the present invention can be ionic or nonionic surfactants, preferably nonionic, such as for example the polysorbate 80 (also named Tween® 80).

[0039] The liposomes according to the invention can be prepared by means of conventional techniques, e.g. those described in the experimental section.

[0040] In particular, as described in the experimental section, the liposomes can be prepared by means of the lipid film hydration method. Such method includes the preparation of an organic phase containing the liposome-forming lipids, and at the same time the preparation of an aqueous phase comprising the components which will compose the core of aqueous solution, such as for example lactoferrin, hyaluronic acid (if present) and other functional agents (e.g., cryoprotectants). It has been observed that the order of addition of the components to the aqueous phase dose not significantly change the characteristics (size, polydispersity index and Z-potential) of the obtained liposomes, and therefore it is possible to prepare the aqueous phase by adding the components comprised in it in any order.

[0041] It has also been observed that the liposomes can be prepared without the use of an ultrasonic probe. The ultrasonic probe can cause the release of metals which could later be chelated by lactoferrin, thus making the product partially inactive. Therefore, advantageously, for the preparation of the liposomes, according to the present invention, an ultrasonic bath can be used (e.g., the ultrasonic bath Transsonic Digitals, produced by Elma GmbH).

[0042] Further object of the invention is a composition comprising the product of the invention according to the description above and pharmaceutically suitable excipients.

[0043] The composition according to the invention can comprise agents suitable to modulate its viscosity and/or preservatives and/or stabilizing agents and/or agents suitable to modulate its osmolarity.

[0044] The composition of the invention is particularly advantageous when used to prevent and/or treat ocular diseases, in particular hyposphagma, dry eye syndrome and ocular inflammatory diseases and complications thereof, and therefore

said pharmaceutically suitable excipients will be excipients conventionally used in ocular topical compositions.

[0045] Compositions for ophthalmic topical use according to the invention can be suspensions of liposomes in an aqueous medium of suitable viscosity, e.g. in order to prepare eye drops.

[0046] With the term "ocular topical compositions" or "ophthalmic topical compositions" it is meant compositions directly administered to the eye, preferably at the anterior area of the external tunic (or fibrous tunic) of the eye and/or in the conjunctival sac.

[0047] The liposomes used in the composition of the invention have advantageously a positive surface charge, in order to improve their adhesion to the ocular microenvironment, in particular to the fibrous tunic of the eye; they can have a Z-potential value as described above.

[0048] The osmolarity of the composition of the invention can advantageously have the osmolarity values set forth above. The composition of the invention having the above osmolarity avoids to cause osmotic stresses to the ocular microenvironment once it is administered by ocular topical route. Such osmolarity can be regulated by means of osmolarity modulators as described above, e.g. in amounts from 1 to 30%, preferably from 5 to 25%, more preferably from 7 to 20%. By way of example, it has been found that it is possible to obtain a final osmolarity value of about 300 mOsm/kg when the composition of the invention comprising liposomes comprising hyaluronic acid contains about 9.93% hydroxypropyl-β-cyclodextrin and about 7% trehalose. Still by way of example, it has been found that it is possible to obtain a final osmolarity value of about 300 mOsm/kg when the composition of the invention comprising liposomes comprising chitosan contains about 5% hydroxypropyl-β-cyclodextrin and about 5% trehalose.

[0049] In the present invention, the percentage amounts of the components, unless otherwise specified, refer to the weight percent of the components to the total volume of the final composition (or formulation).

[0050] Advantageously, the composition of the invention can comprise:

I) liposome-forming lipids in an amount in the range from 1% to 5%, preferably from 2% to 4%, more preferably 3%; and
II) lactoferrin in an amount in the range from 0.5% to 8%, preferably from 1% to 4%, still more preferably of 2%; and a component selected from
III) hyaluronic acid in an amount in the range from 0.0001% to 0.5%, preferably from 0.0005% to 0.1%, more preferably from 0.001% to 0.02%, still more preferably of 0.01%; or
IV) chitosan in an amount in the range from 0.02% to 2%, preferably from 0.1% to 1%, more preferably of 0.2%.

[0051] Preferably, the composition of the invention can comprise liposome-forming lipids in the amount of 1.5%.

[0052] Preferably, the composition of the invention can comprise lactoferrin in the amount of 0.8%.

[0053] As it is possible to observe in the experimental section, compositions of the invention comprising the above stated amounts proved to be effective in the prevention and/or treatment of ocular diseases.

[0054] The composition of the invention can be prepared by means of conventional methods for the preparation of compositions comprising liposomes.

[0055] Advantageously, according to the present invention, the composition and/or the core of aqueous solution inside the liposomes can have a neutral or slightly acidic pH, e.g. a pH between 5 and 8, preferably between 5.4 and 7, when the composition of the invention is applied at the ocular topical level. Therefore, the composition of the invention and/or the product of the invention can have, as functional agents, also pH modulators, such as for example buffers. Such pH modulators can be present in an amount suitable to provide the desired pH based on the type of administration and/or product of the invention, e.g. the pH as described above.

[0056] The composition of the invention, as well as the products contained in it, in order to be administered by ocular topical route, may require to be sterile or essentially sterile, e.g. to fulfill the regulatory requirements. For this purpose, it is possible to sterilize the composition of the invention, as well as the liposomes contained in it, by γ-ray irradiation, e.g. at a dose of 25 kGy, or 10 kGy.

[0057] In order to increase the stability of the composition of the invention, as well as of the liposomes contained in it, it is possible to freeze-drying the composition and the liposomes. An example of freeze-drying process of the composition of the invention is provided in the experimental section.

[0058] It is further an object of the present invention the composition of the invention, as well as the product of the invention, for their use as medicament.

[0059] Indeed, as it can be observed in the experimental section, the composition of the invention and the products comprised in it are useful to prevent and/or treat the ocular diseases. For example, the product of the invention, as well as the compositions of the invention comprising the product of the invention, proved to be useful in the prevention and the treatment of the ocular inflammatory diseases.

[0060] In the present invention, with "inflammation" it is meant the known natural nonspecific defense mechanism which can come after the detrimental action of physical, chemical and/or biological agents. With "ocular inflammation" or "ocular inflammatory diseases" it is meant the inflammation as described above which affects any structure of the eye (e.g., posterior chamber, ciliary area, pupil, anterior chamber, cornea, iris, crystalline lens capsule and nucleus,

ANEXO

conjunctiva, retina vessels, optic nerve, sclera and retina). Examples of the ocular inflammatory diseases can be conjunctivitis, chalazion, stye, blepharoconjunctivitis and keratitis.

[0061] Due to the efficacy of the composition and product of the invention in the treatment of the inflammation, the composition and the product of the invention can also be used in the diseases due to complications of ocular inflammation, such as for example in the ocular infections due to *Pseudomonas aeruginosa*.

[0062] The composition of the invention, as well as the product of the invention, proved also to be useful in the treatment of dry eye syndrome and hyposphagma, in particular when the liposome comprises chitosan.

[0063] As a matter of fact, it is known that the dry eye syndrome depends on the reduction of the lactoferrin concentration in the lacrimal fluid which occurs with the aging of the eye. Advantageously, the delivery of lactoferrin in the eye through the liposome and the composition of the invention allow to restore the optimal lactoferrin concentration, thus solving this way the dry eye syndrome.

[0064] Moreover, the composition and the product of the invention, as demonstrated in the experimental section, proved to be suitable for the ocular topical administration, since they do not cause irritation following their administration and are highly tolerated in the ocular microenvironment. Therefore, the composition of the invention, as well as the product of the invention, can be used in the prevention and/or the treatment of ocular diseases.

[0065] In the present invention, with "diseases of the eye" or "ocular diseases" it is meant those diseases which affect any structure of the eye, e.g. the structures described above, and comprise the ocular inflammatory diseases as described above. Preferably, such diseases of the eye are dry eye syndrome, hyposphagma, conjunctivitis, chalazion, stye, blepharoconjunctivitis and keratitis.

[0066] The invention will be better understood thanks to the not limitative exemplary figures and examples, reported below.

DESCRIPTION OF THE FIGURES

[0067]

Figure 1 shows a plot referring to the results of a test on the therapeutic activity of the products of the invention, described in detail in Example 8.

Figure 2 shows a plot referring to the results of a test on the prophylactic activity of the products of the invention, described in detail in Example 9.

EXPERIMENTAL SECTION

Example 1

Preparation of the products of the invention

[0068] The liposome preparation has been carried out by means of the lipid film hydration method illustrated below. First of all, an oil phase has been prepared by adding, under stirring, the lipids forming the lipid bilayer of the liposome and other compounds (see Table 1 below for the qualitative and quantitative composition of the oil phase) to ethanol, until the formation of a homogeneous phase. Later, ethanol has been removed under reduced pressure by means of a rotary evaporator (Buchi R-210). A lipid film has been then obtained. In order to assure the complete evaporation of the solvent, the lipid film has been fully dried by using a nitrogen flux. Later, an aqueous phase has been prepared by adding to water the components which will be part of the core of aqueous solution inside the liposome (see Table 1 below for the qualitative and quantitative composition of the aqueous phase). The so prepared aqueous phase has been added to the lipid film (step of lipid film hydration) and the mixture has been homogenized by using an ultrasonic bath (Transsonic Digitals), thus obtaining the formation of liposomes. Finally, the so obtained liposomes underwent two cycles of homogenization process at 800 mbar and ambient temperature by means of the Stransted-pressure cell homogeniser-FPG12800 instrument.

[0069] According to the above described method, three formulations (F1, F2 and F3) of the products of the invention have been prepared. In F1 formulation, the liposomes comprise lactoferrin and chitosan, while in F2 and F3 compositions, the liposomes comprise lactoferrin and hyaluronic acid. For F1, chitosan has been added after the step of lipid film hydration and before the two cycles of homogenization. The qualitative and quantitative composition of F1, F2 and F3 is set forth in Table 1.

Table 1

Formulation		Component and % amount (w/v)	Oil or aqueous phase
F1	Liposomes comprising lactoferrin and chitosan	Lipoid S75 3%	Oil phase
		Cholesterol 0.1%	Oil phase
		Tocopherol 0.002%	Oil phase
		Chitosan 0.2%	Added later
		Lactoferrin 2%	Aqueous phase
		Tween® 80 0.3%	Aqueous phase
F2	Liposomes comprising lactoferrin and hyaluronic acid	Lipoid S75 3%	Oil phase
		Cholesterol 0.1%	Oil phase
		Tocopherol 0.002%	Oil phase
		Lactoferrin 2%	Aqueous phase
		Hyaluronic acid 290 kDa 0.01%	Aqueous phase
		Tween® 80 0.3%	Aqueous phase
F3	Liposomes comprising lactoferrin and hyaluronic acid	Lipoid S80 1.5%	Oil phase
		Cholesterol 0.1%	Oil phase
		Tocopherol 0.002%	Oil phase
		Lactoferrin 0.8%	Aqueous phase
		Hyaluronic acid 1600 kDa 0.1%	Added later
		Tween® 80 0.3%	Aqueous phase

Example 2

Characterization of the liposomes

[0070] Liposomes of F1 and F2 prepared according to the above Example have been characterized by determining their average size and the polydispersity index (PI) by means of DLS (using the Zeta Sizer Malvern ZS instrument), and the Z-potential (ZP) by laser Doppler electrophoresis (using the Zeta Sizer Malvern ZS instrument).

[0071] The results of the above characterizations are shown in Table 2.

Table 2

Formulation	Size (nm)	PI	ZP (mV)
F1	79.16 ± 0.43	0.25 ± 0.001	32.9 ± 0.8
F2	85.55 ± 0.62	0.20 ± 0.001	23.5 ± 0.4

[0072] The size of the F1 and F2 liposomes previously determined by DLS has been checked by transmission electron microscope analysis (TEM) after negative staining. The TEM analysis confirmed the size determined by DLS of F1 and F2 liposomes. Moreover, the TEM analysis highlighted the smooth and spherical surface of F1 and F2 liposomes.

Example 3

Preparation of additional liposomes

[0073] Additional liposomes have been prepared, shown in Table 3, according to the method described in Example

ANEXO

1. The aqueous phase and the oil phase of F1.1, F1.2, F1.3 and F1.4 liposomes qualitatively and quantitatively correspond to those of F1 formulation described in Table 1, while the aqueous phase and the oil phase of F2.1, F2.2, F2.3 and F2.4 liposomes qualitatively and quantitatively correspond to those of F2 formulation described in Table 1. To such additional liposomes, after two cycles of homogenization, have been added:

- 5% hydroxypropyl-β-cyclodextrin and 5% trehalose to F1.1, F1.2, F1.3 and F1.4 liposomes;
- 9.93% hydroxypropyl-β-cyclodextrin and 7% trehalose to F2.1, F2.2, F2.3 and F2.4 liposomes.

[0074] The liposomes of the present example have been characterized as described in Example 2. The results of such characterizations are set forth in Table 3.

Table 3

Formulation	Size (nm)	PI	ZP (mV)
F1.1	89.95 ± 0.64	0.257 ± 0.009	34.3 ± 0.51
F1.2	88.87 ± 0.95	0.259 ± 0.005	36.9 ± 0.66
F1.3	89.10 ± 0.02	0.261 ± 0.004	35.7 ± 0.17
F1.4	88.46 ± 0.64	0.263 ± 0.003	34.4 ± 0.58
F2.1	79.71 ± 0.17	0.204 ± 0.01	20.20 ± 0.37
F2.2	78.37 ± 0.36	0.200 ± 0.004	20.63 ± 2.10
F2.3	78.14 ± 0.19	0.205 ± 0.005	21.84 ± 0.62
F2.4	77.36 ± 0.10	0.205 ± 0.007	21.13 ± 0.41

[0075] The osmolarity values of all formulations are set forth in Table 3 and are around 300 mOsm/kg. Such values have been determined by using the Advanced® Model 3320 Micro-Osmometer instrument (Advanced® Instruments, Inc., Norwood, MA, USA).

Example 4

Sterilization of the liposomes

[0076] The F2 liposomes have been sterilized by using γ rays at a dose of 25 kGy.

[0077] After such sterilization, the sterilized F2 liposomes have been characterized again in order to check that the above described sterilization process does not affect their structure. The results of such characterizations are set forth in Table 4.

Table 4

Formulation	Sterilization	Size (nm)	PI	ZP (mV)	Osmolarity (mOsm/kg)
F2	Before	85.55 ± 0.62	0.20 ± 0.001	23.5 ± 0.4	273
	After	92.54 ± 0.61	0.203 ± 0.008	28.5 ± 0.56	279

[0078] The results shown in Table 4 confirm that F2 liposomes do not undergo any substantial change of their characteristics after the sterilization treatment.

[0079] A sterilization treatment as described above has been carried out equally to F1 liposomes.

Example 5

Freeze-drying process of the liposomes

[0080] Liposomes F1 to F1.4 and F2 to F2.4 have been freeze-dried by means of the following freeze-drying process:

Table 5

Step	Time (hours)	Temperature (°C)	Pressure (mBar)
Freezing	8	-80	Atmospheric P
Freezing	1	-30	Atmospheric P
Primary drying	3	-30	0.350
Primary drying II	1	-15	0.350
Secondary drying	12	+10	0.350

[0081] The freeze-drying process as described above allows the long-term storage of the liposomes, preserving the original chemical-physical characteristics after reconstitution.

Example 6

Evaluation of the *in vitro* ocular irritation by means of HET CAM test

[0082] The *in vitro* test described in the present example has been carried out in order to evaluate if the ocular topical administration of the liposomes could cause irritation to the eye. To such purpose, the *in vitro* HET CAM test as described in ICCVAM-Recommended Test Method Protocol has been carried out: Hen's Egg Test - Chorioallantoic Membrane (HET-CAM) Test Method.

[0083] The HET CAM test has been carried out by observing the irritation effects (bleeding, vasoconstriction and clotting) induced on the chorioallantoic membrane (CAM) of 10 days embryonated eggs by applying 0.3 ml of liposomes under test and calculating the ocular irritation index ("OII") according to the formula described in Table 6. OII can be grouped in the four categories set forth in Table 6.

Table 6

Calculation of OII (HET CAM)	OII	Classification
OII = (301 - H) * 5/300 + (301 - v) x 7/300 + (301 - C) * 9/300 H: bleeding, v: vasoconstriction, C: clotting	0-0.9	Not-irritant
	1-4.9	Slightly irritant
	5-8.9	Moderately irritant
	9-21	Irritant

[0084] The liposomes under examination in the present test are F1 and F2 liposomes. By means of the same method, the following controls have been also tested: SDS 1% (positive control with slow irritation), 0.1 N NaOH (positive control with fast irritation) and NaCl 0.9% (negative control).

[0085] The embryonated eggs for this test have been obtained by the G.A.L.L.S.A. farm, Tarragona, Spain. The eggs are kept at a temperature of 12 ± 1 °C for at least 24 hours before placing them into the incubator at controlled temperature (37.8 °C) and humidity (50-60%) during the incubation days.

[0086] The data have been analyzed as mean ± standard deviation at the moment when the injury occurred (n = 3/group).

[0087] The results of the HET CAM test demonstrated that:

- SDS 1% and 0.1 N NaOH have irritating effects (both positive controls);
- NaCl has not irritating effects (negative control); and
- F1 and F2 liposomes have not irritating effects, have an ocular irritation index corresponding to that of the not-irritating products.

[0088] Therefore, it has been demonstrated, by means of the present *in vitro* test, that the products of the invention do not cause ocular irritation.

ANEXO

Example 7

Evaluation of the *in vitro* ocular irritation by means of Draize test

[0089] The *in vitro* test described in the present example has been carried out in order to evaluate if the ocular topical administration of the products of the invention could cause irritation to the eye. To this purpose, the Draize irritation test has been carried out. Such test has been carried out by using male albino rabbits from New Zealand of 2.5 kg average got from the San Bernardo farm (Navarra).

[0090] The present test has been carried out by placing the sample to be evaluated inside the conjunctival sac of the left eye of the albino rabbits. A moderate massage has been carried out to guarantee the correct circulation. The occurrence of irritation has been observed both at the moment of application and after one hour, by using the right eye as negative control (n = 3/group). According to the present example, the samples to be evaluated were F1 liposomes and F2 liposomes.

[0091] The evaluation of the irritation has been carried out by directly observing the anterior segment of the eye, detecting the possible injuries of conjunctiva, iris and cornea as shown in Table 8. The ocular irritation index ("OII") has been calculated based on the observed injuries and the formula set forth in Table 7.

Table 7

Calculation of OII (Draize test)
OII = Cornea (A * B * 5) + Iris (A * 5) + Conjunctiva (A + B + C) * 2

Table 8

Structure	**Injury**	**Evaluation**	**Score**
CORNEA	*A) Level of opacity* - Absence of ulcers - Diffused areas - Translucent areas - Opalescent areas - Full opacity	 0 1 2 3 4	Corneal score: A * B * 5 Maximum score: 80
	B) *Affected area* - None - One fourth or less - More than a quarter but without means - More than half but less than three quarters - More than three quarters up to a whole plane	 0 1 2 3 4	
IRIS	*A) Score of the damage to iris* - Normal - Presence of deep wrinkles, congestion, puffiness, moderate circumncorneal inj ection	 0 1	Radial score: A * 5 Maximum score:10
	- No reaction to light, hemorrhage, extensive damage (injury)	2	
CONJUNCTIVA	*A) Redness* - Normal eye - Some vessels clearly injected - Diffused redness - Highly diffused redness	 0 1 2 3	Corneal score: (A + B + C) * 2 Maximum score: 20

(continued)

	B) Chemosis or inflammation		
	- None	0	
	- Partial	1	
	- Pronounced with partial dysfunction of the eyelids	2	
	- Eyelids more or less closed	3	
	- Eyelid dropping	4	
	C) Secretions		
	- None	0	
	- Any anomalous amount	1	
	- Humidity and wet eyelash of the eyelids	2	
	- Periocular humidity	3	

[0092] The results of the present test revealed that both F1 and F2 liposomes are not irritating (OII = 0). Indeed, the animals did not show any *in vivo* sign of irritation both at the moment of application, and after one hour. The present test has therefore confirmed the results of the test of the previous Example, demonstrating that the products of the invention do not cause ocular irritation and are therefore suitable to be administered by ocular topical route.

Example 8

In vivo treatment of ocular inflammation

[0093] The ability of *in vivo* treatment of the inflammation by F2 liposomes by means of the below set forth irritation test has been evaluated.

[0094] Inflammation in the eye of male albino rabbits as described in Example 7 is induced by applying a drop of eye drops containing 0.5% arachidonic acid sodium salt (SA - irritating agent) at time 0. After 30 minutes, the sample under examination is administered to the inflamed eye. Finally, the ocular inflammation index is evaluated at different time points. In the present test, the samples under examination were:

I) 50 μl of free lactoferrin (not encapsulated into the lipid bilayer of liposomes) dissolved in PBS (comparative example);
II) 50 μl of F2 liposomes.

[0095] As positive control (C+ - comparative), a rabbit administered with SA at time 0, without any administration after 30 minutes, has been used.

[0096] The ocular inflammation has been evaluated for each time point at 30, 60, 90, 120, 150, 180 and 210 minutes and the inflammation index has been consequently calculated for each time point according to the tables of the previous Example.

[0097] The results of the present test are shown in Figure 1. In particular, Figure 1 shows the values of ocular inflammation score of the positive control (C), free lactoferrin (I) and F2 liposomes at the minutes set forth above. In Figure 1, the order of the bars represent the ocular inflammation indexes is C+, I and F2 for all the measurements at the minutes set forth above. Moreover, in Figure 1 the comparison of F2 liposomes or free lactoferrin (I) to the positive control (C+) is represented as *p<0.05, ** p<0.01, *** p<0.001, **** p<0.0001, while the comparison of F2 liposomes to the free lactoferrin (I) is represented as $p<0.05, $$p<0.01, $$$p<0.001, $$$$p<0.0001. The results shown in Figure 1 demonstrate that the product of the invention, in particular that one comprising the hyaluronic acid (F2), is effective in treating the ocular inflammation. In particular, the products of the invention proved to be particularly effective in the treatment of inflammation already after 60 minutes from their administration. The products of the invention proved also to be surprisingly more effective than free lactoferrin in the treatment of inflammation also in the long-term, possibly as a consequence of the sustained release of lactoferrin and hyaluronic acid.

Example 9

In vivo prevention of ocular inflammation

[0098] The ability of *in vivo* prevention of the inflammation by F1 and F2 liposomes by means of the below set forth

irritation test has been evaluated.

[0099] The samples under examination are applied at time 0 to the eye of male albino rabbits as described in Example 7. After 30 minutes, a drop of eye drops containing 0.5% arachidonic acid sodium salt (SA - irritating agent) is applied to the same eye. Finally, the ocular inflammation index is evaluated at different time points. In the present test, the samples under examination were F1 liposomes and F2 liposomes. As positive control (C+ - comparative), a drop of eye drops containing 0.5% arachidonic acid sodium salt (SA - irritating agent) has been applied to the eye of a male albino rabbit at minute 30, without prior application of any liposome.

[0100] The ocular inflammation has been evaluated for each time point at 60, 90, 120, 150, 180 and 210 minutes after the administration of F1 and F2 formulations and the inflammation index (OII) has been consequently calculated for each point in time according to the tables of Example 7.

[0101] The results of the present test are shown in the plot of Figure 2. In particular, Figure 2 shows the values of ocular inflammation score of the positive control (C+), the formulation of F1 liposomes, and the formulation of F2 liposomes, at the minutes set forth above. In Figure 2, the order of the bars representing the ocular inflammation indexes is C+, F1 and F2 for all the measurements at the minutes set forth above.

[0102] Moreover, in Figure 2, the values are expressed as mean ± standard deviation, *p<0.05, **p<0.01, ***p<0.001 and ****p<0.0001 significantly lower than the inflammatory effects induced by SA; the values are expressed as mean ± standard deviation, $^{\$}$p<0.05, $^{\$\$}$p<0.01, $^{\$\$\$}$p<0.001 and $^{\$\$\$\$}$p<0.0001 significantly lower than the inflammatory effect induced by the other liposome formulations developed.

[0103] The results shown in Figure 2 demonstrate that there is efficacy in the prevention of ocular inflammation of liposomes of F1 and F2 formulations; in particular, for the formulations of liposomes comprising hyaluronic acid (F2). Such efficacy in the prevention of the inflammation is present already 30 minutes after the inflammatory stimulus of the liposomes comprising hyaluronic acid. In addition the results show that F1 liposomes comprising chitosan provide better results with respect to C+ positive control and require longer time to provide the prevention effect with respect to F2 liposomes comprising hyaluronic acid. It is believed that this is due to the gradual and sustained release of lactoferrin characterizing the products of the invention comprising chitosan.

Example 10

Hyposphagma treatment

[0104] The present test has been carried out in order to determine the reduction level of hyposphagma by the products of the invention. According to the present test, hyposphagma has been induced in the rabbit by means of the method described below. The reduction level of hyposphagma has been evaluated by using biodegradable systems and controlled administration.

[0105] The test has been performed on 9 rabbits. In order to realize this test, the rabbis have been administered with an intramuscular anesthesia (ketamine/xylazine) and an ocular topical anesthesia (procaine in drops). Once the rabbits have been anesthetized, the fur of one of the two ears has been shaved and then the shaved ear has been cleaned with alcohol. From the auricular marginal vein 0.2 ml of blood has been extracted, and immediately after the extraction, 0.1 ml of the previously extracted blood has been injected in the superior conjunctival area of the rabbit eye. The rabbits have then been randomly sorted in 3 different groups, to which different treatments in the form of ocular drops have been applied:

I) control group: Saline serum (positive control);
II) ocular drops of liposomes comprising lactoferrin and hyaluronic acid (F2 liposomes); and
III) ocular drops of liposomes comprising lactoferrin and chitosan (F1 liposomes).

[0106] Once the rabbit has been reawakened, the reduction level of hyposphagma with respect to the control group (as described below) after 8, 24, 48, 72, 96 and 120 hours following the induction of the same has been evaluated. The treatment with ocular drops is applied daily. Hyposphagma is evaluated with a millimetric scale at time zero and during its daily evolution by the treatment. Later the rabbit will be sacrificed by means of anesthesia followed by a pentobarbital dose. The obtained results have been analyzed by using an ANOVA test to observe if significant effects are produced with respect to the control group.

[0107] The preliminary results deriving from what reported in the present example have demonstrated a greater efficacy of F2 and F1 with respect to the control group in the treatment of hyposphagma.

Example 11

Treatment of dry eye

[0108] The present test has been carried out in order to determine the reduction level of dry eye by the products of the invention. According to the present test, dry eye has been induced in the rabbit by means of the method described below. The reduction level of dry eye has been evaluated by using biodegradable systems and controlled administration.

[0109] The test has been performed on 9 rabbits. During the first 3 weeks, the rabbit has been treated with ocular drops of 0.1% benzalkonium chloride two times per day (morning and afternoon, weekend included). This treatment is required to guarantee a statistically significant effect (n=3/group). After the three weeks of preparation, the treatment has been applied (see the following bulleted list) during one week. The rabbits have been randomly sorted in 3 different groups:

I) control group: Saline serum (positive control);
II) ocular drops of liposomes comprising lactoferrin and hyaluronic acid (F2 liposomes); and
III) ocular drops of liposomes comprising lactoferrin and chitosan (F1 liposomes).

[0110] At the end of the treatment, the Schirmer test and the staining with fluorescein (under anesthesia) have been performed in order to evaluate the extension of the treatment of dry eye for each single group. Later the rabbits have been sacrificed.

[0111] The preliminary results of the present example have demonstrated a greater efficacy of F2 and F1 with respect to the control group in the treatment of dry eye.

Claims

1. A product made of liposomes, which comprises lactoferrin and a component selected from hyaluronic acid or chitosan, for its use in the prevention and/or treatment of ocular diseases.

2. The product according to claim 1, **characterized in that** said ocular diseases are inflammatory ocular diseases, preferably said inflammatory ocular diseases are selected from the group comprising conjunctivitis, chalazion, stye, blepharoconjunctivitis and keratitis.

3. The product according to claim 1, **characterized in that** said ocular diseases are selected from the group comprising dry eye syndrome and hyposphagma.

4. The product according to any one of the preceding claims, **characterized in that** said liposomes have a positive Z-potential charge, preferably said Z-potential charge is greater than or equal to 10 mV, more preferably it is greater than or equal to 15 mV, still more preferably it is greater than or equal to 20 mV.

5. The product according to any one of the preceding claims, **characterized in that** said liposomes have a size lower than or equal to 200 nm, preferably lower than or equal to 150 nm, more preferably lower than or equal to 100 nm, still more preferably it is in the range from 70 nm to 100 nm.

6. The product according to any one of the preceding claims, **characterized in that** the core of aqueous solution inside said liposomes has an osmolarity in the range from 200 to 500 mOsm/Kg, preferably from 250 to 450 mOsm/Kg, more preferably it is about 310 mOsm/Kg.

7. The product made of liposomes, which comprises lactoferrin and a component selected from hyaluronic acid or chitosan, **characterized in that** said liposomes have a size lower than or equal to 200 nm, and that the core of aqueous solution inside said liposomes has an osmolarity in a range from 200 to 500 mOsm/Kg.

8. A composition comprising the product as described in claim 7 and pharmaceutically suitable excipients.

9. The composition according to claim 8, **characterized in that** it is an ocular topical composition.

10. The composition according to claim 8 or 9, **characterized in that** it comprises:

ANEXO

I) liposome-forming lipids in an amount in the range from 1% to 5%, preferably from 2% to 4%, more preferably 3%; and
II) lactoferrin in an amount in the range from 0.5% to 8%, preferably from 1% to 4%, still more preferably of 2%; and a component selected from
III) hyaluronic acid in an amount in the range from 0.0001% to 0.5%, preferably from 0.0005% to 0.1%, more preferably from 0.001% to 0.02%, still more preferably of 0.01%; or
IV) chitosan in an amount in the range from 0.02% to 2%, preferably from 0.1% to 1%, more preferably of 0.2%.

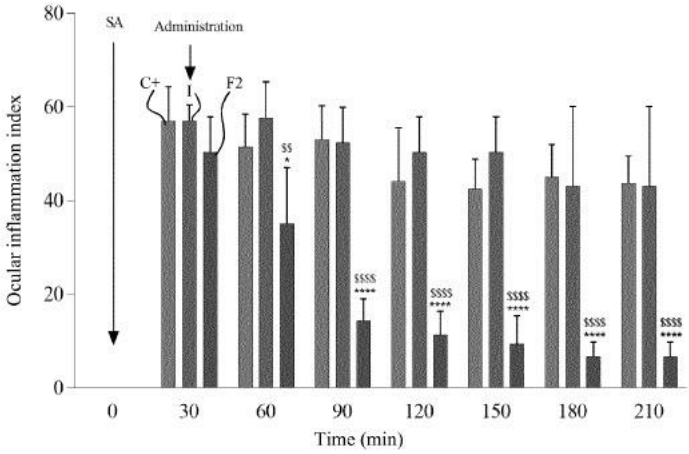
SA
Administration
C+
I
F2
Ocular inflammation index
80
60
40
20
0
$$
$$$$
****
0
30
60
90
120
150
180
210
Time (min)

Fig. 1

ANEXO

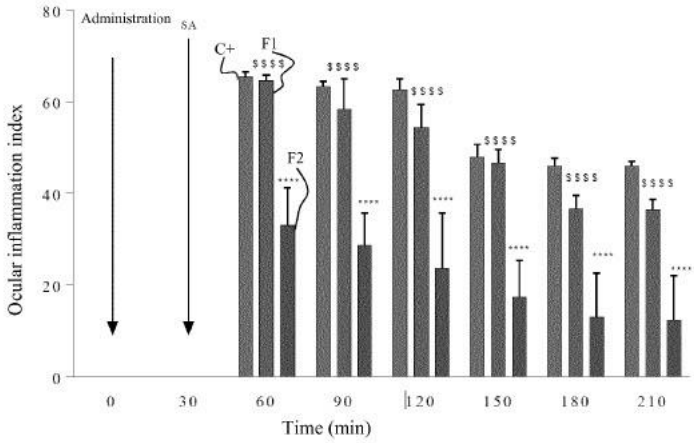
Administration
SA
C+
F1
F2
$$$$
****
Ocular inflammation index
Time (min)
0
30
60
90
120
150
180
210
0
20
40
60
80

Fig. 2

Europäisches Patentamt
European Patent Office
Office européen des brevets

EUROPEAN SEARCH REPORT

Application Number
EP 19 18 9078

DOCUMENTS CONSIDERED TO BE RELEVANT

Category	Citation of document with indication, where appropriate, of relevant passages	Relevant to claim	CLASSIFICATION OF THE APPLICATION (IPC)
Y	MARTA VICARIO-DE-LA-TORRE ET AL: "Novel Nano-Liposome Formulation for Dry Eyes with Components Similar to the Preocular Tear Film", POLYMERS, vol. 10, no. 4, 11 April 2018 (2018-04-11), page 425, XP055575757, DOI: 10.3390/polym10040425 * abstract * * paragraphs [02.2], [03.1] * * page 10, last paragraph - page 11 *	1-10	INV. A61K9/127 A61K38/40 A61K47/36 A61K31/722 A61K31/728
Y	FUJIHARA T ET AL: "Lactoferrin suppresses loss of corneal epithelial integrity in a rabbit short-term dry eye model", JOURNAL OF OCULAR PHARMACOLOGY AND THERAPEUT, MARY ANN LIEBERT, INC., NEW YORK, NY, US, vol. 14, no. 2, 1 January 1998 (1998-01-01), pages 99-107, XP009074064, ISSN: 1080-7683 * abstract *	1-10	
A	EP 2 016 937 A1 (UNIV MADRID COMPLUTENSE [ES]) 21 January 2009 (2009-01-21) * paragraphs [0001], [0009], [0011], [0012], [0013] - [0021] * * claims *	1-10	

-/--

TECHNICAL FIELDS SEARCHED (IPC)
A61K

The present search report has been drawn up for all claims

Place of search	Date of completion of the search	Examiner
The Hague	3 December 2019	Epskamp, Stefan

CATEGORY OF CITED DOCUMENTS
X : particularly relevant if taken alone
Y : particularly relevant if combined with another document of the same category
A : technological background
O : non-written disclosure
P : intermediate document

T : theory or principle underlying the invention
E : earlier patent document, but published on, or after the filing date
D : document cited in the application
L : document cited for other reasons

& : member of the same patent family, corresponding document

EPO FORM 1503 03.82 (P04C01)

ANEXO

Europäisches Patentamt
European Patent Office
Office européen des brevets

EUROPEAN SEARCH REPORT

Application Number
EP 19 18 9078

DOCUMENTS CONSIDERED TO BE RELEVANT

Category	Citation of document with indication, where appropriate, of relevant passages	Relevant to claim	CLASSIFICATION OF THE APPLICATION (IPC)
A	LI N ET AL: "Liposome coated with low molecular weight chitosan and its potential use in ocular drug delivery", INTERNATIONAL JOURNAL OF PHARMACEUTICS, ELSEVIER, NL, vol. 379, no. 1, 8 September 2009 (2009-09-08), pages 131-138, XP026471271, ISSN: 0378-5173, DOI: 10.1016/J.IJPHARM.2009.06.020 [retrieved on 2009-06-25] * abstract *	1-10	
A	TRIF M ET AL: "Liposomes as possible carriers for lactoferrin in the local treatment of inflammatory diseases", PROCEEDINGS OF THE SOCIETY FOR EXPERIMENTAL BIOLOGY AND MEDICINE, SAGE PUBLICATIONS LTD, GB, vol. 226, no. 6, 1 January 2001 (2001-01-01), pages 559-564, XP003011978, ISSN: 0037-9727 * abstract * * page 560, left-hand column, paragraph 3 *	1-10	TECHNICAL FIELDS SEARCHED (IPC)

The present search report has been drawn up for all claims

Place of search	Date of completion of the search	Examiner
The Hague	3 December 2019	Epskamp, Stefan

CATEGORY OF CITED DOCUMENTS

X : particularly relevant if taken alone
Y : particularly relevant if combined with another document of the same category
A : technological background
O : non-written disclosure
P : intermediate document

T : theory or principle underlying the invention
E : earlier patent document, but published on, or after the filing date
D : document cited in the application
L : document cited for other reasons

& : member of the same patent family, corresponding document

EPO FORM 1503 03.82 (P04C01)

ANNEX TO THE EUROPEAN SEARCH REPORT ON EUROPEAN PATENT APPLICATION NO. EP 19 18 9078

This annex lists the patent family members relating to the patent documents cited in the above-mentioned European search report. The members are as contained in the European Patent Office EDP file on The European Patent Office is in no way liable for these particulars which are merely given for the purpose of information.

03-12-2019

Patent document cited in search report	Publication date	Patent family member(s)	Publication date
EP 2016937 A1	21-01-2009	EP 2016937 A1	21-01-2009
		ES 2284398 A1	01-11-2007
		ES 2535189 T3	06-05-2015
		PL 2016937 T3	31-07-2015
		WO 2007125134 A1	08-11-2007

EPO FORM P0459

For more details about this annex : see Official Journal of the European Patent Office, No. 12/82